Tonje Dobrowen Fredriksen

Quantitative Doppler Methods in Cardiovascular Imaging

Thesis for the degree of Philosophiae Doctor

Trondheim, November 2014

Norwegian University of Science and Technology
Faculty of Medicine
Department of Circulation and Medical Imaging

NTNU – Trondheim
Norwegian University of
Science and Technology

NTNU
Norwegian University of Science and Technology

Thesis for the degree of Philosophiae Doctor

Faculty of Medicine
Department of Circulation and Medical Imaging

© Tonje Dobrowen Fredriksen

ISBN 978-82-326-0536-1 (printed ver.)
ISBN 978-82-326-0537-8 (electronic ver.)
ISSN 1503-8181

Doctoral theses at NTNU, 2014:312

Printed by NTNU-trykk

Kvantitative Doppler-metoder i blodstrømsavbildning

Måling av blodhastigheter med ultralyd kan si noe om tilstedeværelse og utvikling av enkelte hjerte- og karsykdommer. Både forkalkninger i blodårene og lekkasjer i hjerteklaffene kan oppdages ved hjelp av slike hastighetsmålinger, og ved tidlig diagnostisering kan pasienten få riktig oppfølging og risikoen for dødsfall reduseres betydelig.

Hastighetsmålinger kan gjøres ved å sende korte ultralydpulser inn i kroppen. Ved å gjøre en frekvensanalyse av de reflekterte pulsene kan man lage et hastighetsspekter, som viser blodhastighetene som funksjon av tid. Et slikt spekter vil ha en nøyaktighet som er bestemt av avbildningstiden av et gitt blodvolum – lengre avbildningstid gir større nøyaktighet. Ved høye hastigheter og/eller stor vinkel mellom ultralydstrålen og blodstrømmen, vil man derfor få en redusert nøyaktighet.

Vi har utviklet en ny spektraldopplermetode som vi har kalt ”2-D tracking Doppler”. Denne metoden tar i bruk ufokuserte lydbølger, samt en teknikk kalt parallell stråleforming. Ved å bruke den nye metoden kan man følge blodet i den retningen det beveger seg, noe som gir lengre avbildningstid for et gitt blodvolum, og dermed større nøyaktighet i hastighetsspekteret. I denne avhandlingen presenterer vi resultater fra flere typer forsøk som viser at når vinkelen mellom ultralydstrålen og blodstrømmen er stor, får man mer nøyaktige hastighetsmålinger med 2-D tracking Doppler-metoden, enn med en tradisjonell metode.

Vinkelen mellom ultralydstrålen og blodhastighetsretningen må bestemmes for å få korrekte hastigheter. Dette gjør man vanligvis manuelt ved å studere ultralydbildet, noe som kan være utfordrende ved komplekse strømningsfelt. Med 2-D tracking Doppler-metoden vil man få et bredere hastighetsspekter hvis man velger feil vinkel. Vi viser at denne egenskapen ved metoden kan brukes til å finne vinkelen automatisk, og med større nøyaktighet enn med den tradisjonelle metoden.

Vi har også utviklet en metode for å beregne størrelsen på hjertelekkasjer ved å kombinere spektraldoppler med parallell stråleforming. Hjertelekkasjer består som regel av en strøm av blod med svært høye hastigheter. Ved å estimere hastighetene til blodet i mange punkter ved lekkasjen kan man derfor få informasjon om hvor stor lekkasjen er. Vi har gjort en simuleringsstudie for å finne det optimale oppsettet for metoden, og vi viser at med dette oppsettet ser det ut til at man kan estimere både blodstrømsvolumet til lekkasjen og omfanget av den svært nøyaktig.

Tonje Dobrowen Fredriksen
Institutt for sirkulasjon og bildediagnostikk, NTNU
Hovedveileder: Hans Torp
Biveileder: Bjørn Olav Haugen
Finansieringskilde: MI Lab

Ovennevnte avhandling er funnet verdig til å forsvares offentlig for graden Philosophiae Doctor (PhD) i medisinsk teknologi. Disputas finner sted i Auditoriet, Medisinsk Teknisk Forskningssenter, torsdag 13. november 2014 kl. 12:15.

Abstract

Ultrasound imaging of blood flow in the heart and blood vessels has become an essential part of diagnosing diseases related to the circulatory system. By using different Doppler methods, the blood flow may be visualized or quantified. In this work we take advantage of the opportunities given by the introduction of parallel processing of ultrasound data to develop new quantitative Doppler methods.

Pulsed wave (PW) Doppler is a technique for measuring blood velocities, providing the full velocity spectrum in a specific region of interest. The maximum velocities may be found by delineation of the spectral envelope, and may be used to estimate the severity of stenoses or valve leakages. However, PW Doppler suffers from several challenges, which makes quantitative analysis problematic. To limit spectral broadening, we created a new method called 2-D tracking Doppler, which incorporates information from several parallel receive beams. Spectra with improved resolution and signal-to-noise ratio were produced for a large span of beam-to-flow angles. The new method was tested using *in vitro* and *in vivo* recordings. A signal model was derived and the expected Doppler power spectra were calculated, showing good agreement with experimental data.

Experiments were performed to investigate how the 2-D tracking Doppler method depends on the tracking angle. It was shown that the spectra have lowest bandwidth and maximum power when the tracking angle is equal to the beam-to-flow angle. This may facilitate new techniques for velocity calibration. It was shown that the velocity calibration errors may be lower for the 2-D tracking Doppler method than for a conventional PW Doppler approach, and especially for large beam-to-flow angles.

In heart disease, the quantification of valve regurgitation is a remaining challenge. In this thesis, we have investigated a new technique to estimate the size of regurgitant jets using spectral Doppler and parallel beamforming. A modality that uses high pulse repetition frequency 3-D Doppler was devised, to isolate the backscattered signal power from the vena contracta, that is the narrowest flow region of a regurgitant jet. A simulation study was performed to test and optimize the new method, suggesting a feasible setup for the transmit- and receive beams. Cross-sectional power Doppler images of simulated regurgitations of various sizes were generated, and the regurgitant volumes were accurately estimated. Since the velocity-time integral and the orifice area are extracted from a single recording, the proposed method may give more robust volume estimates than methods where the velocities and the area are measured from separate recordings.

Preface

This thesis is submitted in partial fulfillment of the requirements for the degree of *Philosophiae Doctor* (Ph.D.) at the Faculty of Medicine of the Norwegian University of Science and Technology (NTNU). The research was funded by *Medical Imaging Laboratory* (MI-Lab), and was carried out at the Department of Circulation and Medical Imaging. The main supervisor has been Professor Hans Torp from Department of Circulation and Medical Imaging, NTNU and co-supervisor has been MD, PhD Bjørn Olav Haugen.

Acknowledgements

There are many people that have shared their knowledge and time with me in the process of producing this thesis, and they all deserve the most sincerely thanks. I also want to express my gratitude to NTNU, MI-Lab and the Department of Circulation and Medical Imaging for equipping me with all possible tools and opportunities.

My amazing fellow PhD students have been invaluable to me, both for work and social reasons. Because of you, all the conference trips we have attended have been filled with social, fun and memorable experiences. I especially would like to thank Solveig for being my accomplice when exploring the life as a PhD student. I also want to share the most grateful thanks to the genius couple Ekroll/Avdal, for all your help and support during the work of publishing papers. You have been the best consultants for all my questions, work related or not.

There are also many people "in the corridor" that have helped me a lot. First I would like to thank my ex-supervisor Torbjørn, for all the effort and work that you put into the first part of my PhD. I also would like to thank Svein Arne for all the hours you have spent battling the E9 scanner with me, and Bastien for your infinite expertise in simulation software and scanner programming. I especially want to thank Hans for always taking the time to guide me, in spite of a well of other duties. With all your experience and knowledge, it has been a great comfort that so much of my work has gone through your filters.

Last, but not least, I want to thank all of you that have taken care of me outside the work office. This thesis would never have come to be without you.

Table of Contents

Abbreviations

B-mode	Brightness mode
CCA	Common carotid artery
CW	Continuous wave
ECA	External carotid artery
EROA	Effective regurgitant orifice area
$F_{\#}$	F-number
FFT	Fast Fourier transform
FWHM	Full width half maximum
HPRF	High pulse repetition frequency
ICA	Internal carotid artery
IQ	In-phase Quadrature
M-mode	Motion mode
MR	Mitral regurgitation
PISA	Proximal isovelocity surface area
PRF	Pulse repetition frequency
PRT	Pulse repetition time
PW	Pulsed wave
RF	Radio frequency
ROI	Region of interest
Rx	Receive
SNR	Signal-to-noise ratio
Tx	Transmit

Chapter 1

Introduction

Ultrasound imaging is a technique with many advantages; it is real-time, non-invasive, relatively cheap, highly available, and without harmful effects. Among the different possible image types, the well-known B-mode image displays a two-dimensional cross-section of the tissue being imaged, while the Doppler images can visualize the blood flow. In addition to imaging, ultrasound can be used for quantitative measurements, such as elastography and flow estimation.

It was in the late 50's that Satomura in Japan found that it was possible to measure heart movement using the shift in frequency of backscattered ultrasound [1], a wave effect proposed by Doppler about a hundred years earlier. The method was soon adapted to blood velocity measurements [2, 3], and researchers in Trondheim were among the first to utilize it. In the 1970s, Rune Aaslid and Jarle Hoen found that it was possible to non-invasively measure pressure drops across heart valves, by extracting the Doppler shift and applying a simplified solution to the Bernoulli equation [4]. A pulsed echo Doppler flow velocity meter (PEDOF) [5], invented by Bjørn Angelsen, had an integrated system of both pulsed wave and continuous wave Doppler, and was soon applied in the clinics by cardiologist Liv Hatle [6, 7].

One of the most frequently used quantitative measurements in clinical Doppler ultrasound today is to measure the maximum blood velocities. In the heart, estimates of peak velocity are used to derive the pressure gradient across a cardiac valve using the modified Bernoulli equation [8]. In arteries, increased velocities occur in the region of a stenosis, and the degree of stenosis may be derived directly from the maximum velocity [9]. At valve leakages, the significance of the regurgitation is determined from the regurgitant volume, which can be estimated from the maximum velocities and the orifice area [10].

Maximum velocities can be estimated by delineating the envelope of velocity spectra, produced by either continuous wave Doppler (CW) or pulsed wave Doppler (PW). When using CW Doppler, a continuous wave of ultrasound is sent into the body, in distinction to PW Doppler where short pulses of ultrasound are used. This means that for CW Doppler, there is no limit on the maximum velocities that can be measured, but there is no depth resolution. For PW Doppler, however, the measurement location is defined, but the maximum velocities that can be measured are limited by the pulse repetition frequency (PRF).

A band of velocities are usually displayed in the spectra, representing the blood

velocities present in the insonified volume. However, the spectra may broaden additionally because of the transit time effect. The transit time is the effective observation time of the blood scatterers in the received signal. For PW Doppler the insonified volume is limited by the beam width and the pulse length. The scatterers pass through the insonified volume during a short time interval, limiting the achievable velocity resolution. This is particular challenging when the beam-to-flow angle is large or when high-velocity jets are present, e.g., in stenotic regions. Spectrum broadening leads to overestimation of the maximum velocities, which may decrease diagnostic confidence and makes quantitative analysis more challenging and less reproducible.

A method for generating velocity spectra with reduced spectral broadening, called velocity matched spectrum, has previously been published [11]. By tracking the scatterers along the direction of the flow, the transit time was increased, giving a better velocity resolution in the spectrum. A similar method is the butterfly search technique [12], developed by Alam and Parker. In this method, the complex demodulated signal is sampled on different delay trajectories (butterfly lines) in the slow time-fast time space. To estimate the mean velocity, the butterfly lines on which the variance is minimal are searched for. Both methods only track along the beam direction and have therefore shown improved performance only for small beam-to-flow angles.

Conventional Doppler techniques can only measure the axial component of blood flow. The blood velocity is estimated by multiplying the measured velocity with an angle correction factor of $1/\cos\theta$, where θ is the manually chosen beam-to-flow angle. As the angle correction factor tends to infinity as θ approaches $90°$, the velocity estimates are very sensitive to angle estimation errors for large beam-to-flow angles.

Several techniques have been suggested to overcome the angle dependence in Doppler ultrasound. Cross-beam vector Doppler has been one of the main approaches to 2-D flow imaging since the onset of the idea in the 1970s. Using triangulation, the 1-D velocity estimates from two different angles of insonation can be used to reconstruct a 2-D velocity vector [13]. Another approach has been described by J. Jensen *et al.* [14, 15], where both the velocity magnitude and angle is determined using a cross-correlation technique. The angle is found from beamforming directional signals in a number of directions and then selecting the angle with the highest normalized correlation. However, these methods only estimate the mean velocity, and may be biased because of clutter filtering issues or spatial averaging.

Velocity estimation is particularly challenging in the heart, as the heart lies deep within the body, partly concealed by ribs and surrounded by the lungs, and contains complex flow patterns with unclear boundaries. Estimates of both the flow velocities and directions can help diagnose and predict several diseases. Flow near stenotic and leaky valves are of particular clinical interest. Mitral regurgitation (MR) is the backflow of blood through the mitral valve, and it is one of the most common valvular heart diseases. The disease can cause dyspnea and be life-threatening, but mortality is reduced by surgical procedures [16, 17]. Accurate assessment of the disease is crucial for timing the intervention before the heart remodels with the development of permanent heart failure and increased mortality.

2-D color Doppler jet area measurements are used to diagnose mitral regurgitation, but the method may not give an accurate estimate of the severity of the regurgitation.

A number of factors have been reported to influence the accuracy, which include instrument settings, geometric orifice characteristics, blood viscosity, and jet properties such as momentum, velocity, pressure gradient, and eccentricity [18]. The color Doppler images can also be used to measure the width of the narrowest region of the jet, called the vena contracta. The vena contracta is a measure of the effective orifice size, and by assuming a circular geometry, the orifice area can be estimated.

The regurgitant flow volume is another parameter used when grading MR. It can be calculated by multiplying the orifice area with the velocity-time integral, found by either PW Doppler or CW Doppler. Since the velocity-time integral is calculated by taking the envelope of the velocity spectrum, errors may be introduced because of the aforementioned problems.

Another suggestion for quantification of MR is the proximal isovelocity surface area method (PISA) [19]. The method has gain popularity the recent years, and it is now recommended by the echo guidelines [10]. It measures the flow convergence zone proximal to the regurgitant valve, using 2-D color Doppler. By assuming a hemispheric shape of the inflow region, the volume flow rate is predicted. However, the accuracy of the method is controversial, and it has been shown that it underestimates functional MR because of the assumption about circular orifices [20, 21]. An extension of PISA that assumes hemielliptic in addition to hemispheric inflow regions avoids some of these problems [22], but it involves complicated measurements in several image planes.

PW Doppler measurements have also been used directly to measure the regurgitant flow volume. In laminar blood flow, such as the vena contracta, the backscattered power is proportional to the amount of blood passing through the sample volume [23]. This principle was used by Buck *et al.* [24], who measured the flow volume from the power-velocity integral by using a single wide transmit beam and a narrow beam for calibration. Hergum *et al.* [25, 26] extended this principle in the method MULDO, by using the sum of several narrow beams as a composite measurement beam and selecting one of these as a reference beam. A more robust estimate was then achieved, but still with overestimation of small orifices because of the limited spatial resolution, and some underestimation of large orifices as a result of the stochastic nature of the Doppler signals.

Recent technical advances have enabled parallel processing of ultrasound data, which in turn have enabled 3-D imaging. 3-D B-mode imaging was initially anticipated to solve the MR quantification problem, but the images are not yet of sufficient quality for direct planimetry of the regurgitant orifice. 3-D color Doppler images of the regurgitant jet, however, are used for quantification in some clinics today, but the accuracy of the measurements are limited by many of the same factors as mentioned for the 2-D color Doppler methods.

3-D PISA methods with less geometric assumptions than the 2-D methods have recently been developed and tested by several investigators [27, 28]. By directly measuring the area of the isovelocity surface, improved flow rate estimation accuracy has been shown. However, methods that derive PISA from volumetric color Doppler data suffer from the fundamental limitation regarding angle dependence of color Doppler imaging. The 3-D methods must identify the entire curvature of the isovelocity surface, including the most peripheral PISA surface, which may represent a large

Doppler imaging angle [29].

The introduction of parallel processing of data has also improved 2-D imaging. By using broad ultrasound beams on transmit and forming multiple image lines on receive; more information is available per acquisition. This has revolutionized color Doppler imaging, but improvements for spectral Doppler estimation techniques are still preliminary. However, with the possibility of simultaneous acquisition of Doppler signals from a 2-D region, new opportunities arise for both method development and improvement of existing techniques.

1.1 Aims of Study

The overall aim of this study is to develop cardiovascular Doppler methods for more accurate estimation of maximum blood flow velocities and orifice area. All the contributions focus on developing methods that use pulsed wave (PW) Doppler imaging in a combination with parallel receive beams. The two main aims of this study are to improve the accuracy and reproducibility of PW Doppler measurements, and to develop new and more robust methods for assessing the severity of valvular regurgitations.

1. **Improve accuracy and reproducibility of PW Doppler measurements**: A previously published method called velocity matched spectrum [11] has shown reduced spectral broadening for small beam-to-flow angles. By using plane wave transmissions and parallel beamforming, the tracking can be done for a wide range of beam-to-flow angles. By adapting the velocity matched spectrum method for use in a 2-D imaging region, this study aims to:

    - Improve the spectral resolution in PW Doppler for large beam-to-flow angles.
    - Investigate the angle dependency of the new method, and how it can be utilized for velocity calibration.

2. **Develop new and more robust methods for assessing the severity of valvular regurgitations**: By acquiring PW Doppler signals from many parallel beams, both information about the jet velocities and the orifice area is available from a single acquisition, which may give more accurate estimates of the regurgitant volume. By generating multiple simultaneous velocity spectra from parallel beams, this study aims to:

    - Extract qualitative information about the cross-sectional area of the vena contracta in regurgitant jets from PW Doppler measurements.
    - Develop a method for estimating the orifice area, orifice shape and regurgitant volume of mitral regurgitations.

1.2 Thesis Outline

The contributions included in this thesis are summarized in Section 1.4, discussed in Section 1.5 and presented in their complete form in Chapters 2-5. To ease the reading of the contributions, some background on the main topics is provided in the following section. This includes some theory about PW Doppler imaging and the potential errors of the technique when used for maximum velocity estimation. In addition, some background on mitral regurgitation is given, including a short description of some of the most common ultrasound techniques for assessment of this disease.

1.3 Background

1.3.1 Pulsed Wave (PW) Doppler

In medical ultrasound, several Doppler techniques are used for blood flow visualization and measurement. While color Doppler gives an overview of the mean velocities in a large region, PW Doppler and continuous wave (CW) Doppler produce spectral displays showing the velocity distribution in a single sample volume. In Fig 1.1 an example of a color Doppler display (left) and a PW Doppler display (right) is shown. The velocities in the color Doppler image are encoded in colors given by the colorbar in the upper right corner. In the PW Doppler spectrum, the intensity of the Doppler signal for a particular velocity and moment in time is displayed as the brightness at that point on the display. The rest of this section will describe the process of generating such a PW Doppler spectrum, and parts of the Doppler terminology will be explained.

In *PW Doppler*, short ultrasound pulses are transmitted, which allows for depth resolution by calculating the time of flight of the pulse. Generally, the pulses are transmitted in a single direction with a *pulse repetition frequency* (PRF) that allows for the pulse to propagate to the depth of interest and back again, before a new pulse is transmitted. The signal from a PW Doppler recording can be arranged in a 2-D matrix, as illustrated in Fig. 1.2, where the received signal is divided into segments of duration equal to the pulse repetition time (PRT). The vertical axis is called *fast time* and the horizontal axis is called *slow time*, reflecting how frequently the data is sampled in the respective directions. In the figure, a moving satterer is sampled at depth z_1, which results in the low-frequent *slow time signal* shown in the lower part of the figure.

If the blood is moving, the frequency of the backscattered signal will be altered from the transmitted frequency. This change in frequency is a phenomenon called the *Doppler effect*, and it can be used to measure the velocity of the moving scatterers. The Doppler shift, f_D, for a two-way system is given by the following equation:

$$f_D = 2f_0 \frac{v\cos(\theta)}{c} \tag{1.1}$$

[30], where f_0 is the transmitted frequency, c is the sound propagation velocity, v is the velocity of the scatterer and θ is the angle between the velocity direction and the

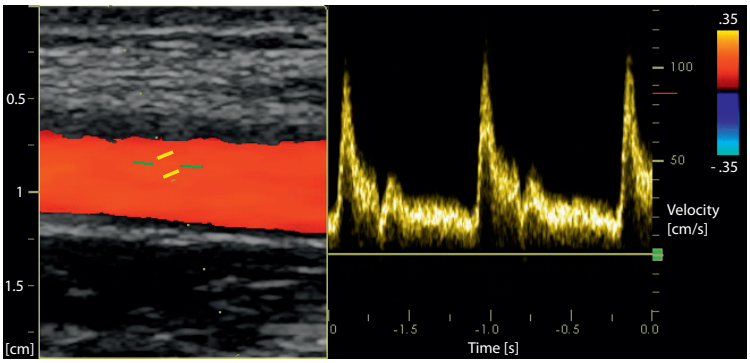

Figure 1.1: Color Doppler imaging (left) and PW Doppler imaging (right) of flow in a carotid artery is demonstrated. A B-mode image of the carotid artery is shown in the background of the color Doppler image. The axial velocities in the color Doppler image are encoded in colors given by the colorbar in the upper right corner. Red color indicates flow towards the transducer and blue color indicates flow away from the transducer. The colorbar has units in cm/s. The PW Doppler spectrogram provides velocity information from a sample volume inside the artery, indicated by the two yellow parallel lines in the color flow image. The green line indicates the direction of the flow compared to the ultrasound beam, which was manually chosen by the examiner. The maximum velocities given by the PW Doppler spectrum are approximately 1 m/s.

ultrasound beam. The equation is valid when $v \cos\theta \ll c$, which is the case for medical ultrasound imaging.

In PW Doppler, the transmitted pulse contains a band of frequencies that is much broader than the Doppler frequency shift. This makes it difficult to extract the Doppler shift by spectral analysis in fast time. However, by sending multiple pulses, the Doppler shift may be extracted after a Fourier transform in slow time. By inserting the resulting Doppler frequencies in (1.1), the velocities of the scatterers are found. In the ultrasound scanner, the Doppler spectrum is continuously updated in a real-time spectral Doppler display with the blood velocity as the vertical axis and time as the horizontal axis.

In Fig. 1.3, the Fourier domain signals of a stationary scatterer (clutter) and a moving scatterer (blood) are illustrated. The 2-D Fourier domain (upper graph) is obtained by a 2-D Fourier transform of the PW Doppler signals in the slow- and fast time directions. The vertical axis gives the frequencies in the received signal, and the horizontal axis gives the Doppler frequencies. A spectrum corresponding to a conventional PW Doppler spectrum (identical to the slow time Fourier transform) is obtained by projecting the 2-D Fourier signals down to the Doppler frequency axis, as illustrated in the lower graph of Fig. 1.3. It can be observed that each frequency in the received signal corresponds to a unique Doppler frequency shift. The signals from the stationary scatterers are usually removed by a high pass filter (clutter filter).

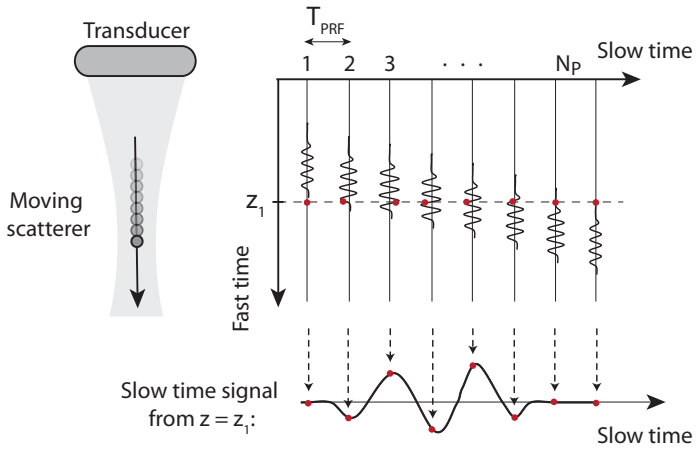

Figure 1.2: Illustration of PW Doppler signals in the slow- and fast time directions. An ultrasound transducer transmits a pulse that is scattered by a moving scatterer at z_1. The slow time signals are sampled at z_1, resulting in the sampled waveform shown in the lower part.

1.3.2 Maximum Velocity Estimation Errors

PW Doppler measurements of the peak systolic velocity are widely used for determining the severity of stenoses in blood vessels. The method is used to determine which patients that need further examinations, but in some institutions, the peak velocity measurement is the only diagnostic technique used prior to surgery [30]. In the heart, maximum velocities are used to calculate the severity of stenosis or of valve leakages. However, errors are frequently introduced in the estimates, which may lead to serious misdiagnosis.

There are several sources of error in maximum velocity estimation. *Spectral broadening* is the primary intrinsic error in the ultrasound system. An infinitely long observation time is needed to measure a velocity accurately. In PW Doppler, a relatively small sample volume is used, which means that for high velocities, the blood will pass rapidly through the sample volume, resulting in a short observation time and broadening of the estimated velocity spectrum. The effect is also called *transit time* broadening, and it causes the measured peak frequency to be higher than the value corresponding to the true peak velocity.

Because of the pulsatile flow profile in the circulatory system, accelerated flow is usually present, which may give rise to an increase in spectral bandwidth. Using a common femoral artery waveform, Bastos et al. [31] showed that for observational windows of very short duration, e.g., 2 ms, broadening will be dominated by the transit time rather than by the effects of acceleration. However, for longer windows, the effects of accelerations become more evident.

Another important source of error is the angle used for velocity calibration. Only

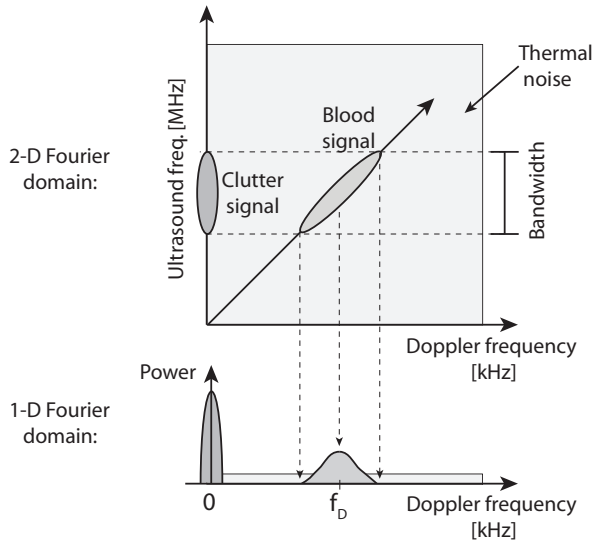

Figure 1.3: Illustration of PW Doppler signals in the Fourier domain. In the 2-D Fourier domain, the blood signal is located along an inclined line that extends through the origin. The clutter signal is located around zero Doppler frequency. The bandwidth of the pulse restricts the signal along the vertical axis. A spectrum corresponding to a conventional PW Doppler spectrum is obtained by projecting the 2-D Fourier signals down to the Doppler frequency axis.

the velocity component in the axial direction is measured by conventional Doppler techniques and the Doppler angle must be found manually by inspecting the ultrasound images. At large beam-to-flow angles (greater than 60°), the apparent Doppler shift is small, and minor errors in angle accuracy can result in large errors in velocity.

Aliasing is an error caused by an insufficient sampling rate in slow time. According to sampling theory, a signal can be reconstructed unambiguously as long as the true frequency (e.g., the Doppler shift) is less than half the sampling rate. Thus, the pulse repetition frequency must be at least twice the maximum Doppler frequency shift encountered in the measurement. The maximum measurable velocity is also called the *Nyquist limit*, and the velocities that exceed this limit are aliased. In a spectral Doppler display, this means that the signals wrap around to negative amplitude as false reversed flow. By applying a baseline-shift, velocities up to twice the Nyquist limit may be resolved, as long as the direction of flow is known. Around twice the Nyquist limit, the clutter filter will remove the signal, and at even higher velocities, the velocity duplicates may get intermixed.

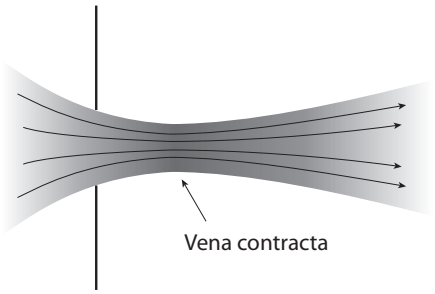

Figure 1.4: Illustration of the vena contracta in a jet flow. The vena contracta is found slightly downstream of the orifice and is the point where the cross-sectional area is at its minimum.

1.3.3 The Mitral Valve and Mitral Regurgitation

The purpose of the heart valves is to direct blood flow in one direction through the heart, passing oxygenated blood to the body, and deoxygenated blood to the lungs. For different reasons the valves may not close properly, causing a backflow (regurgitation) of blood through the valve when it is supposed to be closed. Large regurgitations will eventually cause heart failure, dyspnea and there may be an increased risk of mortality. *Mitral regurgitation (MR)* is one of the most common forms of valvular heart disease.

The *mitral valve* is situated between the left ventricle and the left atrium and it consist of two leaflets that together are typically 4-6 cm^2 in area. It is common to distinct whether MR is caused by abnormalities in the valve itself (organic MR) or if it is caused by left ventricular dilation and dysfunction (functional MR). Organic MR, with calcified, thickened or prolapsing leaflets, may have a nearly circular regurgitant orifice. Functional MR, on the other hand, may have a crescent–shaped regurgitant orifice. The mitral regurgitation flow velocity is always high, usually greater than 4 m/s with peak velocities up to 6 or 7 m/s [32]. This is due to the high systolic pressure gradient between the ventricle and atrium.

Clinicians are encouraged to use several methods when assessing the severity of MR. Both the heart dimensions and function should be evaluated, in addition to several flow parameters, such as flow direction or distribution. The color flow area of the regurgitant jet can be used for diagnosing MR, but the method is not recommended for quantifying the severity [10].

Vena contracta width is a semiquantitative measure of the severity of MR. Vena contracta is the point in a fluid jet where the cross-sectional area of the jet is at its minimum and the fluid velocity is at its maximum. It is found slightly downstream of the orifice, which, for the case of MR is in the left atrium. The flow in this region is laminar and studies suggest that the vena contracta width is relatively independent of hemodynamic variables [33, 34]. An illustration of the vena contracta is shown in Fig. 1.4.

The vena contracta area represents a direct measure of the *effective* regurgitant

orifice area (EROA), which is smaller than the regurgitant orifice area, and it can be estimated by measuring the vena contracta width from a color Doppler recording and assuming a circular geometry. When a measure of the EROA has been obtained, the regurgitant volume, RgV, can be estimated by using the formula:

$$RgV = EROA \cdot VTI \tag{1.2}$$

[35], where VTI is the velocity time integral of the MR jet found from a CW Doppler recording.

A quantitative method for evaluation of mitral regurgitation is the *proximal isovelocity surface area* (PISA) method. It is based on the principle that when fluid passes through a small circular orifice, there is flow acceleration just proximal to the orifice (flow convergence zone). The flow converges towards the orifice in hemispheric layers of equal velocity. By measuring the radius of one of these hemispheres (called the PISA radius), the severity of the regurgitation can be estimated. In general, a small PISA radius corresponds to a mild regurgitation, and a large PISA radius corresponds to a severe regurgitation.

In practice, the PISA radius is measured from a color Doppler recording by adjusting the PRF so that the aliasing velocity forms a hemispheric shape in the color Doppler display. From the PISA radius, the instantaneous regurgitant flow (RgF) can be calculated as

$$RgF = 2\pi \cdot r^2 \cdot v_a \ , \tag{1.3}$$

where r is the PISA radius of the convergence zone and v_a is the aliasing velocity. Note that the error is squared if the radius is measured incorrectly. By also performing a CW Doppler measurement, it is possible to estimate the effective regurgitant orifice area (EROA) and the regurgitant volume. The EROA is calculated by dividing the instantaneous regurgitant flow with the peak velocity of the regurgitant jet, assesed by CW Doppler. The regurgitant volume can then be obtain by (1.2), where the velocity-time integral is obtained from the CW Doppler recording.

In order to find the mechanism of the MR, a more detailed examination of the valve can be performed by transesophageal echocardiography, which involves passing a small ultrasound probe into the patient's esophagus (down the throat). The probe is then located closer to the heart than for transthoracic echocardiography (standard echocardiography), and a higher ultrasound frequency can be used, which results in an increased image quality.

1.4 Summary of Contributions

Two main studies are presented in the contributions. The 2-D tracking Doppler method is developed in Chapter 2 and is further investigated in Chapter 3. Methods for quantifying mitral regurgitation are investigated in Chapters 4 and 5. In the following, a summary of the two studies are given, presenting the motivation and the main results.

1.4.1 2-D Tracking Doppler (Chapters 2 and 3)

Pulsed wave (PW) Doppler is an important tool in cardiovascular diagnostics, and it can be used when estimating the maximum velocities at stenoses or valve leakages. However, errors are frequently introduced in the estimates because of spectral broadening and incorrect choice of the beam-to-flow angle. Errors from both effects become worse with larger beam-to-flow angles.

To increase the robustness of maximum velocity estimation, we have developed a new spectral estimation technique called 2-D tracking Doppler, based on an algorithm first described by Torp and Kristoffersen[11]. Whereas conventional PW Doppler algorithms sample the scatterer movement over time from a fixed position, the proposed algorithm samples at varying positions in space, resulting in an increased observation time and decreased spectral broadening. In the initial version of the technique, tracking of the blood scatterers was done in the axial direction, improving the spectral resolution for small beam-to-flow angles. In this work the method has been adapted for tracking blood with any beam to-flow angle, by utilizing plane wave transmission and parallel beamforming.

In the proposed method, the Doppler signal is resampled in the flow direction from a 2-D region. Several slow-time instances of the resampled signal are further summed along straight lines in a domain spanned by space and slow-time, where summation along different angles contribute to the power in different velocity cells of the power spectrum.

The new method was tested using simulations, *in vitro* ultrasound recordings from a flow phantom, and *in vivo* recordings from the human carotid artery. The resulting 2-D tracking Doppler spectra showed reduced spectral broadening and increased signal-noise-ratio (SNR) compared with Doppler spectra generated by a conventional PW Doppler method. A signal model was derived and the expected Doppler power spectra were calculated, showing good agreement with both simulations and experimental data. Improved spectral resolution was shown especially for large beam-to-flow angles.

Experiments were performed to investigate how the 2-D tracking Doppler method depends on the tracking angle. Results from both simulations and *in vitro* and *in vivo* recordings showed that the spectra broaden when using an erroneous tracking angle. Using the signal model, it was shown that the spectra have lowest bandwidth and maximum power when the tracking angle is equal to the beam-to-flow angle. The findings resulted in two proposals for velocity calibration, where the minimum full width at half maximum (FWHM) or the maximum power of the 2-D tracking Doppler spectra is used to predict the Doppler angle. The techniques were tested using *in vitro* recordings of flow in a straight tube, at beam-to-flow angles at 63°, 73° and 83°. It was shown that the velocity calibration errors may be lower for the FWHM method than for a conventional PW Doppler approach, and especially for large beam-to-flow angles.

With an *in vivo* example it was demonstrated that the 2-D tracking Doppler method is suited for measurements in a patient with carotid stenosis.

Two papers are concerned with this topic: "2-D Tracking Doppler: A New Method

to Limit Spectral Broadening in Pulsed Wave Doppler"*, which was a joint work with Ingvild Kinn Ekroll, and* "Investigations of Spectral Resolution and Angle Dependency in a 2-D Tracking Doppler Method"*, which was a joint work with Jørgen Avdal.*

1.4.2 Quantification of Mitral Regurgitation (Chapters 4 and 5)

Estimating the size of mitral regurgitation (MR) is crucial to identify which people are in need of surgery, but the existing methods are complex and have limitations. Therefore, new methods to quantify the regurgitation are needed.

We have investigated how parallel beamforming applied in a PW Doppler mode can improve the diagnosis of MR. By using a plane wave on transmit, it was possible to have a continuous acquisition for the Doppler processing. This gave us the same resolution in time as conventional pulsed wave (PW) Doppler, with the added benefit of the lateral resolution provided by the multiple receive beams. Using a matrix array transducer, these receive beams could cover a three dimensional region in space, enabling the estimation of Doppler spectra from a grid of beams spread across the MR orifice. A high pulse repetition frequency allowed us to isolate the backscattered Doppler power from the core of the high-velocity regurgitant jet.

We have proposed a qualitative method where multiple simultaneous velocity spectra are generated from parallel receive beams and combined into an enhanced velocity spectrum. This composite velocity spectrum has colors representing the number of beams intersecting the jet. The algorithm for determining the color of each velocity bin is based on power thresholding. The method was validated using simulations of flow in a straight tube, and in one individual with MR. It successfully generated velocity spectra that contained information about the lateral extent of high velocity flow, both from the simulations and from the *in vivo* recording. Hence, the spectra gave information about the size of regurgitant jets, in addition to all the information the cardiologist is used to get from a pulsed wave Doppler recording.

Another proposal in this thesis is a quantitative method where the signal from the receive beams are interpolated in space using 2-D spline interpolation and velocity spectra are generated from each of the interpolated beams. A single spectrum is displayed, and a velocity-time region that only includes the high velocities of the jet is manually chosen from the spectrum. The signal from the vena contracta is then isolated and the cross-sectional area can be displayed as a 2-D image. The size of the area is found by first averaging the chosen region in the velocity and time directions, and then thresholding the resulting power in each of the interpolated beams. The regurgitant volume is found by estimating the velocity-time-integral and multiplying with the estimated area.

The method was optimized and tested using simulations. A flat transmit beam at the depth of interest (10 cm), was searched for, to ensure consistent estimation results for different jet sizes and locations. The transmit beam found best suited for the method was a diverging beam with an opening angle of 6° and with transmit apodization using a Tukey window with taper ratios of 45% and 5% in the azimuth and elevation directions respectively. To further optimize the method, we investigated

the effects of different numbers of receive beams and the density of which they are sampled. With 16 receive beams, the regurgitant volume estimates depended on the position of the jet and gave biased results for small regurgitations, while 64 beams gave sufficiently increased accuracy and robustness.

The simulation results from the MR estimation tests showed that the method provides accurate estimates of the regurgitant volume when using the optimal parameters. From the cross-sectional power Doppler images of the regurgitation, information about both the cross-sectional area and shape could be extracted. Since the velocity-time integral and the orifice area are extracted from a single recording, the proposed method may give more robust flow volume estimates than methods where the velocities and the area are measured from two separate recordings.

This work is described in two papers: "Quantification of Mitral Regurgitation Using PW Doppler and Parallel Beamforming" *and* "Regurgitant Volume Quantification Using 3-D Pulsed Wave Doppler". *The former is based on a proceeding published in the 2011 IEEE International Ultrasonics Symposium Proceedings.*

1.5 Discussion

This thesis has mainly been concerned with two topics in cardiovascular imaging; the general improvement of spectral velocity analysis, and the quantification of valvular regurgitation. In both studies we have combined PW Doppler with parallel beamforming, and hence, increased the information available for each transmitted ultrasound beam.

1.5.1 2-D Tracking Doppler

A new technique for generating angle corrected velocity spectra with reduced spectral broadening has been developed. The results showed that the method could provide velocity spectra with increased velocity resolution, especially for large beam-to-flow angles, and also give information about the Doppler angle. By tracking the blood scatterers along straight lines in a 2-D region, the observation time was increased and the spectral broadening due to the transit time effect was reduced.

The new technique is based on a previously published method [11], that produces velocity spectra with reduced spectral broadening. By tracking the scatterers along the direction of the flow, the transit time was increased, giving a better velocity resolution in the spectrum. A similar approach was taken by K. Ferrara in "Wideband maximum likelihood velocity estimation" [36], and by Alam and Parker in the "butterfly search" technique [12]. However, these methods do not provide a spectrum display, and are not suited for maximum velocity estimation. All these approaches are limited to track along the direction of the beam, resulting in improved performance for small beam-to-flow angles only. By using plane transmit waves and parallel receive beams we have extended this principle to spectral velocity estimation at any beam-to-flow angle.

The 2-D tracking Doppler method was investigated for varying tracking angles using simulations, *in vitro* and *in vivo* experiments, focusing on situations with large beam-to-flow angles, where limitations in velocity estimation and calibration are most evident. It was shown that when applied to the same data, the 2-D tracking Doppler method reduced spectral broadening and increased the signal-noise-ratio (SNR) compared with a conventional spectral estimation technique. The increased SNR can be explained by the statistical properties of the blood signal compared with the noise signal. Along trajectories where the velocity is constant, the signal will match in phase when summed, whereas the contribution from noise will not.

2-D tracking Doppler spectra were calculated using an extended version of the signal model used in [11]. The extended model takes the correlation between the signals from multiple receive beams into account, and includes thermal noise and clutter filtering. A uniform, constant and in-plane flow was assumed. The predicted spectra therefore describe an ideal situation where the flow direction is in the imaging plane and no velocity gradients are present. Any out-of-plane movement would shorten the tracking length; hence broaden the main lobe of the power spectrum. Also, an infinitely large plane wave is assumed in the model, and no edge effects are therefore present. However, the predicted spectra corresponded well with both the *in vitro* results and the spectra generated from Field II simulations.

The tracking trajectory was in the first part of this study determined from a B-mode image of the geometry and chosen as a straight line. As for conventional spectral Doppler techniques, determining the beam-to-flow angle may be problematic when the flow field is complex and does not follow the flow boundaries. Estimating the correct beam-to-flow angle is especially important when calibrating velocity spectra at large beam-to-flow angles, as the angle correction factor tends to infinity as the beam-to-flow angle approaches 90°. We used the signal model to investigate how the 2-D tracking Doppler spectra changes when the tracking angle is chosen different from the beam-to-flow angle. It was shown that the spectra broaden when the incorrect angle is chosen and that the spectra have lowest bandwidth and maximum power when the tracking angle is equal to the beam-to-flow angle. This may facilitate new techniques for velocity calibration, either automatically or manually by e.g. adjustment of the tracking angle, while observing the effect on the spectral display.

Angle estimation by the minimum FWHM and the maximum power was tested and analyzed using repeated measurements of *in vitro* flow. The estimated angles by the minimum FWHM had a bias of less than 4.4% for all the investigated beam-to-flow angles. Angles measured from B-mode images were used as a ground truth in the analysis, and a possible inaccuracy in these measurements could explain the calculated bias in the angle estimates. The velocity calibration errors corresponding to the angles estimated from the minimum FWHM were compared with the maximum velocity errors expected when using a conventional PW Doppler method. The maximum velocity errors of the conventional method increase rapidly for large beam-to-flow angles, whereas the estimated velocity calibration errors of the 2-D tracking Doppler method had a standard deviation of less than 6% for all the investigated angles (63°, 73° and 83°). This indicates that the 2-D tracking Doppler method may be used for automatic angle correction of velocity spectra, providing more robust velocity

estimates than a conventional approach, for large beam-to-flow angles.

A challenge *in vivo* is that spatial velocity gradients in the tracking direction and surrounding low velocities may broaden the spectra. However, in many applications the primary interest is the quantification of maximum velocities, for instance in cases of valvular insufficiency or in stenotic regions, where the high velocity flow can be distinguished from the low velocities in the spectra. In this work, the technique was tested for *in vivo* recordings of the carotid artery; in one healthy volunteer and in one patient with carotid stenosis. For both scenarios, the 2-D tracking Doppler method gave better velocity resolution than the conventional PW Doppler method. For the case with the stenosis, the velocity-time waveform was also easier to delineate in the 2-D tracking Doppler spectrum because of clutter that was overlapping with the high velocities in the conventional spectrum. This ability of the tracking technique to resolve the velocity ambiguity problem, when the maximum velocity is beyond the Nyquist limit, has earlier been shown for normal blood flow in the aorta in the axial direction [11].

To limit spectral broadening of the velocity spectra, the flow has to be constant for a certain length. Curved flow fields, accelerated flow and turbulent flow were not considered in this work, all of which may limit the useful tracking length. In this work, the tracking length was set between 1 and 2 cm (at the highest velocities), which might be longer than the distance of constant flow in more complex flow fields. Spectral broadening because of a limited tracking length might reduce the angle sensitivity of the 2-D tracking Doppler technique. Also, flow direction may vary through the heart cycle, and in regions of complex flow the accuracy of the angle estimation may be limited. However, in the most challenging cases, these effects will also limit the quality of conventional PW Doppler in a similar way.

The combination of an increased spectral resolution and more robust velocity calibration for large beam-to-flow angles may give both challenges and opportunities in vascular imaging. Most importantly, the increased robustness for large beam-to-flow angles may facilitate reliable velocity estimation for angles above 60°. This can improve blood velocity estimation in regions with near-transversal flow, for instance in vascular imaging or when imaging the heart from a parasternal view. However, as the 2-D tracking method produces narrower spectra, and hence might give lower maximum velocity estimates than conventional approaches, introducing the method in the clinics could result in a need for revision of the guidelines for thresholds and treatment.

1.5.2 Quantification of Mitral Regurgitation

Methods for assessing the severity of valvular regurgitations, and mitral regurgitation (MR) in particular, have been developed. The aim was to develop robust methods that are less user-dependent and faster to perform than the methods used in the clinics today. The standard diagnostic imaging procedures include an integrated assessment of several parameters using multiple imaging modalities. Both qualitative and quantitative methods are used, but most are dependent on scanner settings and on geometric assumptions. This makes the procedures both time-consuming and largely

dependent on the skills of the sonographer.

Two methods for evaluation of valvular regurgitation were developed in this work, both combining PW Doppler imaging with parallel receive beamforming. They were both successful in providing information about the jet size from a single PW Doppler recording. Using a single broad beam on transmit and parallel beams on receive; a continuous acquisition was achieved, which allowed for a regular PW Doppler processing of the received signals. As only the beams intersecting the jet contain high velocity signals, the PW spectra generated from the parallel beams included spatial information of the jet.

Both methods are based on thresholding. The threshold was chosen to a value some decibels below the maximum intensity of the dataset. This may lead to underestimations of some regurgitations because of statistical fluctuations of the Doppler signals. A threshold that is independent of the maximum intensity should therefore be considered.

A high pulse repetition frequency (HPRF) was used to acquire the high velocity Doppler signals from the regurgitant jets. With HPRF acquisition several pulses are transmitted before the deep echoes from the first pulse has returned to the probe, meaning that the received echoes from multiple sample volumes along the beam are mixed together. This range ambiguity introduced by HPRF acquisition is not important for measuring the velocity of regurgitant jets, as the signals received from the ambiguous sample volumes are removed by a clutter filter as long as the beam only intersects one jet. This is usually the case for transthoractic imaging.

The first proposed method was semi-quantitative, giving information about the jet size by color coding the PW Doppler spectrum. Since PW Doppler measurements are part of the standard procedures when evaluating MR, the proposed method added information to the images without adding additional time or effort for the examiner.

Colored spectra generated from simulations of flow in straight tubes were successful in differentiating between small, medium and large tubes. However, a 2-D probe was used in the simulations, meaning that the receive beams were located in a 1-D line across the flow, limiting the information available about jet size and geometry. The method was also implemented on a scanner with a 3-D probe, and tested on a patient with mitral regurgitation. The scanner available for testing could produce a maximum of 16 parallel receive beams, which restricted the field of view and the density of the receive beams. The resulting spectrum contained colors that seemed reasonable, as the low velocity clutter was colored in a color representing a large area, and the high velocities were colored in a color representing a smaller area. However, it was later found that the number of parallel receive beams used in this study is not adequate for accurately estimating the jet size.

The second proposed method was a quantitative method that estimates the regurgitant volume, produces a cross-sectional power Doppler image of the vena contracta and generates a velocity spectrum from a single PW Doppler recording. By displaying the cross-sectional power Doppler image, the shape and size of the regurgitant orifice may be found. The cross-sectional power Doppler image may also be used as a tool when searching for the jet and positioning the probe. By multiplying the cross-sectional area of the vena contracta with the velocity-time integral, angle-

independent estimates of the flow volume is achieved. As the cross-sectional area and the velocity-time integral are estimated from the exact same position, the volume estimates may be more robust than estimates done using two separate recordings.

Different beam configurations were tested by simulating the beam profiles and the received Doppler signal. Especially the receive beam number and density was investigated, and it was shown that 16 parallel receive beams are inadequate when estimating the regurgitant volume. Large variations in the two-way intensity profile was found when using 4x4 parallel receive beams, which may be a result of the limited beams available for the interpolation algorithm. Using 4x4 parallel receive beams, a beam spacing of 0.9 times the Rayleigh criterion was needed to cover an area of 1x1 cm. In theory, the beam spacing given by the Rayleigh criterion should be enough to fully reconstruct the signals from any intermediate beams through interpolation. However, Rayleigh beam spacing resulted in large intensity variations in the two-way beam profiles, also for 64 receive beams. A diverging transmit beam and 64 receive beams, sampled with a beam spacing of half the Rayleigh criterion was suggested as the configuration best suited for the method.

The proposed method makes no assumptions about the geometry of the orifices, and it should be possible to measure the area of multiple jets, eccentric jets and asymmetric jets as long as they can fit inside the measurement area. For orifices extending beyond the measurement area, the volume estimates will be underestimated. A measurement area of approximately 1x1 cm was used in this work, but by using more receive beams and a broader transmit beam, the area may be extended. A broader transmit beam, however, will result in lower signal-noise-ratio, which might be a challenge when measuring at the depth of the mitral valve.

The method should be tested *in vivo* when a sufficient amount of parallel receive beams is available. Some challenges are expected *in vivo* because of more complex flow patterns, such as velocity gradients and turbulent flow. Because of the random nature of Doppler signals from blood, a lot of averaging in time is required, which could be a challenge if the regurgitation is only present during a short time interval, or if the vena contracta moves from frame to frame. However, should the method prove to give valid estimates *in vivo*, it could be an important tool when evaluating MR.

1.6 Concluding Remarks

Maximum velocity estimates are frequently used when diagnosing cardiovascular diseases. We have developed new Doppler methods to increase the accuracy and robustness of such estimates.

To limit spectral broadening, we have created a method called 2-D tracking Doppler, that increase the effective observation time of the scatterers by incorporating information from several parallel receive beams. Spectra with improved resolution and signal-to-noise ratio were produced using simulations, and *in vitro* and *in vivo* recordings for a large span of beam-to-flow angles. A signal model was derived and the expected Doppler power spectra were calculated, showing good agreement with experimental data. It was shown that the spectra have lowest bandwidth and

maximum power when the tracking angle is equal to the beam-to-flow angle. This may facilitate new techniques for velocity calibration.

The increased resolution and robustness of the velocity estimates for large beam-to-flow angles may facilitate velocity estimation above 60°; hence improve blood velocity estimation in regions with near-transversal flow. Regions of accelerated or disturbed flow may still present a challenge; however, it was demonstrated significant improvement in spectral resolution for flow in a stenotic carotid artery. For the same case, it was shown that the 2-D tracking Doppler technique resolves the velocity ambiguity problem that results from aliasing. This is the first time that this has been demonstrated for such a complex flow pattern.

A new technique for estimating the size of regurgitant jets, using spectral Doppler and parallel beamforming, has been proposed. By estimating both the velocity-time-integral and the orifice area from a single pulsed wave recording, robust estimates of the regurgitant flow volume may be achieved. A simulation study was performed to test and optimize the new method, suggesting a feasible setup for the transmit and receive beams. 2-D images of simulated regurgitations of varying sizes were generated and the cross sectional areas of the regurgitations were accurately estimated. In further studies, the method should be implemented on a scanner and validated in an *in vitro* study. The technique should then be tested on patients with mitral regurgitation, comparing the regurgitant volume estimates with estimates from existing quantitative methods, such as PISA or the vena contracta width.

1.7 List of Publications

In addition to published and unpublished manuscripts included in this thesis, written and oral contributions have been made to national and international conferences. A list of the material to which the candidate has been a contributor is included in the following.

Papers included in the thesis

1. **Tonje Dobrowen Fredriksen**, Ingvild Kinn Ekroll, Lasse Løvstakken and Hans Torp, "2-D Tracking Doppler: A New Method to Limit Spectral Broadening in Pulsed Wave Doppler", *IEEE Transactions on Ultrasonics, Ferroelectrics and Frequency Control*, vol. 60, no. 9, pp. 1896-1905, 2013.

2. **Tonje Dobrowen Fredriksen**, Jørgen Avdal, Ingvild Kinn Ekroll, Torbjørn Dahl, Lasse Løvstakken and Hans Torp, "Investigations of Spectral Resolution and Angle Dependency in a 2-D Tracking Doppler Method", *IEEE Transactions on Ultrasonics, Ferroelectrics and Frequency Control*, vol. 61, no. 7, pp. 1161-1170, 2014.

3. **Tonje Dobrowen Fredriksen**, Hans Torp and Torbjørn Hergum, "Quantification of Mitral Regurgitation Using PW Doppler and Parallel Beamforming", based on a conference proceeding published in *2011 IEEE International Ultrasonics Symposium Proceedings*.

4. **Tonje Dobrowen Fredriksen**, Bjørn Olav Haugen and Hans Torp, "Regurgitant Volume Quantification Using 3-D Pulsed Wave Doppler".

Additional conference presentations, posters and proceedings

1. **Tonje Dobrowen Fredriksen**, Torbjørn Hergum and Hans Torp, "3D Cardiac Doppler – Flow Phantoms", Poster at *The Joint National PhD conference in Medical Imaging and the Annual MedViz conference, 2011*

2. **Tonje Dobrowen Fredriksen**, "3D Cardiac Doppler - Developing real-time 3D echocardiographic Doppler methods for qualitative and quantitative evaluation of valvular regurgitation", Presentation at *The Artimino Conference on Medical Ultrasound Technology, 2011*

3. **Tonje Dobrowen Fredriksen**, Hans Torp and Torbjørn Hergum, "Quantification of Mitral Regurgitation Using PW Doppler and Parallel Beamforming", Poster and proceeding at *The 2011 IEEE International Ultrasonics Symposium*

4. **Tonje Dobrowen Fredriksen**, Ingvild Kinn Ekroll, Lasse Løvstakken and Hans Torp, "2D Tracking Doppler: A New Method to Limit Spectral Broadening in Pulsed Wave Doppler", Poster and proceeding at *The 2012 IEEE International Ultrasonics Symposium* and poster at *The 4th National PhD Conference in Medical Imaging, 2012*

5. **Tonje Dobrowen Fredriksen**, Ingvild Kinn Ekroll, Lasse Løvstakken and Hans Torp, " Increasing the Transit Time in PW Doppler using Plane Waves on Transmit and Parallel Beams on Receive", Poster at *The 5th National PhD Conference in Medical Imaging, 2013*

References

[1] S. Satomura, "Ultrasonic Doppler method for the inspection of cardiac functions," *J. Acoust. Soc. Am*, vol. 29, no. 11, pp. 1181–1957, 1957.

[2] S. Satomura, "Study of the Flow Patterns in Peripheral Arteries by Ultrasonics," *J. Acoust. Soc. Jpn*, 1959.

[3] D. Franklin, W. Schlegal, and R. Rushmer, "Blood flow measured by Doppler frequency shift of backscattered ultrasound," *Science*, vol. 132, no. 3478, pp. 564–565, 1961.

[4] J. Holen, R. Aaslid, K. Landmark, and S. Simonsen, "Determination of Pressure Gradient in Mitral Stenosis with a Non-invasive Ultrasound Doppler Technique," *Acta Medica Scandinavica*, vol. 199, no. 1-6, pp. 455–460, 1976.

[5] B. A. J. Angelsen and A. O. Brubakk, "Transcutaneous measurement of blood flow velocity in the human aorta," *Cardiovascular Research*, vol. 10, no. 3, pp. 368–379, 1976.

[6] L. Hatle, A. Brubakk, A. Tromsdal, and B. Angelsen, "Noninvasive assessment of pressure drop in mitral stenosis by Doppler ultrasound.," *British heart journal*, vol. 40, pp. 131–40, Mar. 1978.

[7] L. Hatle, B. Angelsen, and A. Tromsdal, "Noninvasive assessment of atrioventricular pressure half-time by Doppler ultrasound," *Circulation*, vol. 60, pp. 1096–1104, Nov. 1979.

[8] R. B. Stamm and R. P. Martin, "Quantification of pressure gradients across stenotic valves by Doppler ultrasound," *Journal of the American College of Cardiology*, vol. 2, pp. 707–718, Oct. 1983.

[9] E. G. Grant, C. B. Benson, G. L. Moneta, A. V. Alexandrov, J. D. Baker, E. I. Bluth, B. a. Carroll, M. Eliasziw, J. Gocke, B. S. Hertzberg, S. Katanick, L. Needleman, J. Pellerito, J. F. Polak, K. S. Rholl, D. L. Wooster, and R. E. Zierler, "Carotid artery stenosis: gray-scale and Doppler US diagnosis–Society of Radiologists in Ultrasound Consensus Conference.," *Radiology*, vol. 229, pp. 340–6, Nov. 2003.

[10] P. Lancellotti, L. Moura, L. A. Pierard, E. Agricola, B. A. Popescu, C. Tribouilloy, A. Hagendorff, J.-L. Monin, L. Badano, and J. L. Zamorano, "European Association of Echocardiography recommendations for the assessment of valvular regurgitation. Part 2: mitral and tricuspid regurgitation (native valve disease).," *European journal of echocardiography : the journal of the Working Group on Echocardiography of the European Society of Cardiology*, vol. 11, pp. 307–32, May 2010.

[11] H. Torp and K. Kristoffersen, "Velocity matched spectrum analysis: A new method for suppressing velocity ambiguity in pulsed-wave Doppler," *Ultrasound in medicine & biology*, vol. 21, no. 7, pp. 937–944, 1995.

[12] S. Alam and K. Parker, "The butterfly search technique for estimation of blood velocity," *Ultrasound in medicine & biology*, vol. 21, no. 5, pp. 657–670, 1995.

[13] B. Dunmire, K. W. Beach, K. Labs, M. Plett, and D. E. Strandness, "Cross-beam vector Doppler ultrasound for angle-independent velocity measurements.," *Ultrasound in medicine & biology*, vol. 26, pp. 1213–35, Oct. 2000.

[14] J. Kortbek and J. A. Jensen, "Estimation of velocity vector angles using the directional cross-correlation method.," *IEEE transactions on ultrasonics, ferroelectrics, and frequency control*, vol. 53, pp. 2036–49, Nov. 2006.

[15] J. Jensen and N. Oddershede, "Estimation of velocity vectors in synthetic aperture ultrasound imaging," *Imaging, IEEE Transactions on*, vol. 25, no. 12, pp. 1637–1644, 2006.

[16] M. Enriquez-Sarano, J.-F. Avierinos, D. Messika-Zeitoun, D. Detaint, M. Capps, V. Nkomo, C. Scott, H. V. Schaff, and A. J. Tajik, "Quantitative determinants of the outcome of asymptomatic mitral regurgitation.," *The New England journal of medicine*, vol. 352, pp. 875–83, Mar. 2005.

[17] M. Enriquez-Sarano, C. W. Akins, and A. Vahanian, "Mitral regurgitation.," *Lancet*, vol. 373, pp. 1382–94, Apr. 2009.

[18] B. A. Lin, A. S. Forouhar, N. M. Pahlevan, C. A. Anastassiou, P. A. Grayburn, J. D. Thomas, and M. Gharib, "Color Doppler jet area overestimates regurgitant volume when multiple jets are present.," *Journal of the American Society of Echocardiography: official publication of the American Society of Echocardiography*, vol. 23, pp. 993–1000, Sept. 2010.

[19] F. Recusani, G. S. Bargiggia, A. P. Yoganathan, A. Raisaro, L. M. Valdes-Cruz, H. W. Sung, C. Bertucci, M. Gallati, V. A. Moises, and I. A. Simpson, "A new method for quantification of regurgitant flow rate using color Doppler flow imaging of the flow convergence region proximal to a discrete orifice. An in vitro study," *Circulation*, vol. 83, pp. 594–604, Feb. 1991.

[20] Y. Matsumura, S. Fukuda, H. Tran, N. L. Greenberg, D. A. Agler, N. Wada, M. Toyono, J. D. Thomas, and T. Shiota, "Geometry of the proximal isovelocity surface area in mitral regurgitation by 3-dimensional color Doppler echocardiography: difference between functional mitral regurgitation and prolapse regurgitation.," *American heart journal*, vol. 155, pp. 231–8, Feb. 2008.

[21] P. Kahlert, B. Plicht, I. M. Schenk, R.-A. Janosi, R. Erbel, and T. Buck, "Direct assessment of size and shape of noncircular vena contracta area in functional versus organic mitral regurgitation using real-time three-dimensional echocardiography.," *Journal of the American Society of Echocardiography: official publication of the American Society of Echocardiography*, vol. 21, pp. 912–21, Aug. 2008.

[22] C. Yosefy, R. A. Levine, J. Solis, M. Vaturi, M. D. Handschumacher, and J. Hung, "Proximal flow convergence region as assessed by real-time 3-dimensional echocardiography: challenging the hemispheric assumption.," *Journal of the American Society of Echocardiography : official publication of the American Society of Echocardiography*, vol. 20, pp. 389–96, Apr. 2007.

[23] B. A. J. Angelsen, "A theoretical study of the scattering of ultrasound from blood.," *IEEE transactions on bio-medical engineering*, vol. 27, pp. 61–7, Feb. 1980.

[24] T. Buck, R. A. Mucci, J. L. Guerrero, G. Holmvang, M. D. Handschumacher, and R. A. Levine, "The Power-Velocity Integral at the Vena Contracta: A New Method for Direct Quantification of Regurgitant Volume Flow," *Circulation*, vol. 102, pp. 1053–1061, Aug. 2000.

[25] T. Hergum, T. R. Skaug, K. Matre, and H. Torp, "Quantification of valvular regurgitation area and geometry using HPRF 3-D Doppler.," *IEEE transactions on ultrasonics, ferroelectrics, and frequency control*, vol. 56, pp. 975–82, May 2009.

[26] T. R. Skaug, T. Hergum, B. H. Amundsen, T. Skjaerpe, H. Torp, and B. O. Haugen, "Quantification of mitral regurgitation using high pulse repetition frequency three-dimensional color Doppler.," *Journal of the American Society of Echocardiography : official publication of the American Society of Echocardiography*, vol. 23, pp. 1–8, Jan. 2010.

[27] J. A. de Agustín, P. Marcos-Alberca, C. Fernandez-Golfin, A. Gonçalves, G. Feltes, I. J. Nuñez Gil, C. Almeria, J. L. Rodrigo, L. Perez de Isla, C. Macaya, and J. Zamorano, "Direct Measurement of Proximal Isovelocity Surface Area by Single-Beat Three-Dimensional Color Doppler Echocardiography in Mitral Regurgitation: A Validation Study.," *Journal of the American Society of Echocardiography : official publication of the American Society of Echocardiography*, pp. 815–823, June 2012.

[28] P. Thavendiranathan, S. Liu, S. Datta, S. Rajagopalan, T. Ryan, S. R. Igo, M. S. Jackson, S. H. Little, N. De Michelis, and M. A. Vannan, "Quantification of chronic functional mitral regurgitation by automated 3-dimensional peak and integrated proximal isovelocity surface area and stroke volume techniques using real-time 3-dimensional volume color Doppler echocardiography: in vitro and clini," *Circulation. Cardiovascular imaging*, vol. 6, pp. 125–33, Jan. 2013.

[29] S. H. Little, "Is it Really Getting Easier to Assess Mitral Regurgitation Using the Proximal Isovelocity Surface Area?," *Journal of the American Society of Echocardiography : official publication of the American Society of Echocardiography*, vol. 25, pp. 824–6, Aug. 2012.

[30] R. S. C. Cobbold, *Foundations of Biomedical Ultrasound*. Oxford University Press, Inc., 2007.

[31] C. Bastos, P. Fish, and F. Vaz, "Spectrum of Doppler ultrasound signals from nonstationary blood flow," *IEEE transactions on ultrasonics, ferroelectrics, and frequency control*, vol. 46, no. 5, pp. 1201–1217, 1999.

[32] J. K. Oh, R. A. Nishimura, J. B. Seward, and A. J. Tajik, "Differentiation of Aortic Stenosis Jet From Mitral Regurgitation by Analysis of Continuous-Wave Doppler Spectrum: Illustrative Cases," *Echocardiography*, vol. 3, no. 1, pp. 55–60, 1986.

[33] H. Baumgartner, H. Schima, and P. Kühn, "Value and limitations of proximal jet dimensions for the quantitation of valvular regurgitation: an in vitro study using Doppler flow imaging," *Journal of the American Society of Echocardiography*, vol. 4, no. 1, pp. 57–66, 1991.

[34] A. Schmidt, T. da Silva Júnior, A. Pazin-Filho, L. Otávio Murta Júnior, O. César Almeida-Filho, L. Gallo-Júnior, J. Antonio Marin-Neto, and B. Carlos Maciel, "Effects of changing blood viscosity and heart rate on vena contracta width as evaluated by color Doppler flow mapping. An in vitro study with a pulsatile flow model.," *Echocardiography (Mount Kisco, N.Y.)*, vol. 25, pp. 133–40, Feb. 2008.

[35] P. A. Grayburn, N. J. Weissman, and J. L. Zamorano, "Quantitation of Mitral Regurgitation," *Circulation*, vol. 126, pp. 2005–2017, Oct. 2012.

[36] K. W. Ferrara and V. R. Algazi, "A new wideband spread target maximum likelihood estimator for blood velocity estimation. I. Theory.," *IEEE transactions on ultrasonics, ferroelectrics, and frequency control*, vol. 38, pp. 1–16, Jan. 1991.

Chapter 2

2-D Tracking Doppler: A New Method to Limit Spectral Broadening in Pulsed Wave Doppler

Tonje D. Fredriksen, Ingvild K. Ekroll, Lasse Lovstakken, and Hans Torp
Medical Imaging Lab and Deptartment of Circulation and Medical Imaging
Norwegian University of Science and Technology (NTNU)
Trondheim Norway

Transit time broadening is a major limitation in pulsed wave (PW) Doppler, especially when the angle between the flow direction and the ultrasound beam is large. The associated loss in frequency resolution may give severe overestimation of blood velocities, and finer details in the spectral display are lost. By using plane wave transmissions and parallel receive beamforming, multiple PW Doppler signals can be acquired simultaneously in a 2-D region. This enables tracking of the moving blood scatterers over a longer spatial distance to limit transit time broadening.
In this work, the new method was tested using *in vitro* ultrasound recordings from a flow phantom, and *in vivo* recordings from a human carotid artery. The resulting 2-D tracking Doppler spectra showed significantly reduced spectral broadening compared with Doppler spectra generated by the Welch's method. The reduction in spectral broadening was 4-fold when the velocity was 0.82 m/s and the beam-to-flow angle was 62°. A signal model was derived and the expected Doppler power spectra were calculated, showing good agreement with experimental data. Improved spectral resolution was shown for beam-to-flow angles between 40° and 82°.

2.1 Introduction

Pulsed wave (PW) Doppler is an important tool in cardiovascular diagnostics, by which the complete spectrum of blood or tissue velocities is estimated. It is typically displayed as a 2-D sonogram with velocity along the y-axis and time along the x-

axis. The spectral power is displayed in a gray scale. Fundamentally, the spectrum of velocities presented will broaden because of the so-called transit time effect. Even though a uniform velocity field is present, a spectrum of velocities will be estimated and displayed. The transit time is the effective observation time of the blood scatterers in the received signal. The scatterers pass through the insonified volume during a short time interval, and as the velocity increases, the transit time decreases, resulting in more severe spectral broadening for high velocities. This limitation makes it more challenging to delineate the true maximum velocity as a function of time, decreasing diagnostic confidence and making quantitative analysis more challenging and less reproducible. In the context of blood velocity measurements, delineation is particular challenging when high-velocity jets are present, e.g., in stenotic regions. The transit time is usually limited by the pulse length. However, if the beam-to-flow angle is large, the transit time will be given by the beam width. This is illustrated in Fig. 2.1, where PW Doppler spectra from two situations are shown. The beam-to-flow angles are small and large in the left and right image panels, respectively.

There have been many attempts to improve spectrum and mean frequency estimation of Doppler signals, but most techniques base the spectral estimation on samples originating from one spatial position. Recent approaches to increase the spectral resolution in PW Doppler include nonparametric methods previously used in direction-of-arrival estimation, such as the Capon minimum variance estimator [1] and the amplitude and phase estimation (APES) approach [2]. As opposed to the data-independent Welch's method, these two are data-dependent, or data-adaptive, signal processing techniques. The adaptive property is the source of the improved frequency resolution and lower leakage in the resulting spectra [3]. It was recently reported that the observation window in PW Doppler could be reduced using two versions of these estimators; the blood spectral power Capon method (BPC) and the blood spectral amplitude and phase estimation (BAPES) technique [4]. It was also shown in a clinical feasibility study that the methods could work robustly for vascular imaging [5]. However, the transit time presents a fundamental limitation to the gain in spectral resolution when using these techniques [6]. To obtain improved delineation both in low- and high-velocity regions, ways to increase the observation time should be investigated.

A method for generating velocity spectra with reduced spectral broadening, called velocity matched spectrum, has previously been published [7]. By tracking the scatterers along the direction of the flow, the transit time was increased, giving a better velocity resolution in the spectrum. A similar method is the butterfly search technique [8], developed by Alam and Parker. In this method, the complex demodulated signal is sampled on different delay trajectories (butterfly lines) in the slow time-fast time space. If the delay trajectory matches the scatterer movement, all the data samples will have similar values and their variance will be low. To estimate the mean velocity, the butterfly lines on which the variance is minimal are searched for. Both of these methods use focused transmissions and are limited to track along the direction of the beam. They have therefore shown improved performance only for small beam-to-flow angles.

We have now extended the velocity matched spectrum method to allow for

tracking in a 2-D space. An enabling technology for 2-D tracking is parallel receive beamforming, a technique now implemented in most high-end ultrasound imaging systems. This technology allows for the instantaneous acquisition of multiple image lines in 2-D, without affecting the desired pulse repetition frequency (PRF), by using plane wave transmissions. Using this scheme, we can acquire data that makes it possible to follow blood or tissue scatterers in 2-D space over time. Whereas conventional PW Doppler algorithms sample the scatterer movement over time from a fixed position, the proposed algorithm samples at varying positions in space, resulting in an increased observation time and decreased spectral broadening.

A related approach has been described by Jensen and Oddershede [9], in which the mean velocity is estimated in the flow direction. The method is based on synthetic aperture imaging, in which defocused emissions are used to achieve dynamic focusing both on transmit and receive in a 2-D region. Directional beamforming was done in the flow direction, and a cross-correlation technique was used to estimate the flow velocity. In the 2-D tracking Doppler approach, directional beamforming is obtained by interpolating the signal from multiple parallel beams along a line in the flow direction. However, as opposed to Jensen's method, in which the mean velocity is estimated, the 2-D tracking Doppler method produces a Doppler spectrum display.

In this work, plane wave transmissions and parallel receive beams are used to track the blood scatterers from pulse to pulse and to construct a Doppler spectrum display with reduced spectral broadening. The method is tested both *in vitro* and *in vivo*. For evaluation of the method, conventional PW Doppler spectra are estimated and compared with the 2-D tracking Doppler spectra. Although conventional PW Doppler methods usually use focused beams on transmit, we also use the term *conventional* when using Doppler signals acquired from plane wave transmissions. The 2-D tracking Doppler algorithm is described in Section 2.2.1. The signal model presented in Section 2.2.2 is used for simulating the expected velocity spectra. In Section 2.3 the experimental work is described. The results are presented in Section 2.4 and discussed in Section 2.5.

2.2 Methods

The acquisition in the 2-D tracking Doppler method consists of two parts: First the signal is acquired from a 2-D region in space. Then, the signal is resampled along an oblique line in space. To be able to describe the signal before and after resampling, some terminology must be defined: The *fast time* has time steps given by the sampling rate in the axial direction, and is indexed with t. The *slow time* has time steps given by the pulse repetition time (PRT) and is indexed with k. In literature, the term *M-mode* usually refers to data from one scan line as a function of time (slow time). When using the 2-D tracking Doppler method, it is convenient to extend the meaning of the term M-mode to include any line in space as a function of time. M-mode can then refer to a 2-D matrix that has axes given by an oblique line in space and slow time. x and z are spatial coordinates in azimuthal and axial directions, respectively. r is a distance along the direction of the oblique line. In the Fourier domain, the corresponding temporal

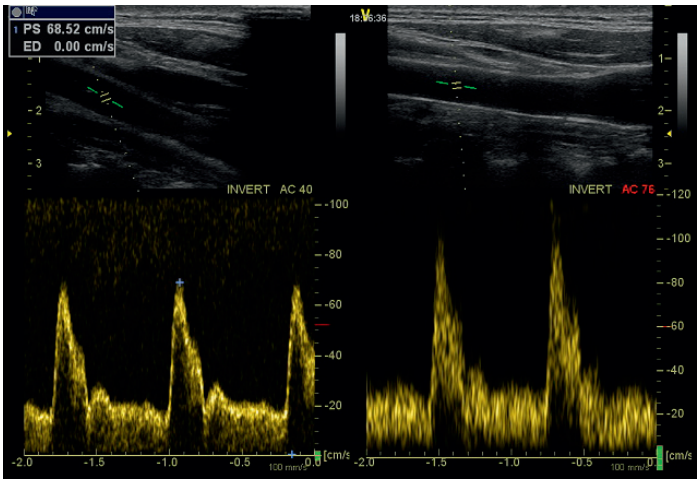

Figure 2.1: Two screenshots from a high-end ultrasound scanner, Vivid E9 (GE Vingmed Ultrasound, Horten, Norway). B-mode images of a carotid artery are shown at the top. PW Doppler spectra are shown at the bottom. The beam-to-flow angle was 40° for the recording to the left, and 76° for the recording to the right. The spectral broadening is prominent in the recording with the largest beam-to-flow angle.

frequency axes are f_z in the axial direction, f_θ along the oblique line, and f_D in slow time.

The new method is based on the properties of the 2-D fast Fourier transform (FFT). Flow estimation based on the 2-D FFT has been discussed by many authors [10–12]. Velocity spectra can be generated by taking the 2-D FFT of the signal in the fast- and slow time directions and integrating along lines of differing slope that pass through the origin [10]. The slope of each line corresponds to one particular velocity and is given by the relation between the Doppler frequency, f_D, and the transmitted frequency, f_z:

$$f_D = \frac{2 f_z v_z}{c} \ ,$$

where v_z is the velocity component of the scatterers in the axial direction and c is the speed of sound. If the flow contains one single velocity, the spectral content of the signal will extend along a line with angle $\phi = \arctan^{-1}(c/(2v_z))$.

It has previously been shown [7] that integration along lines of differing slope in the 2-D FFT is equivalent to summation along lines of differing slope in the fast time-slow time domain. Signal from scatterers with constant velocity that move along the ultrasonic beam will make skewed lines in the fast time-slow time domain. When summation is done along such a skewed line, a peak in the velocity spectrum is observed. Shortened transit time and broadening of the spectrum will occur when the flow is not in the direction of the beam. In this work, we propose a technique in which the scatterers are followed between parallel beams instead of just along one

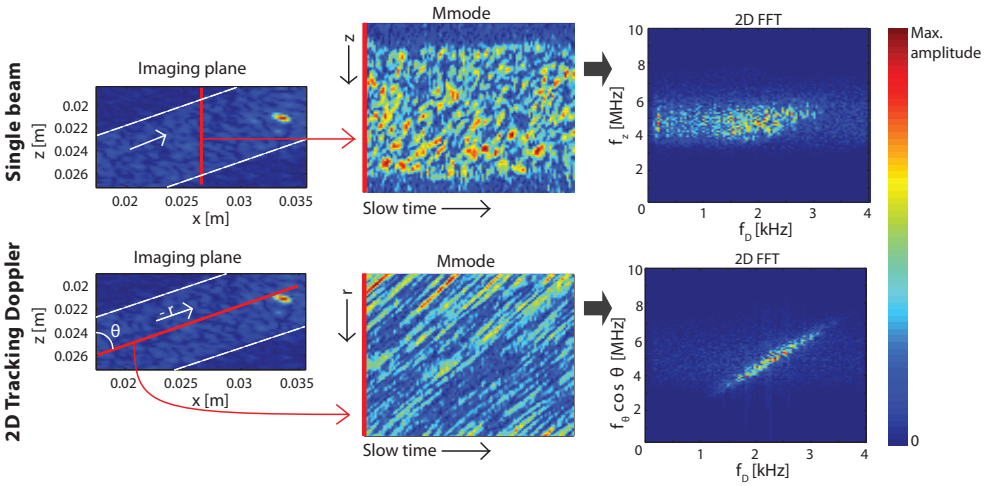

Figure 2.2: Tracking of the scatterers using a single ultrasonic beam is compared with tracking of the scatterers using several parallel beams (2-D tracking Doppler). The beam-to-flow angle, θ, is 62°. The images to the left show the imaging plane. The flow is in the direction of the white arrow. The red line illustrates the tracking trajectory. In the images in the middle, the signal from the red line is displayed as a function of time (M-mode). The signal lines in the 2-D tracking Doppler M-mode are much thinner and extend farther than in the single-beam M-mode. In the images to the right, the complex pre-envelope signal is displayed in the 2-D Fourier domain. They show a signal that is more concentrated along a skewed line in the 2-D tracking Doppler approach compared with the single-beam approach. The intensities are displayed in a color scale given by the color bar to the right.

ultrasonic beam. The new method is therefore suited for situations with any beam-to-flow angle. In the Fourier domain this is equivalent to summation along lines in the $f_\theta f_D$ domain. The flow direction can be determined manually by assuming that the flow is aligned with the blood vessel.

In Figure 2.2, the Doppler signal from a single ultrasonic beam direction, consistent with the method in [7], is compared to tracking of the scatterers using several parallel beams (2-D tracking Doppler). The beam-to-flow angle is 62°. By using the 2-D tracking Doppler approach, the signal can be extracted from a line that follows the direction of the flow. The signal forms lines in the 2-D tracking Doppler M-mode image that are much thinner and extend further than in the single-beam M-mode image, making it better suited for tracking. The 2-D tracking Doppler 2-D FFT image shows a signal that is concentrated along a skewed line. In the single-beam approach, the shortened transit time makes the signal more dispersed. As the beam in the single-beam approach traverses across the blood vessel, scatterers near the vessel walls are also contributing to the signal. The blood near the walls is slowly moving and is found as low Doppler frequencies in the single-beam 2-D FFT image.

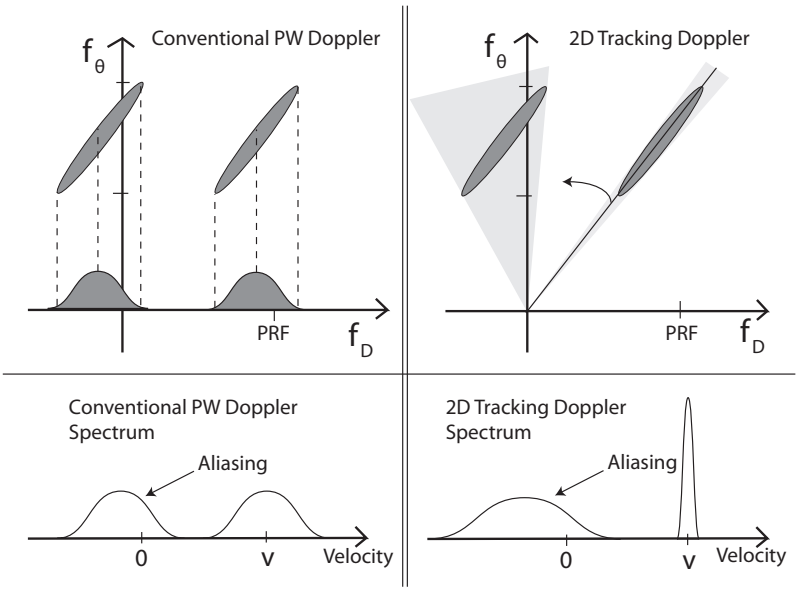

Figure 2.3: Diagrams of the 2-D frequency spectrum of a Doppler signal. The left panel illustrates how the frequency spectrum is projected down to the Doppler axis when using conventional PW Doppler methods. In the right panel, the 2-D tracking Doppler method sums the signal along oblique lines of varying angles in the Fourier domain, corresponding to different velocities. When reaching the angle corresponding to the true velocity (black solid line), the signal will extend along that line. The contribution to the velocity spectrum from aliasing will spread over a larger range of velocities, but with reduced amplitude.

The Doppler signal has a 2-D frequency spectrum with a finite bandwidth given by the bandwidth of the received pulse and the transit time. In Fig. 2.3, the 2-D tracking Doppler method is illustrated in the 2-D Fourier domain. The f_θ axis is the temporal frequency axis in the direction of flow. If $\theta = 0$, the axis corresponds to the f_z axis. The left panel of Fig. 2.3 illustrates how the frequency spectrum is projected down to the Doppler axis when using conventional PW Doppler methods. As indicated in the diagram, the spectrum of a sampled signal will be repeated at every N times the sampling frequency, where N is an integer. Velocity ambiguity can therefore occur. The right panel illustrates how the 2-D tracking Doppler method sums the signal for different angles in the Fourier domain. Utilizing the full 2-D spectrum, the 2-D tracking Doppler method can distinguish between the true velocities and the aliased parts.

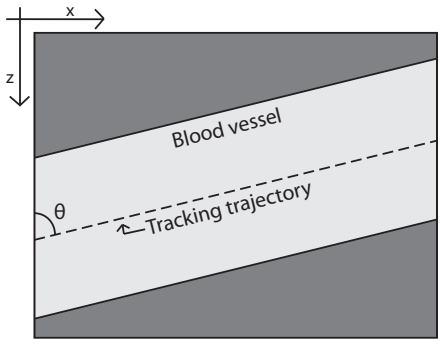

Figure 2.4: Diagram of the imaging plane. The tracking trajectory was chosen to follow the direction of the blood flow in the middle of the vessel.

2.2.1 The Algorithm

The 2-D tracking Doppler spectra can be calculated from the complex pre-envelope signal, $u(x, z, k)$, or from the complex demodulated (IQ) signal, $u_{IQ}(x, z, k)$. The signal samples are extracted, using 2-D spline interpolation, along a user-defined straight line following the direction of the flow, as shown in Fig. 2.4. The data are further processed using a previously published method, velocity matched spectrum [7], to obtain a velocity spectrum.

The signal is processed in two steps:

1. Generating the M-mode Matrix:

   Data samples are selected along a straight line in space for all k. For a specific beam-to-flow angle, θ, the signal can be written as

   $$u_\theta(r, k) = u(r \sin\theta + x_0, r \cos\theta + z_0, k) \ ,$$
   $$u_{IQ,\theta}(r, k) = u_{IQ}(r \sin\theta + x_0, r \cos\theta + z_0, k) \ ,$$

   where r is the distance along the straight line from an arbitrary point $[x_0, z_0]$ on the line.

2. Generating the velocity spectrum $\hat{p}(v)$:

   Summation is done along straight lines in the M-mode matrix. The slope of each line corresponds to a particular velocity, and the sum along the line contributes to the power in one velocity cell in the velocity power spectrum. Since u_{IQ} is complex demodulated, a phase correction factor must be included to account for the axial motion. A sliding-window approach is applied in the slow-time

direction using a smooth window to reduce side lobes.

$$\hat{p}(v) = \left| \sum_k w(k) u_\theta(r_0 + kvT, k_0 + k) \right|^2$$
$$= \left| \sum_k w(k) u_{IQ,\theta}(r_0 + kvT, k_0 + k) e^{i\omega_d k \Delta t} \right|^2 ,$$

$$\Delta t = \frac{2vT\cos\theta}{c} ,$$

where w is the window function with length N and defined for $k \in [-N/2, N/2]$, v is a velocity, r_0 and k_0 are the center positions in range and time, ω_d is the angular demodulation frequency, and T is the pulse repetition time.

The corresponding expression for a conventional velocity spectrum is given by

$$\hat{p}_{conv}(v) = \left| \sum_k w(k) u_\theta(r_0, k_0 + k) e^{i\omega_0 k \Delta t} \right|^2$$
$$= \left| \sum_k w(k) u_{IQ,\theta}(r_0, k_0 + k) e^{i\omega_0 k \Delta t} \right|^2 ,$$

when the data are taken from a single point r_0 in space, and ω_0 is the received center frequency.

2.2.2 Signal Model

The method was investigated by simulating the expected Doppler power spectra using an extended version of the signal model presented in [13] and [7]. The following derivations will add thermal noise, clutter filtering, and tracking of the scatterers between parallel beams to the model. When deriving the expressions for the expected Doppler power spectra, it is convenient to use the complex pre-envelope of the received signal, but the same calculations apply to the IQ signal.

The constructed complex pre-envelope signal, $s(x, z, k)$, is sampled along a line with angle θ, with respect to the z-axis. This can be described as a multiplication of the signal with a delta function:

$$s_\theta(r, k) = s(x, z, k) \cdot \delta(z - x\tan\theta) ,$$

where r is a continuous variable. The signal can be characterized by its autocorrelation function, defined as

$$R_{s_\theta}(\rho, m) \equiv \langle s^*_\theta(r, k) s_\theta(r + \rho, k + m) \rangle ,$$

where ρ and m are lags along the oblique line and in slow time, respectively; $*$ denotes the complex conjugate; and $\langle\rangle$ is the expectation value operator. By including a noise term, $n(r,k)$, the thermal noise in the signal is accounted for, giving a combined signal

$$s_n(r,k) = s_\theta(r,k) + n(r,k) \ .$$

and its autocorrelation function

$$R_{s_n}(\rho,m) = R_{s_\theta}(\rho,m) + N_0\delta(\rho)\delta(m) \ , \tag{2.1}$$

where N_0 is the noise power.

Clutter filtering is done in slow time, with a high-pass filter with impulse response $h(k)$. Band-pass filtering in fast time is done with a filter $b(r)$ to match the bandwidth of the sampled signal. The frequency response of $b(r)$ is assumed to be flat over the signal bandwidth. The filtered signal and its autocorrelation function is given by

$$\begin{aligned} s_f(r,k) &= s_n(r,k) \otimes_r b(r) \otimes_k h(k) \ , \\ R_{s_f}(\rho,m) &= R_{s_n}(\rho,m) \otimes_\rho b_2(\rho) \otimes_m h_2(m) \ , \end{aligned} \tag{2.2}$$

where $\otimes$ means convolution and the subscript $_2$ indicates short notation for the autocorrelator operator, $b_2(\rho) = \langle b^*(r)b(r+\rho)\rangle$. Inserting (2.1) into (2.2) and utilizing that $s_\theta(r,k)$ and $b(r)$ has the same bandwidth, we get

$$\begin{aligned} R_{s_f}(\rho,m) &= R_{s_\theta}(\rho,m) \otimes_\rho b_2(\rho) \otimes_m h_2(m) \\ &\quad + N_0 b_2(\rho) \otimes_\rho \delta(\rho) \cdot h_2(m) \otimes_m \delta(m) \\ &= R_{s_\theta}(\rho,m) \otimes_m h_2(m) + N_0 b_2(\rho) \cdot h_2(m) \ . \end{aligned} \tag{2.3}$$

The velocity spectrum is then given by

$$\begin{aligned} \hat{p}(v) &= \left| \sum_k w(k) s_f(r_0 + kvT, k_0 + k) \right|^2 \\ &= \sum_{k_1,k_2} w^*(k_1) w(k_2) \\ &\quad \cdot s_f^*(r_0 + k_1 vT, k_0 + k_1) s_f(r_0 + k_2 vT, k_0 + k_2) \ , \end{aligned}$$

and its expectation value is

$$\begin{aligned} \langle \hat{p}(v) \rangle &= \sum_{k_1,k_2} w^*(k_1) w(k_2) \\ &\quad \cdot \langle s_f^*(r_0 + k_1 vT, k_0 + k_1) s_f(r_0 + k_2 vT, k_0 + k_2) \rangle \\ &= \sum_k w_2(k) R_{s_f}(kvT, k) \ , \end{aligned} \tag{2.4}$$

where $k = k_2 - k_1$. Inserting (2.3) into (2.4), we get

$$\begin{aligned}\langle \hat{p}(v) \rangle &= \sum_k w_2(k)(R_{s_\theta}(kvT, k) \otimes_k h_2(k) \\ &+ N_0 b_2(kvT) h_2(k)) \\ &= \sum_{k,n} w_2(k) R_{s_\theta}(kvT, k-n) h_2(n) \\ &+ \sum_k w_2(k) N_0 b_2(kvT) h_2(k) \ . \end{aligned} \tag{2.5}$$

In [13] and [7] it is assumed that we have a zero-mean Gaussian process. If we also assume that the correlation length in blood is much shorter than the wavelength [14], the blood random field is white. Adding the assumption that the blood field is stationary and has a uniform velocity v_0 in the direction θ, the autocorrelation function can be written in terms of the pulse-echo response, g(r):

$$R_{s_\theta}(\rho, m; v_0) = g_2(\rho - m v_0 T) \ . \tag{2.6}$$

By inserting (2.6) into (2.5), we obtain the expected power spectrum for the 2-D tracking Doppler method:

$$\begin{aligned}\langle \hat{p}(v \mid v_0) \rangle &= \sum_{k,n} w_2(k) g_2(kvT - (k-n)v_0 T) h_2(n) \\ &+ \sum_k w_2(k) N_0 b_2(kvT) h_2(k) \ . \end{aligned} \tag{2.7}$$

Using the same signal model, but only considering samples originating from a fixed position in space, we can calculate the expected power spectrum for the conventional PW Doppler method:

$$\begin{aligned}\langle \hat{p}_{conv}(v) \rangle &= \sum_k w_2(k) R_{s_f}(0, k) e^{-i\omega_0 k \Delta t} \\ &= \sum_{k,n} w_2(k) R_{s_\theta}(0, k-n) h_2(n) e^{-i\omega_0 k \Delta t} \\ &+ \sum_k w_2(k) N_0 b_2(0) h_2(k) e^{-i\omega_0 k \Delta t} \ , \end{aligned} \tag{2.8}$$

where ω_0 is the received center frequency. By inserting (2.6) into (2.8), we get

$$\begin{aligned}\langle \hat{p}_{conv}(v \mid v_0) \rangle &= \sum_{k,n} w_2(k) g_2(-(k-n)v_0 T) h_2(n) e^{-i\omega_0 k \Delta t} \\ &+ \sum_k w_2(k) N_0 b_2(0) h_2(k) e^{-i\omega_0 k \Delta t} \ . \end{aligned} \tag{2.9}$$

The final expressions of the expected Doppler power spectra include the autocorrelation of the pulse-echo response, g_2. To calculate g_2, the spectral density function, $G(f_x, f_z)$, of the received signal must be modeled. This can be done using the principles of the Fraunhofer approximation, which states that the lateral variation of the ultrasound field at the focal depth can be approximated as the Fourier transform of the product of the aperture and apodization functions [15]. The Fourier transform of this ultrasound field is thus a scaled version of the aperture and the apodization function. In fast time, the frequencies are centered on $2f_0/c$, where f_0 is the center frequency of the received signal [16].

The sampling of the signal along a line with angle θ has been described by a multiplication of the signal with a delta function, $\delta(z - x\tan\theta)$. In the spatial Fourier domain this corresponds to a convolution of the spectral density function with another delta function:

$$G_\theta(f_\theta) = G(f_x, f_z) \otimes \delta(f_z - f_x \tan(\theta + 90°)) \big|_{(f_\theta \sin\theta, f_\theta \cos\theta)} \ ,$$

where G_θ is the spectral density function along the axis f_θ which has an angle θ with respect to the f_z axis. As illustrated in Fig. 2.5, the convolution can be described as a projection of the spectral content of the signal to a line with angle θ which extends through the origin. $\mathbf{G}_\theta$ can be found numerically by summing the spectral contribution from each radial frequency:

$$\mathbf{G}_\theta = \sum_{f_z} w_a \left(\frac{\mathbf{f}_\theta - f_z \cos\theta}{0.5\, B_x(f_z) \sin\theta} \right) G_z(f_z) \ ,$$

where w_a is the apodization function, B_x is the bandwidth, and G_z is the spectral density function along the f_z axis.

The Wiener-Khinchin theorem states that the power spectral density of a wide-sense-stationary random process is the Fourier transform of the corresponding autocorrelation function [17]. $\mathbf{g_2}$ can therefore be found by taking the inverse Fourier transform of $\mathbf{G}_\theta$.

$$\mathbf{g_2} = \mathcal{F}^{-1}(\mathbf{G}_\theta) \ .$$

2.3 Experiments

The 2-D tracking Doppler method was tested both *in vitro* and *in vivo*, and compared with a conventional PW Doppler method. Recordings were done using a SonixMDP ultrasound scanner with a 5-MHz linear probe and a SonixDAQ for channel data acquisition (Ultrasonix, Richmond, BC, Canada). The acquisition consisted of continuous plane wave transmissions with a PRF of 4 kHz. The RF channel data was IQ-demodulated and low-pass filtered to reduce the noise bandwidth, and beamformed using a Hamming window over the active receive aperture. Details of the acquisition setup and the post processing parameters are given in Table 2.1.

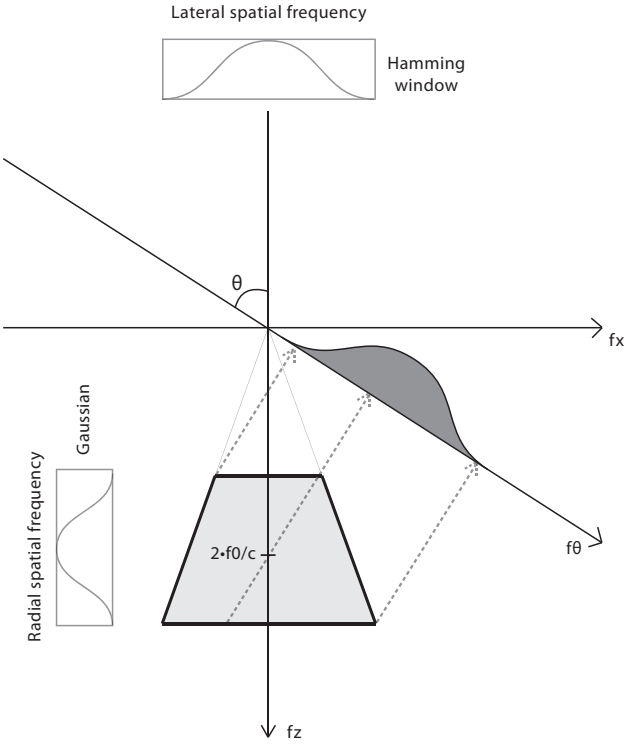

Figure 2.5: Diagram of the signal in the Fourier domain. Sampling the signal along a straight line in space is the same as projecting the signal to a line with the same angle in the Fourier domain. The beam-to-flow angle is θ, the radial distribution of frequencies is assumed to be Gaussian, and the lateral distribution is given by the apodization function, which is a Hamming window.

Conventional PW Doppler spectra were estimated from the same data sets using the Welch's method. Estimates from range samples over 2 mm were averaged to reduce the variance. No range averaging was applied to the signal because the receive filter was adapted to the bandwidth of the transmitted pulse. The slow-time window length was 32 samples for both methods. The tracking length was approximately 1.5 cm for the 2-D tracking Doppler method. The 2-D tracking Doppler estimates were averaged in the direction of the flow. The SNR was high both *in vitro* and *in vivo*. White noise was therefore added in the post processing of the data to mimic a more realistic clinical situation with moderate SNR.

Table 2.1: Parameters

Acquisition setup		Post-processing parameters	
Parameter	Value	Parameter	Value
Tx center frequency	5 MHz	Tracking length	1.5 cm
Pulse periods	2.5	Window	Hamming
PRF	4 kHz	Window length	32 samples
F-number	1.4	HP-filter	FIR, order 50
		HP-filter cutoff	32 Hz

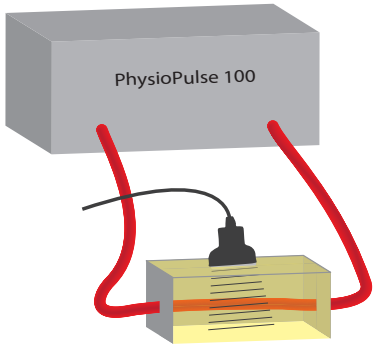

Figure 2.6: The experimental setup. The flow phantom consisted of a tube with an inner diameter of 6 mm that was coupled to a flow loop. A pulsatile flow was achieved using the PhysioPulse 100 Flow System. The phantom was filled with a blood-mimicking fluid.

2.3.1 *In Vitro* Recordings

In vitro flow studies give a controlled situation of the flow and are easily repeatable. Therefore, to investigate the performance of the new method, recordings were done using a flow phantom representing a carotid artery. The experimental setup is illustrated in Fig. 2.6. The flow phantom consisted of a silicon tube with an inner diameter of 6 mm that was coupled to a flow loop. The tube was partly surrounded by a stiff silicon layer, creating an imaging distance of approximately 2 to 3 cm. A pulsatile flow was achieved using the PhysioPulse 100 Flow System (Shelley Medical Image Technologies, London, ON, Canada). The phantom was filled with a blood-mimicking fluid that has been tested and described by Ramnarine *et al.* [18]. The fluid exhibited characteristics very similar to those of blood, but produced stronger backscattered echoes. The probe was mechanically tilted to produce beam-to-flow angles of 62° and 82°.

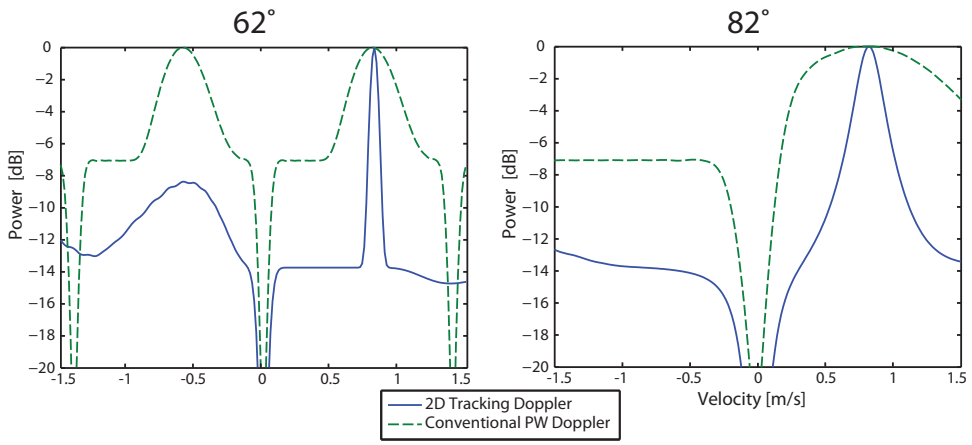

Figure 2.7: Simulations of the expected Doppler power spectra. The expected conventional Doppler power spectra are shown in dashed green curves and the expected 2-D tracking Doppler power spectra are shown in solid blue curves. The spectra in the left and right panel were simulated with a beam-to-flow angle of 62° and 82°, respectively. The simulations were done using a constant velocity of 0.82 m/s. The signal model includes white noise and clutter filtering.

2.3.2 *In Vivo* Recordings

The method was tested on an *in vivo* recording of a carotid artery in a healthy volunteer. The region of interest (ROI) was placed in the common carotid artery, where the blood flow angle was unidirectional. The beam to flow angle was 70°.

2.4 Results

The expected 2-D tracking Doppler power spectra and the expected conventional PW Doppler power spectra were simulated, using (2.7) and (2.9), with a constant velocity of 0.82 m/s and beam-to-flow angles of 62° and 82°. The results are shown in Fig. 2.7. They show a noise floor that is approximately 7 dB lower for the 2-D tracking Doppler spectrum compared with the conventional PW Doppler spectrum. The simulations with a beam-to-flow angle of 62° show a main lobe resolution at -3 dB of approximately 0.1 m/s for the 2-D tracking Doppler spectrum and 0.4 m/s for the conventional PW Doppler spectrum. The simulations with a beam-to-flow angle of 82° show a main lobe resolution at -3 dB of approximately 0.2 m/s for the 2-D Tracking Doppler spectrum and 1.2 m/s for the conventional PW Doppler spectrum.

In Fig. 2.8 the main lobe resolution at -3 dB is plotted with respect to the beam-to-flow angle. The results show improved velocity resolution for beam-to-flow angles between 40° and 82°.

Fig. 2.9 shows conventional PW Doppler spectra and 2-D tracking Doppler spectra

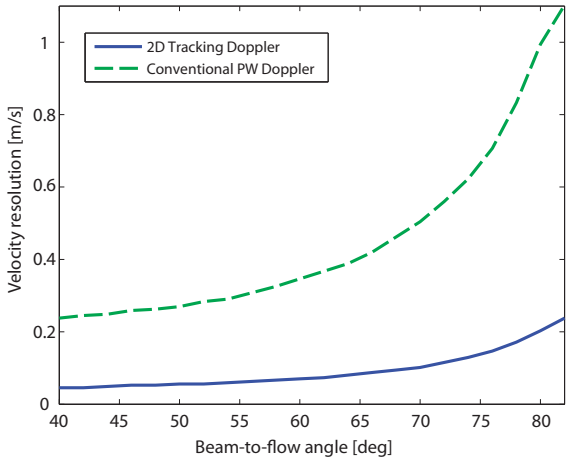

Figure 2.8: The velocity resolution of the simulated Doppler power spectra at -3 dB for beam-to-flow angles between 40° and 82°. The expected velocity resolution for the conventional Doppler power spectra is shown in a dashed green curve and the expected velocity resolution for the 2-D tracking Doppler power spectra is shown in a solid blue curve. The simulations were done using a constant velocity of 0.82 m/s.

generated from *in vitro* ultrasound recordings of pulsatile flow in a straight tube. Usually, the spectral Doppler display is limited to a range of twice the Nyquist velocity with an adjustable baseline. We have included a velocity span of ± two times the Nyquist velocity to capture the aliased velocity waveforms and show the ability to resolve aliasing. In the upper panel spectra the beam-to-flow angle is 62°. For this beam-to-flow angle, two velocity waveforms are observed in each spectrum, but the true velocity waveform stands out more clearly in the display for the 2-D tracking Doppler method than for the conventional method. For the largest velocities in the true velocity waveforms, an approximately 4-fold decrease in the spectral broadening can be observed in the 2-D tracking Doppler spectrum compared with the conventional PW Doppler spectrum. A ripple effect in the velocity waveform can be observed in the 2-D tracking Doppler spectrum. These oscillations indicate that the flow pump was not running evenly. Because of the spectral broadening, they are not visible in the conventional approach. In the lower panel spectra, the beam-to-flow angle was 82°. For this beam-to-flow angle, the velocities in the conventional PW Doppler spectrum are significantly smeared, whereas the velocities in the 2-D tracking Doppler spectrum can still be resolved.

In Fig. 2.10, velocity spectra generated by the 2-D tracking Doppler method and the conventional PW Doppler method are compared with their corresponding simulated velocity spectra. The spectra were generated from a part of the *in vitro* data set containing an approximately constant velocity of 0.82 m/s. The beam-to-flow angle was 62°. The spectral estimates were averaged in time using a window of 17 ms.

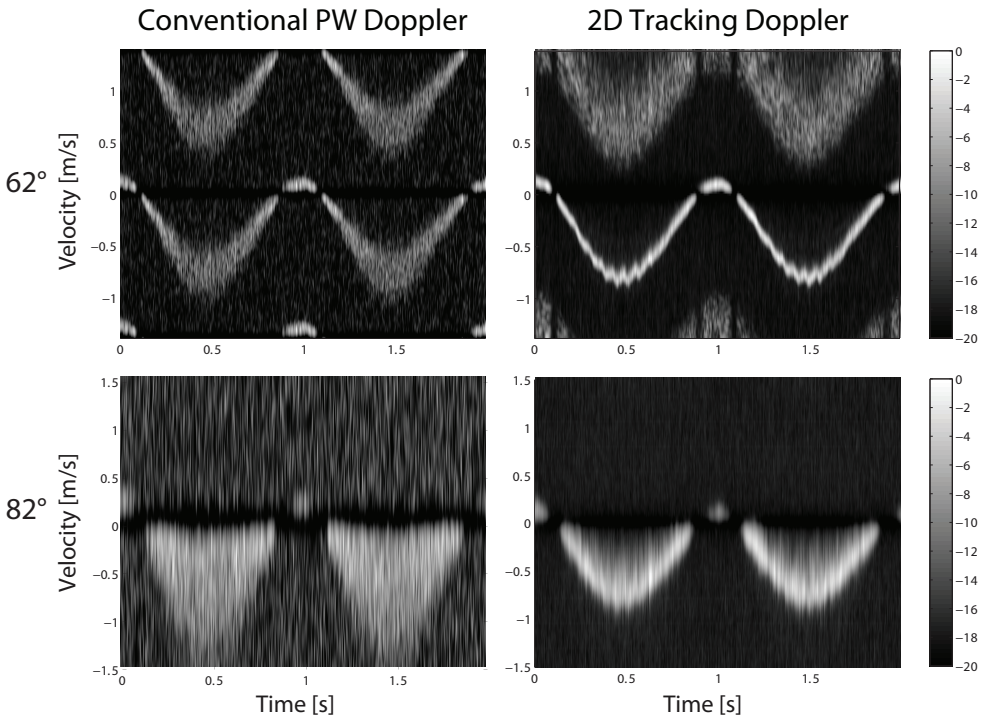

Figure 2.9: Doppler spectra generated from *in vitro* recordings of pulsatile flow in a straight tube. The spectra were generated using a conventional PW Doppler method and the 2-D tracking Doppler method. The dynamic range in decibels is given by the colorbar. The large beam-to-flow angles gave excessive spectral broadening for the highest velocities in the spectra generated by the conventional method. For the 2-D tracking Doppler spectra, the spectral broadening has been reduced.

The simulated velocity spectra were generated using (2.7) and (2.9) and by inserting the same parameters used in the *in vitro* experiment.

Fig. 2.11 shows a conventional PW Doppler spectrum and a 2-D tracking Doppler spectrum generated from an *in vivo* ultrasound recording from the carotid artery of a healthy volunteer. The beam-to-flow angle was 70°. An increased velocity resolution can be observed in the 2-D tracking Doppler spectrum compared with the conventional PW Doppler spectrum, indicating that the method is applicable for *in vivo* imaging.

The two white vertical lines in Fig. 2.11 indicate the time instance used when generating the spectra in Fig. 2.12. The velocity at this time instance was approximately 0.8 m/s. The spectra in Fig. 2.12 show an increase in SNR of approximately 5 dB for the 2-D tracking Doppler method compared with the conventional PW Doppler method. The spectral estimates were averaged in time using a window of 17 ms.

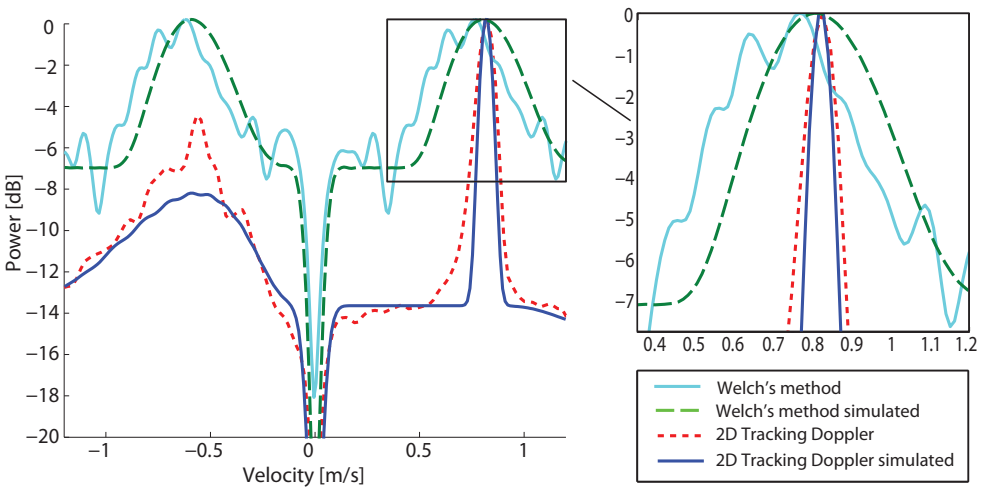

Figure 2.10: Doppler power spectra generated by the 2-D tracking Doppler method and the conventional PW Doppler method. Spectra generated from an *in vitro* recording are compared with their corresponding simulated spectra. The flow had a velocity of 0.82 m/s at an angle of 62° compared with the ultrasound beam.

2.5 Discussion

The results show that spectral broadening can be considerably reduced when applying the 2-D tracking Doppler method compared with a conventional PW Doppler method. This can be explained by the increased transit time that is achieved when following the scatterers in space. An increased velocity resolution can be observed in the spectra generated from both the *in vitro* and *in vivo* ultrasound recordings. The simulation results also show a significant increase in velocity resolution for a wide range of beam-to-flow angles. Similar improvements in velocity resolution have previously been shown with the proposed technique in [7], but only for small beam-to-flow angles. With the new technique, the transmitted beam does not have to be aligned with the direction of the flow, expanding the applicability of the tracking technique.

The 2-D tracking Doppler method is based on a plane wave acquisition. It is well known that the lack of transmit focusing results in reduced penetration depth. Reduced penetration can cause low SNR in situations in which the region of interest is situated at large depths. However, in our experiments the penetration was sufficiently high. Also, the properties of the 2-D tracking Doppler method increase the SNR in the velocity spectra. Flows in cylindrical geometries, such as the straight tube and the carotid artery, have a constant velocity profile in the direction of the flow. By selecting data samples from a line in the middle of the cylinder, the scatterers have approximately equal velocity. The signal will therefore match in both phase and amplitude when summed in the 2-D tracking Doppler algorithm. This results in a better SNR in the 2-D tracking Doppler spectra compared with the conventional PW

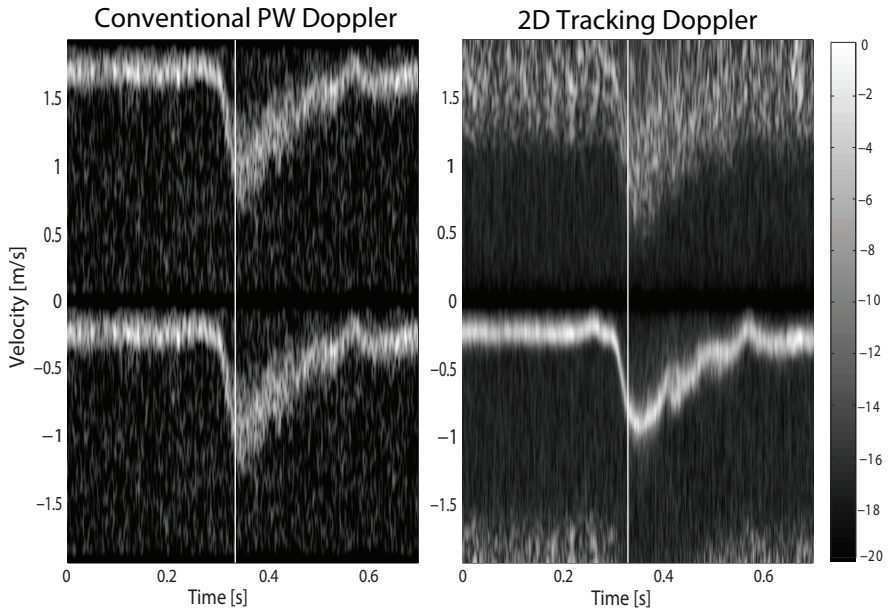

Figure 2.11: Doppler spectra generated from an *in vivo* recording of a carotid artery. The spectra were generated by a conventional PW Doppler method and the 2-D tracking Doppler method. The dynamic range in decibels is given by the color bar. The angle between the flow and the ultrasound beam was 70°, giving excessive spectral broadening for the highest velocities in the conventional spectrum. In the 2-D tracking Doppler spectrum the spectral broadening has been reduced.

spectra, which is evident in both the *in vitro* and *in vivo* results.

Simulations of the expected Doppler power spectra were performed using an extended version of the signal model used in [7]. The model included thermal noise and clutter filtering. Out-of-plane movement was not taken into account. The simulated spectra therefore describe an ideal situation where the flow direction is in the imaging plane and the beam-to-flow angle is measured precisely. Any out-of-plane movement or incorrect positioning of the tracking line would broaden the main lobe in the power spectrum. However, the simulated spectra corresponded well with the spectra generated from the in vitro recordings, showing 4 times increase in spectral resolution, and 7 dB increase in spectral SNR (see Fig. 2.10). This may give new opportunities in blood flow imaging when it is desired to place the probe in an angle that is not parallel with the flow.

The 2-D tracking Doppler approach may have several advantages clinically. First, it may increase quantitative accuracy and reproducibility when tracing the envelope of the Doppler spectrum, because of the estimation and display of spectra with an increased accuracy and resolution. This is especially the case for high-velocity blood flow that we often see in relation to pathology. The 2-D approach to velocity estimation

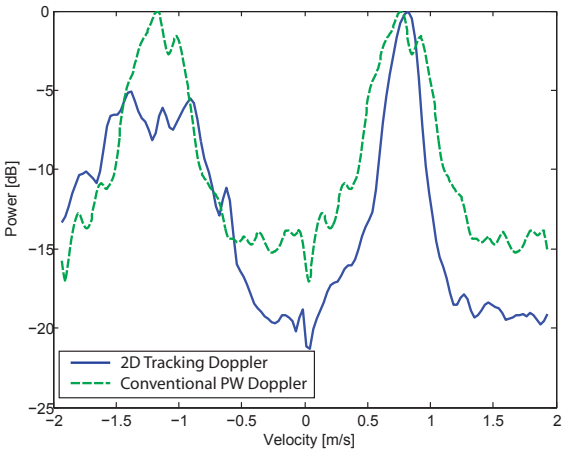

Figure 2.12: Doppler spectra generated from the time instance indicated with the two vertical lines in the *in vivo* recording in Figure 2.11. The velocity is approximately 0.8 m/s. Both the velocity resolution and the SNR are improved by the 2-D Tracking Doppler method compared to the conventional PW Doppler method.

also provides opportunities for resolving the ambiguity problem when the maximum velocity is beyond the Nyquist limit. This has previously been shown for blood flow direction along the ultrasound beam [7].

The use of parallel receive beamforming allows for PW Doppler based on a 2-D or 3-D acquisition scheme such as color Doppler imaging. Using this approach, it is possible to calculate and display multiple simultaneous velocity spectra from arbitrary spatial positions in the image region. This can be useful when quantifying valve leakages or vessel stenosis, and the approach may also help to improve workflow when both color-Doppler imaging and PW Doppler measurements are part of the protocol. The acquisition setup for color Doppler is typically different from that of PW Doppler. For instance, the beam and pulse characteristics are chosen such that an increased spectral broadening is expected in the calculated sonograms when based on color Doppler acquisition. The color Doppler setup, on the other hand, is well suited for tracking purposes (shorter pulses and lower f-number), and by combining retrospective PW Doppler with the tracking technique it is possible to compensate for the decreased transit time in a combined acquisition mode.

An important challenge for the 2-D tracking Doppler method to work in practice is to extract data along the correct trajectory through a 3-D (2-D tracking + time) data set, following the movement of the blood scatterers. In this work, the trajectory was determined from a B-mode image of the artery or tube and chosen as a straight line. This approach may not be suitable for more complex flow fields. Curved flow fields, accelerated flow, and turbulent flow were not considered in this work. To limit broadening of the velocity spectrum, the flow must be constant for a length

corresponding to the tracking length. In this work, the tracking length was 1.5 cm, which could be too long in the aforementioned situations. One solution could be increasing the PRF, which would decrease the required tracking length. Still, high-velocity flow fields that change rapidly in space, such as jet flows, could be a challenge to estimate accurately. Additionally, steady-state flow conditions are assumed, which is true for short time intervals (10 ms [19]) similar to the observation time applied in this work.

2.6 Conclusion

A new method to limit spectral broadening in PW Doppler has been presented. By sampling the in-plane scatterer movement in the direction of flow, an increased transit time was achieved. This was feasible without compromising the pulse repetition frequency by using plane wave transmission and parallel receive beamforming. The velocity spectra generated by the 2-D tracking Doppler method had significantly reduced spectral broadening compared with spectra generated by a conventional PW Doppler method. Increased quantitative accuracy and reproducibility when tracing the envelope of the Doppler spectrum is expected, because of the estimation and display of spectra with increased accuracy and resolution.

References

[1] J. Capon, "High-Resolution Frequency-Wavenumber Spectrum Analysis," *Proceedings of the IEEE*, vol. 57, no. 8, pp. 1408–1418, 1969.

[2] J. Li and P. Stoica, "An Adaptive Filtering Approach to Spectral Estimation and SAR Imaging," *IEEE transactions on signal processing*, vol. 44, no. 6, pp. 1469–1484, 1996.

[3] P. Stoica and R. Moses, *Spectral analysis of signals*. Prentice Hall, Upper Saddle River, 2005.

[4] F. Gran, A. Jakobsson, and J. r. A. Jensen, "Adaptive spectral doppler estimation.," *IEEE transactions on ultrasonics, ferroelectrics, and frequency control*, vol. 56, pp. 700–14, Apr. 2009.

[5] K. L. Hansen, F. Gran, M. M. Pedersen, I. K. Holfort, J. A. Jensen, and M. B. Nielsen, "In-vivo validation of fast spectral velocity estimation techniques.," *Ultrasonics*, vol. 50, pp. 52–9, Jan. 2010.

[6] I. K. Ekroll, H. Torp, and L. Lovstakken, "Spectral Doppler estimation utilizing 2-D spatial information and adaptive signal processing.," *IEEE transactions on ultrasonics, ferroelectrics, and frequency control*, vol. 59, pp. 1182–92, June 2012.

[7] H. Torp and K. Kristoffersen, "Velocity matched spectrum analysis: A new method for suppressing velocity ambiguity in pulsed-wave Doppler," *Ultrasound in medicine & biology*, vol. 21, no. 7, pp. 937–944, 1995.

[8] S. Alam and K. Parker, "The butterfly search technique for estimation of blood velocity," *Ultrasound in medicine & biology*, vol. 21, no. 5, pp. 657–670, 1995.

[9] J. Jensen and N. Oddershede, "Estimation of velocity vectors in synthetic aperture ultrasound imaging," *IEEE Transactions on Medical Imaging*, vol. 25, no. 12, pp. 1637–1644, 2006.

[10] L. Wilson, "Description of broad-band pulsed Doppler ultrasound processing using the two-dimensional Fourier transform," *Ultrasonic imaging*, vol. 315, pp. 301–315, 1991.

[11] W. Mayo, "Two dimensional processing of pulsed Doppler signals," *US Patent 4,930,513*, 1990.

[12] T. Loupas and R. W. Gill, "Multifrequency Doppler: Improving the Quality of Spectral Estimation by Making Full Use of the Information Present in the Backscattered RF Echoes," *IEEE transactions on ultrasonics, ferroelectrics, and frequency control*, vol. 41, no. 4, pp. 522–531, 1994.

[13] H. Torp, K. Kristoffersen, and B. A. J. Angelsen, "Autocorrelation Techniques in Color Flow Imaging: Signal Model and Statistical Properties of the Autocorrelation Estimates," *IEEE transactions on ultrasonics, ferroelectrics, and frequency control*, vol. 41, no. 5, p. 9, 1994.

[14] B. A. J. Angelsen, "A theoretical study of the scattering of ultrasound from blood.," *IEEE transactions on bio-medical engineering*, vol. 27, pp. 61–7, Feb. 1980.

[15] R. S. C. Cobbold, *Foundations of Biomedical Ultrasound*. Oxford University Press, Inc., 2007.

[16] T. Hergum, S. Langeland, E. W. Remme, and H. Torp, "Fast ultrasound imaging simulation in K-space.," *IEEE transactions on ultrasonics, ferroelectrics, and frequency control*, vol. 56, pp. 1159–67, June 2009.

[17] J. G. Proakis and D. G. Manolakis, *Digital Signal Processing. Principles, Algorithms, and Applications.* Pearson Education, Inc., fourth ed., 2007.

[18] K. V. Ramnarine, D. K. Nassiri, P. R. Hoskins, and J. Lubbers, "Validation of a new blood-mimicking fluid for use in doppler flow test objects," vol. 24, no. 3, pp. 451–459, 1998.

[19] P. Vaitkus and R. Cobbold, "A comparative study and assessment of Doppler ultrasound spectral estimation techniques part I: Estimation methods," *Ultrasound in medicine & biology*, vol. 14, no. 8, pp. 661–672, 1988.

Chapter 3

Investigations of Spectral Resolution and Angle Dependency in a 2-D Tracking Doppler Method

Tonje D. Fredriksen[1], Jorgen Avdal[1], Ingvild K. Ekroll[1], Torbjørn Dahl[1,2], Lasse Lovstakken[1], and Hans Torp[1]
[1] MI Lab and Dept. of Circulation and Medical Imaging, NTNU
[2] St Olavs Hospital, Trondheim, Norway

An important source of error in velocity measurements from conventional pulsed wave (PW) Doppler is the angle used for velocity calibration. Because there are great uncertainties and interobserver variability in the methods used for Doppler angle correction in the clinic today, it is desirable to develop new and more robust methods.
In this work, we have investigated how a previously presented method, 2-D tracking Doppler, depends on the tracking angle. A signal model was further developed to include tracking along any angle, providing velocity spectra which showed good agreement with both experimental data and simulations. The full-width at half-maximum (FWHM) bandwidth and the peak value of predicted power spectra were calculated for varying tracking angles. It was shown that the spectra have lowest bandwidth and maximum power when the tracking angle is equal to the beam-to-flow angle. This may facilitate new techniques for velocity calibration, e.g., by manually adjusting the tracking angle, while observing the effect on the spectral display. An *in vitro* study was performed in which the Doppler angles were predicted by the minimum FWHM and the maximum power of the 2-D tracking Doppler spectra for 3 different flow angles. The estimated Doppler angles had an overall error of $0.24° \pm 0.75°$ when using the minimum FWHM. With an *in vivo* example, it was demonstrated that the 2-D tracking Doppler method is suited for measurements in a patient with carotid stenosis.

3.1 Introduction

Blood velocity measurements are essential in cardiovascular diagnostics. Increased flow velocities or abnormal flow patterns can indicate disease and a possible need for surgery. Ultrasound imaging is the primary instrument for cardiovascular diagnostics as the measurements can be done noninvasively and in real-time. High velocity flow is found, for instance, at stenotic regions. The degree of stenosis is normally assessed by using pulsed wave (PW) Doppler to estimate the maximum velocities. With PW Doppler the complete spectrum of velocities are estimated; typically displayed as a 2-D sonogram with velocity along the y-axis and time along the x-axis. PW Doppler analysis of the Doppler signal is usually performed using the fast Fourier transform (FFT) on short data segments in time, acquired from a single sample point in space. For high velocities and large beam-to-flow angles, the blood will pass rapidly through the sample volume, resulting in a short observation time and a broadening of the estimated velocity spectrum. The loss in frequency resolution may give severe overestimation of blood velocities and a risk of misdiagnosis.

Approaches for increasing the transit time include methods that utilize the full 2-D Fourier transform of the signal in the fast- and slow-time directions. Reduced spectral broadening has been shown by several authors [1–4], but only for flow in the axial direction. In [5] we presented a method called 2-D tracking Doppler, which tracks the scatterers along the direction of the flow. The method is based on the principles described in [4], but is adapted for situations with any beam-to-flow angle. By using plane transmit waves and parallel receive beams, it is possible to have instantaneous acquisition of multiple image lines in a 2-D region. By tracking the scatterers along the direction of the flow within this region, the transit time is increased, giving a higher spectral velocity resolution. The method was in [5] tested both *in vitro* and *in vivo* on a carotid artery of a healthy volunteer. The results showed that the 2-D tracking Doppler method could be used to increase the velocity resolution in PW Doppler, especially for large beam-to-flow angles.

In addition to a limited transit time, the greatest source of error in PW Doppler velocity estimation is the angle used for calibrating the spectra. Conventional Doppler techniques can only measure the axial component of blood flow. The blood velocity is estimated by multiplying the measured velocity with an angle correction factor of $1/\cos\theta$, where θ is the estimated beam-to-flow angle. As the angle correction factor tends to infinity as θ approaches 90°, the velocity estimates are very sensitive to angle estimation errors for large beam-to-flow angles. Therefore, clinical guidelines [6] discourage the use of Doppler angles above 60°.

Several techniques have been suggested to overcome the angle dependence in Doppler ultrasound. Cross-beam vector Doppler has been one of the main approaches to 2-D flow imaging since the onset of the idea in the 1970s. Using triangulation, the 1-D velocity estimates from two different angles of insonation can be used to reconstruct a 2-D velocity vector [7]. An alternative dual-beam method has been introduced by Tortoli and colleagues [8], [9], characterized by the different role played by each beam. One of the beams acts as reference, being devoted to estimate only the flow direction. Through the inspection of the spectrum from the reference beam, a 90° beam-to-flow

angle is sought. Such spectra, from transverse flow, are expected to be centered on the zero frequency, and even small deviations from the desired 90° orientation cause noticeable losses of spectral symmetry. However, local secondary flow oscillations, which are often found at atherosclerotic regions [10], may restrict the applicability of the method.

Another approach has been described by J. Jensen and colleagues [11], [12], in which both the velocity magnitude and angle is determined using a crosscorrelation technique. The angle is found from beamforming directional signals in a number of directions and then selecting the angle with the highest normalized correlation. This method has some similarities with the presented method in that minimum spectral bandwidth corresponds to the maximum correlation. However, it only estimates the mean velocity, whereas the 2-D tracking Doppler method produces a full Doppler spectrum display. Mean velocity estimates may have a bias caused by clutter filtering or spatial averaging and they do not provide the peak velocity, as used in e.g., stenosis classification.

Techniques for Doppler angle estimation based on the transit time spectrum broadening effect has been presented by several authors [13–18]. Because the Doppler bandwidth is inversely proportional to the transit time of a scatterer crossing the ultrasound beam, the Doppler angle can be estimated from the resulting Doppler bandwidth. Many promising results have been shown *in vitro*, but the methods have not yet reached clinical practice.

The 2-D tracking Doppler method generates velocity spectra with increased velocity resolution, especially at large beam-to-flow angles. In this work, it is demonstrated that the spectra broaden when the incorrect tracking angle is chosen, compared with spectra with the correct tracking angle. The angle dependency of the 2-D tracking Doppler method will be investigated using simulations and *in vitro* and *in vivo* experiments. Two methods for velocity calibration are proposed; using the Doppler angle given by the minimum spectral broadening or the maximum power. In Section 3.2.1, a brief description of the 2-D tracking Doppler algorithm is given. In Section 3.2.2, the signal model presented in [5] is extended to include incorrect selection of the tracking angle. The experimental work is described in Section 3.3. 2-D tracking Doppler spectra from varying Doppler angles will be presented in Section 3.4, and compared with a conventional PW Doppler method. In Section 3.5, the results are discussed.

3.2 Theory

Two spectral Doppler methods have been applied in this work; the 2-D tracking Doppler method and the more conventional Welch's method. The 2-D tracking Doppler algorithm was described in [5], but will also be summarized in Section 3.2.1.

A signal model was presented in [5] where statistically expected 2-D tracking Doppler spectra were calculated for tracking angles equal to the beam-to-flow angles. In Section 3.2.2, this model will be extended to include tracking along any angle, which allows for investigation of the influence of incorrect tracking angle on the 2-D tracking

Doppler estimates.

3.2.1 The 2-D Tracking Doppler Algorithm

The 2-D tracking Doppler algorithm requires simultaneous acquisition of Doppler signals from a 2-D spatial region. The complex pre-envelope of the received signal is denoted by $u(x, z, k)$, and the in-phase and quadrature demodulated (IQ) signal is denoted by $u_{IQ}(x, z, k)$, where x and z are the spatial coordinates in the azimuth and axial direction, respectively, and k is the slow time index. Post-processing of the data is performed in two steps:

1. The beamformed signal is resampled along a tracking line, using 2-D spline interpolation.

2. The resampled data are processed using the velocity matched spectrum algorithm, first presented in [4] and later applied in [5].

For a chosen tracking angle, θ, the resampled signal can be written as

$$u_\theta(r, k) = u(r \sin\theta + x_0, r \cos\theta + z_0, k) \ , \tag{3.1}$$

$$u_{IQ,\theta}(r, k) = u_{IQ}(r \sin\theta + x_0, r \cos\theta + z_0, k) \ , \tag{3.2}$$

where r is the position along the line through the sample volume point $[x_0, z_0]$. The resampled signal as a function of slow-time was described in [5] as an M-mode matrix. M-mode usually refers to data from one scan line as a function of time (slow time), but is in this context extended to include any straight line in space and slow time.

The signal from scatterers moving with constant velocity will form straight lines in the M-mode matrix, where the slope of each line corresponds to a particular velocity. A velocity spectrum can then be generated by summing the signal along lines with varying slopes.

$$\begin{aligned} \hat{p}(v) &= \left| \sum_k w(k) u_\theta(r_0 + kvT, k_0 + k) \right|^2 \\ &= \left| \sum_k w(k) u_{IQ,\theta}(r_0 + kvT, k_0 + k) e^{i\omega_d k \Delta t} \right|^2 \ , \end{aligned} \tag{3.3}$$

$$\Delta t = \frac{2vT}{c} \cos\theta \ , \tag{3.4}$$

where v is a velocity, r_0 and k_0 are the center positions in range and time, ω_d is the angular demodulation frequency, T is the pulse repetition time, and w is a smooth window function which is zero outside the range $k \in [-N/2, N/2 - 1]$, where N is the window length in number of samples. Because u_{IQ} is complex demodulated, a phase correction factor must be included to account for axial motion.

Using the same formulation as in (3.3), an expression for a conventional, Fourier-based estimate of the power spectrum in a point r_0 can be written as

$$\begin{aligned}\hat{p}_{conv}(v) &= \left|\sum_k w(k)u_\theta(r_0, k_0+k)e^{i\omega_0 k\Delta t}\right|^2 \\ &= \left|\sum_k w(k)u_{IQ,\theta}(r_0, k_0+k)e^{i\omega_0 k\Delta t}\right|^2 ,\end{aligned} \tag{3.5}$$

where ω_0 is the center frequency of the received signal, which may differ slightly from the demodulation frequency, ω_d.

Note that $\hat{p}(v)$ and $\hat{p}_{conv}(v)$ also are functions of r_0 and k. However, these variables were omitted for clarity.

3.2.2 Signal Model

In [5], the statistical expectation values of the power spectra were calculated for tracking angles equal to the beam-to-flow angles. We will now extend the model to include tracking along any angle, by introducing a 2-D point spread function. All motion is assumed to be in the imaging plane. The calculated statistical expectation value of the power spectra will henceforth be referred to as the expected velocity spectra.

The complex pre-envelope of the received signal, $s(x, z, k)$ was in [5] sampled along an oblique line to produce a signal $s_\theta(r, k)$. By adding noise with power N_0, a clutter filter $h(k)$ and a bandpass filter $b(r)$ a signal corresponding to $u_\theta(r, k)$ was constructed. The expected power spectrum for the 2-D tracking Doppler method was shown to be

$$\begin{aligned}\langle\hat{p}(v)\rangle &= \sum_{k,n} w_2(k)R_{s_\theta}(kvT, k-n)h_2(n) \\ &\quad + \sum_k w_2(k)N_0 b_2(kvT)h_2(k) ,\end{aligned} \tag{3.6}$$

where $\langle\rangle$ is the expectation value operator, the subscript $_2$ is a shorthand notation for the autocorrelator operator, and R_{s_θ} is the autocorrelation of s_θ.

In the subsequent formulations in [5], $\theta = \theta_0$ was assumed, where the beam-to-tracking angle is denoted θ and the beam-to-flow angle θ_0. However, by introducing the 2-D point spread function, $f(\vec{r})$, the signal can be evaluated along any tracking angle.

If the blood velocity field is uniform with velocity v_0 at an angle θ_0 and the velocity component in the elevation direction is zero, the autocorrelation of the signal can be written in terms of the autocorrelation of the point spread function:

$$R_{s_\theta}(\rho, m; \vec{v}_0) = f_2(\rho\vec{e}_\theta - m\vec{v}_0 T) , \tag{3.7}$$

$$\vec{v}_0 = v_0 \cdot \vec{e}_{\theta_0} \ , \tag{3.8}$$

where $\vec{e}_\theta$ and $\vec{e}_{\theta_0}$ are unit vectors in the θ and θ_0 directions respectively. Inserting (3.7) into (3.6), we obtain the expected power spectrum for the 2-D tracking Doppler method, given the true velocity $\vec{v}_0$:

$$\begin{aligned}\langle \hat{p}_\theta(v \mid \vec{v}_0) \rangle = &\sum_{k,n} w_2(k) f_2(k\vec{v}T - (k-n)\vec{v}_0 T) h_2(n) \\ &+ \sum_k w_2(k) N_0 b_2(kvT) h_2(k) \ ,\end{aligned} \tag{3.9}$$

$$\vec{v} = v \cdot \vec{e}_\theta \tag{3.10}$$

The geometry of a situation in which $\theta \neq \theta_0$ is shown in Fig. 3.1. The velocity is v_0 and the beam-to-flow angle is θ_0. By choosing a different tracking angle, θ, the point spread function is evaluated at a distance $\vec{r} = k\vec{v}T - k\vec{v}_0 T$ from its center. Assuming an ideal plane wave, where the phase fronts extend in the lateral direction, the estimated velocity spectrum in direction θ will have maximum power when

$$v \cos\theta = v_0 \cos\theta_0 = v_z \ . \tag{3.11}$$

In [5], an expression for the expected power for the conventional PW Doppler spectra was found by using the same signal model, but only considering samples originating from a fixed position in space:

$$\begin{aligned}\langle \hat{p}_{conv}(v) \rangle = &\sum_{k,n} w_2(k) R_{s_\theta}(0, k-n) h_2(n) e^{-i\omega_0 k \Delta t} \\ &+ \sum_k w_2(k) N_0 b_2(0) h_2(k) e^{-i\omega_0 k \Delta t} \ .\end{aligned} \tag{3.12}$$

Inserting (3.7) into (3.12) we get the expected power spectrum for the conventional PW Doppler method, given the true velocity $\vec{v}_0$:

$$\begin{aligned}\langle \hat{p}_{conv}(v \mid \vec{v}_0) \rangle = &\sum_{k,n} w_2(k) f_2(-(k-n)\vec{v}_0 T) h_2(n) e^{-i\omega_0 k \Delta t} \\ &+ \sum_k w_2(k) N_0 b_2(0) h_2(k) e^{-i\omega_0 k \Delta t} \ .\end{aligned} \tag{3.13}$$

3.3 Methods

Velocity spectra were generated by applying the 2-D tracking Doppler algorithm to data from simulations and *in vitro* and *in vivo* recordings. Spectra from one or more

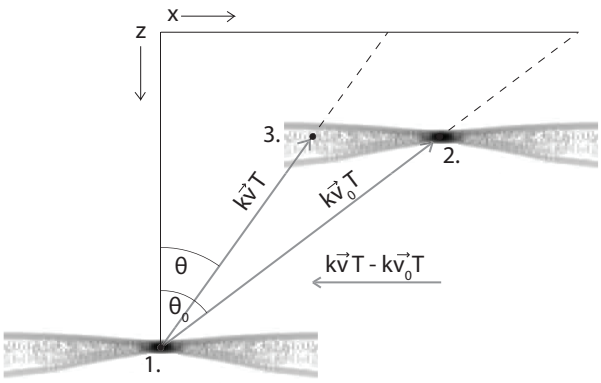

Figure 3.1: Geometric considerations and explanation of the behavior of the 2-D tracking Doppler method when the angle of the tracking trajectory is chosen incorrectly. The diagram shows a point spread function moving from one location to another in the imaging plane. The beam-to-flow angle is θ_0 and the chosen angle for the tracking trajectory is θ. During k pulse repetition periods, the scatterers move a distance kv_0T from point 1 to point 2. When evaluating the signal along a line with angle θ, the maximum correlation is found at point 3. Because of the widened correlation area in the side lobes of the point spread function, the velocity spectrum will broaden. Underestimations of the traveling distance, and hence underestimations of the velocity, will be the result for this scenario. The opposite is true for $\theta > \theta_0$.

tracking angles were generated from a region of interest (ROI). The ROI was chosen as large as possible while ensuring that the flow inside was moving approximately along straight lines with uniform velocities. The tracking length, L, was limited by the size of the ROI for high velocities. For low velocities, L was limited by the temporal window length, N_w, and given by the formula $L = v \cdot N_w \cdot PRT$, where v is the velocity and PRT is the pulse repetition time.

For comparison, velocity spectra were also generated by a conventional PW Doppler method, using (3.13) for the signal model and (3.5) for the *in vitro* and *in vivo* experiments. The same data were used for both spectral estimation techniques, using only a single sample from the tracking line for the conventional method. The same temporal window length was used in the two approaches, and no spatial averaging was performed following any of the two spectral estimation techniques.

3.3.1 Field II Simulations

To validate the new signal model derived in 3.2.2, comparisons were done with the widely used ultrasound simulation program Field II [19], which utilizes an approximate form of the time-domain impulse response function. The blood flow was modeled as a collection of random point scatterers in a simple cylindrical volume with a constant, uniform velocity of 1 m/s at a beam-to-flow angle of 50°. The acquisition and post-

processing parameters were the same as listed in Table 3.1, but with a PRF of 6 kHz.

2-D tracking Doppler spectra were generated by extracting signals from tracking trajectories angled at 20°, 50° and 70° in the cylindrical phantom, and utilizing (3.3) and (3.5). The resulting spectra were qualitatively compared with spectra obtained using (3.9) and (3.13).

3.3.2 Application of the Signal Model

2-D tracking Doppler spectra were generated for different combinations of the beam-to-flow angle, θ_0, and the tracking angle, θ, using the signal model (3.9) and the parameters given in Table 3.1. The spectra were plotted and qualitatively compared with spectra generated from *in vitro* recordings.

To investigate how the spectral width and the maximum power in the 2-D tracking Doppler spectra vary with tracking angle, the signal model (3.9) was used to calculate the expected Doppler power spectra for $\theta_0 = 73°$ and θ ranging from 65° to 77°. The full-width at half-maximum (FWHM) of the spectral main lobes were estimated and compared with the FWHM when $\theta = \theta_0$, to obtain the relative spectral broadening. To be able to compare the FWHM value for different tracking angles, (3.11) was used to estimate the axial velocity components, v_z, of the flow. The spectral broadening and the maximum power were visualized as functions of the velocity calibration error, allowing the bias and sensitivity of angle correction based on either parameter to be evaluated.

3.3.3 *In Vitro* Recordings

To investigate the performance of the 2-D tracking Doppler method for arbitrary tracking angles, recordings were done using a flow phantom for which the correct beam-to-flow angle was easy to identify. The flow phantom consisted of a silicon tube with an inner diameter of 6 mm, coupled to a flow loop driven by the PhysioPulse 100 Flow System (Shelley Medical Image Technologies, London, ON, Canada), giving a slowly pulsating flow. However, only a short time period with approximately constant flow velocities was used for the recording. The tube was partly surrounded by a stiff silicon layer, creating an imaging distance of approximately 3.7 cm and a beam-to-flow angle of 73°. The phantom was filled with a blood-mimicking fluid that has been tested and described by Ramnarine *et al.* [20].

A longitudinal cross section of the tube was imaged using a SonixMDP ultrasound scanner with a 5 MHz linear probe and a SonixDAQ for channel data acquisition (Ultrasonix, Richmond, BC, Canada). The acquisition consisted of continuous plane wave transmissions and the RF channel data was beamformed and complex demodulated offline using Matlab (The MathWorks Inc., Natick, MA). The acquisition setup and post-processing parameters are listed in Table 3.1.

A region of interest (ROI) with center in the middle of the tube was chosen from a B-mode image. Signals from lines of varying slopes centered in the middle of the ROI were extracted and processed using the algorithm given in Section 3.2.1. Both velocity-time spectra and power-velocity plots were used to investigate properties of the

2-D tracking Doppler method. The power-velocity plots were generated by averaging spectral estimates from 100 temporal segments of length 120 with an overlap of 119.

3.3.4 Velocity Calibration Analysis

Repeated measurements of *in vitro* flow were performed using the setup described in Section 3.3.3, with beam-to-flow angles of 63°, 73° and 83°. For each measurement, different directions were tracked with an angular step of 0.2° for the recordings with beam-to-flow angles of 63° or 73°, and an angular step of 0.1° for the recordings with a beam-to-flow angle of 83°. The flow angle was then automatically estimated in two different ways: by minimizing the FWHM, or by maximizing the peak value in the corresponding 2-D tracking Doppler spectrum. The velocity calibration percentage errors, e_{pct}, of the resulting angles, θ, were calculated using the formula

$$e_{pct} = \frac{1/\cos\theta - 1/\cos\theta_0}{1/\cos\theta_0} \cdot 100 \ , \tag{3.14}$$

where θ_0 was measured from B-mode images of the tubes. Both methods for velocity calibration were evaluated by estimating the mean and the standard deviation of 10 independent angle estimates for each of the three beam-to flow angles.

The velocity calibration errors resulting from the minimum FWHM estimates were plotted and compared with the velocity calibration errors expected when using manual angle correction, e.g., from the B-mode or color flow image. To illustrate the potential error which can occur when performing manual angle correction, it was assumed that the Doppler angle can be estimated within ±3°.

3.3.5 *In Vivo* Recordings

The 2-D tracking Doppler method was tested in a patient with a moderate carotid stenosis. The study was approved by The Regional Committee for Medical and Health Research Ethics (REC) in Trondheim, Norway. A color flow image of the artery, recorded with a high-end ultrasound scanner, Vivid E9 (GE Vingmed Ultrasound, Horten, Norway), is shown in Fig. 3.2. Narrowing of the artery, resulting from plaque formation, is causing a high-velocity jet to be formed.

Recordings for the 2-D tracking Doppler method were done in the same way as for the *in vitro* recordings, using the SonixMDP ultrasound scanner with a SonixDAQ for channel data acquisition. The region of interest (ROI) was placed in the stenotic part of the carotid bifurcation. The beam-to-flow angle was estimated, by visual inspection of color flow images, to be approximately 50°. However, it may have varied to some extent during the heart cycle. The acquisition setup and post-processing parameters are listed in Table 3.1.

The tracking line was probed to find the point that maximized the SNR for the conventional PW Doppler method, and a point close to the beginning of the line was selected.

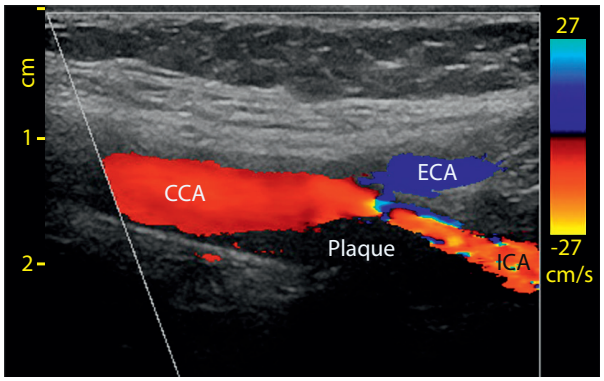

Figure 3.2: A color flow image overlaid on a B-mode image of a carotid artery with moderate carotid stenosis. The image shows the common carotid artery (CCA) bifurcation which divides into the external carotid artery (ECA) and the internal carotid artery (ICA). Plaque formation causes a high velocity jet to be formed, depicted in orange color in the lower right of the image. The recording was done using a high-end Vivid E9 ultrasound scanner.

Table 3.1: Parameters

Acquisition setup		Post-processing parameters		
Parameter	Value	Parameter	*In vivo* value	*In vitro* value
Tx center frequency	5 MHz	Tracking length	1 cm	1.5 cm
Pulse periods	2.5	Window	Hamming	Hamming
PRF	8 kHz	Window length	80 samples	120 samples
F-number	1.4	HP-filter	FIR, order 50	FIR, order 50
		HP-filter cutoff	400 Hz	400 Hz

3.4 Results

3.4.1 Validation of Signal Model

In Fig. 3.3, 2-D tracking Doppler spectra generated from Doppler signals simulated using Field II, and 2-D tracking Doppler spectra predicted by the signal model are shown. The results show good agreement between the spectra from the two models.

3.4.2 Investigations of the Tracking Angle Sensitivity

Fig. 3.4 shows relative broadening and maximum power in Doppler power spectra, predicted using the signal model (3.9). The black line (left y-axis) shows relative broadening of the 2-D tracking Doppler spectra and the gray dashed line (right y-axis) shows the maximum power, plotted with respect to the velocity calibration percentage

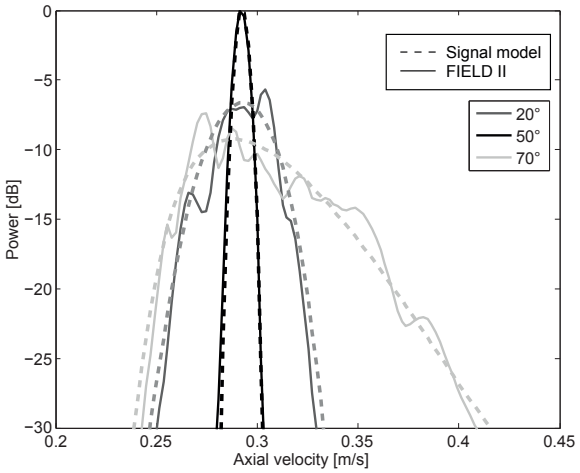

Figure 3.3: 2-D tracking Doppler spectra generated for validation of the signal model (dashed lines) with the Field II software (solid lines).

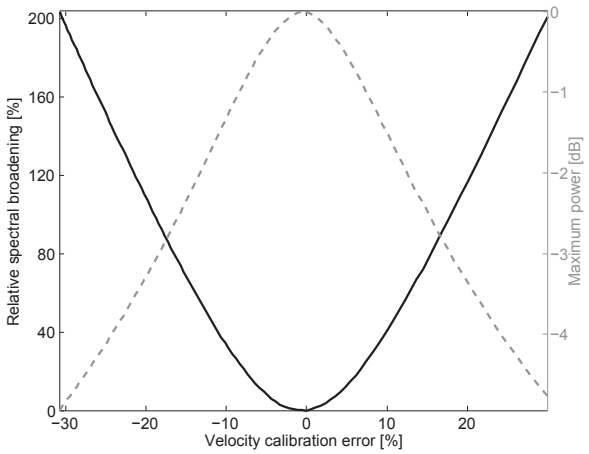

Figure 3.4: Relative broadening (solid line) and maximum power (dashed line) plotted with respect to the velocity calibration error. The FWHM of the spectral main lobe of predicted velocity spectra were estimated for varying θ and compared with the FWHM when $\theta = \theta_0$. The FWHM is at its minimum and the maximum power is at the maximum when the tracking angle is equal to the beam-to-flow angle.

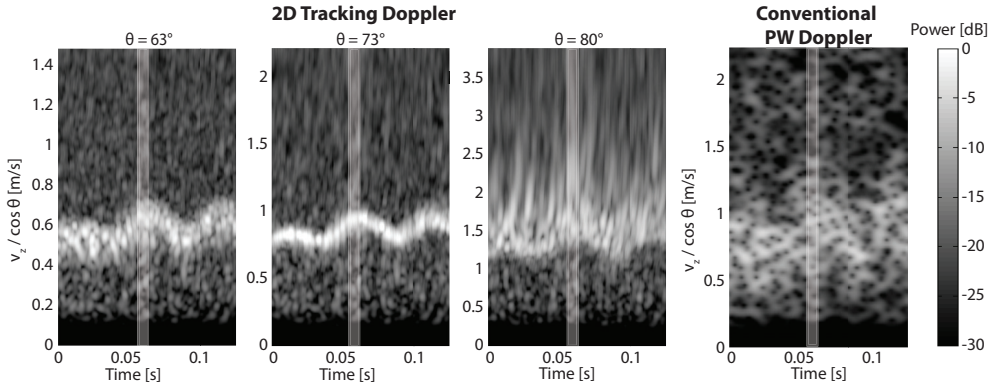

Figure 3.5: Velocity spectra generated from an *in vitro* recording of flow in a straight tube. The three left spectra are generated using the 2-D tracking Doppler method with three different tracking angles, θ. The rightmost spectrum is generated using a conventional PW Doppler method. The velocity axes are scaled using the limits $v_{min} = 0$ and $v_{max} = v_{Nyq}/\cos\theta$, to make the spectra comparable for different tracking angles. The dynamic range in decibels is given by the color bar. The white transparent lines mark the time period used when generating the power-velocity plots in Figs. 3.6 and 3.7(a).

error (3.14). The plot shows that the velocity resolution is highest and the peak power is largest for $\theta = \theta_0$.

In Fig. 3.5, velocity spectra generated from an *in vitro* recording of flow in a straight tube are shown. The 2-D tracking Doppler spectrum with the correct tracking trajectory angle ($\theta = \theta_0 = 73°$) seems to provide the highest contrast and velocity resolution. From this spectrum, it is observed that the flow has a slightly oscillating character around a center velocity of approximately 0.9 m/s. Broadening of the spectra is observed when using incorrect tracking angles. This is most evident for the spectrum with the largest tracking angle.

Figs. 3.6 and 3.7 show power-velocity plots from the *in vitro* recording, at times marked with vertical lines in Fig. 3.5, compared to those predicted using (3.9) and (3.13).

In Fig. 3.6, 2-D tracking Doppler spectra with $\theta = \theta_0 = 73°$ are compared with conventional PW Doppler spectra. The predicted spectra correspond well to the *in vitro* spectra, with some differences due to estimator variance. In addition to an improved velocity resolution, due to the more narrow spectral peaks, the 2-D tracking Doppler spectra have a signal-noise-ratio (SNR) that is about 9 dB higher than the conventional PW Doppler spectra.

In Fig. 3.7 a), 2-D tracking Doppler spectra generated from the *in vitro* recording using three different tracking trajectory angles are shown. Fig. 3.7 b), shows the corresponding velocity spectra predicted by (3.9). To be able to compare the spectra for different tracking angles, equation (3.11) was used to estimate the axial velocity

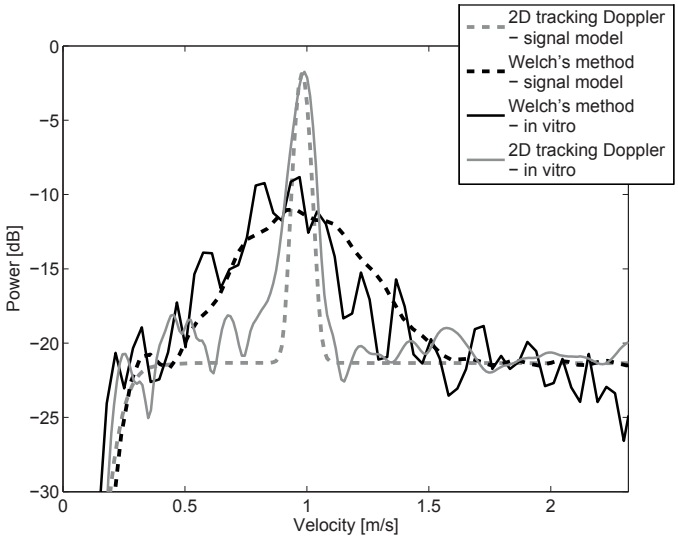

Figure 3.6: Velocity spectra generated from the *in vitro* recording and their corresponding predicted velocity spectra. Short time periods, marked with white vertical lines in Fig. 3.5, were averaged when generating the spectra. Only the 2-D tracking Doppler spectrum with $\theta = \theta_0 = 73°$ and the conventional spectrum are shown here. An increase in velocity resolution may be observed in the 2-D tracking Doppler spectra compared with the conventional PW Doppler spectra.

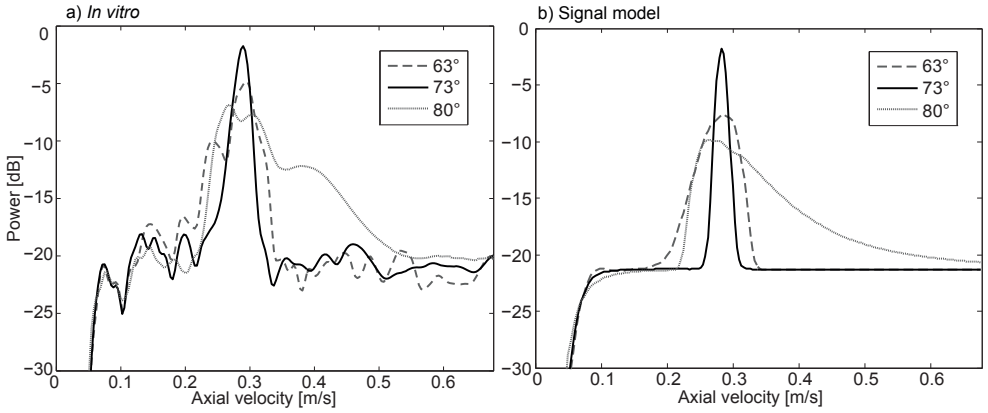

Figure 3.7: (a) Velocity spectra generated from the *in vitro* recording and (b) their corresponding predicted velocity spectra. Short time periods, marked with white transparent lines in Fig. 3.5, were averaged when generating the *in vitro* spectra. Eq. (3.11) was used to estimate the axial velocity component, v_z, of the flow. The highest velocity resolution is found when using the correct tracking angle.

component, v_z, of the flow. The spectra found using the correct tracking angle have the highest velocity resolution and the maximum power. The spectra with $\theta = 63°$ and $\theta = 80°$ seem to have a spectral leakage towards the low and the high velocity region respectively. The same trends are found in the predicted spectra as in the *in vitro* spectra, although the difference in maximum power is slightly larger in the predicted spectra.

3.4.3 Velocity Calibration

In Table 3.2, the mean values and the standard deviations of angle estimates using the minimum FWHM and the maximum power are given. The results show that the mean values of the angles estimated by the maximum power are closer to the angles measured from the B-mode images than the angles estimated by the minimum FWHM. However, the angles estimated by the minimum FWHM have lower standard deviations than the angles estimated by the maximum power.

Table 3.2: Results from the Velocity Calibration Analysis

	63°	73°	83°	Total error
Estimated angle by min. FWHM (°)	63.66 ± 1.05	72.78 ± 0.68	83.28 ± 0.35	0.24 ± 0.75
Velocity calibration error by min. FWHM (%)	2.46 ± 3.70	-1.1 ± 3.85	4.4 ± 5.61	1.92 ± 4.74
Estimated angle by max. power (°)	62.86 ± 2.06	73.10 ± 1.80	83.17 ± 0.37	0.04 ± 1.60
Velocity calibration error by max. power (%)	0.03 ± 7.07	1.55 ± 10.06	2.75 ± 5.63	1.44 ± 7.81

The circles in Fig. 3.8 give the velocity calibration errors in percent for 30 measurements when using the minimum FWHM for Doppler angle estimation. The two lines give the estimated maximum velocity calibration errors for the manual angle correction, given a $\pm 3°$ error in the chosen angle. For the investigated angles, the measured calibration errors for the 2-D tracking Doppler method are smaller than the maximum calibration errors for the conventional approach.

3.4.4 *In Vivo* Imaging

In Fig. 3.9, a conventional PW Doppler spectrum and two 2-D tracking Doppler spectra generated from an *in vivo* recording are shown. The recording was done on a patient with a moderate carotid stenosis. The 2-D tracking Doppler spectrum with

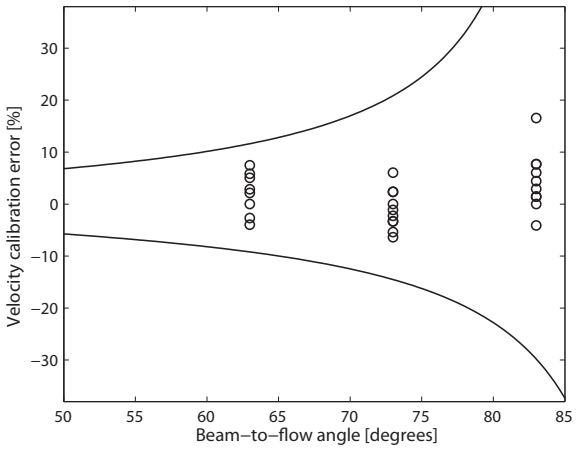

Figure 3.8: Experimental results using the 2-D tracking Doppler method for velocity calibration. The circles give the velocity calibration errors in percent for 30 measurements of *in vitro* flow. The Doppler angles used for velocity calibration were estimated by using the minimum FWHM of the velocity spectra. The two lines gives the velocity calibration errors for the manual angle correction, given a $\pm 3^\circ$ error in the chosen angle.

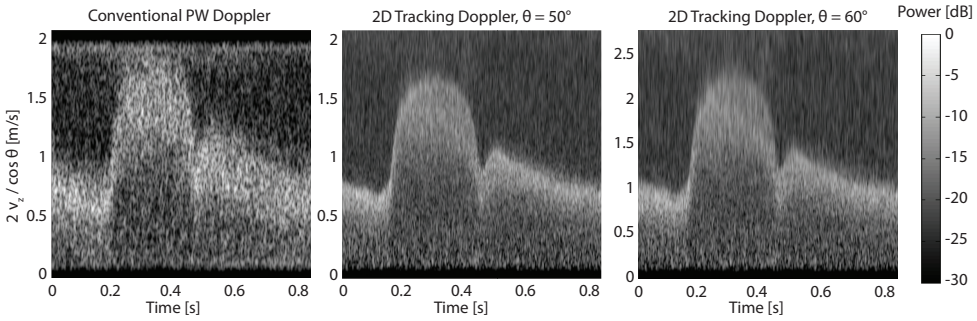

Figure 3.9: Velocity spectra generated from an *in vivo* recording of flow in a carotid artery at a stenotic region. The left spectrum is generated using a conventional PW Doppler method. The two rightmost spectra are generated by the 2-D tracking Doppler method, using tracking angles of 50° and 60°. The velocity axes are scaled using the limits $v_{min} = 0$ and $v_{max} = 2v_{Nyq}/\cos\theta$, to make the spectra comparable for different tracking angles. A higher velocity resolution may be observed in the 2-D tracking Doppler spectrum with $\theta = 50^\circ$, compared with the 2-D tracking Doppler spectrum with $\theta = 60^\circ$. The dynamic range in decibels is given by the color bar.

$\theta = 50°$ has a better velocity resolution than the 2-D tracking doppler spectrum with $\theta = 60°$. By visual inspection, an estimate of the maximum velocity was found to be approximately 1.6 m/s when using the suggested spectral estimation technique, whereas an estimate of this parameter could not be extracted from the conventional PW Doppler spectrum.

3.5 Discussion

In this work, we have investigated properties of the 2-D tracking Doppler method when the tracking direction differs from the flow direction. A motivation for such a study is estimation of the beam-to-flow angle, which is essential for calibration of velocity spectra.

The 2-D tracking Doppler method was investigated for varying tracking angles using simulations, in vitro and in vivo experiments, focusing on situations with high beam-to-flow angles, where limitations in velocity estimation and calibration are most evident. It was shown that when applied to the same data, the 2-D tracking Doppler method reduced spectral broadening and increased the SNR compared with a conventional spectral estimation technique, and further, that it can give information about the beam-to-flow angle. The latter is possible because of relative broadening of the velocity spectrum at erroneous tracking angles.

An erroneous tracking trajectory results in summation of the signal along lines that extend through the side lobes of the point spread function, causing broadening of the velocity spectra. Spectral leakage toward the low- and the high-velocity region was observed for spectra with tracking angles that were too small or too large, respectively. This asymmetric behavior of the spectra may be due to the side lobes of the point spread function, because they are not symmetric around point 3 in Fig. 3.1.

The improved velocity resolution in the 2-D tracking Doppler spectra over conventional spectra is due to the increased transit time, especially at large beam-to-flow angles. When using a large tracking length in the 2-D tracking Doppler method, a long transit time is achieved and the transit time broadening is minimal. However, in complex flow fields, a shorter tracking distance is more appropriate, because the presence of velocity gradients will broaden the spectrum. A compromise in the tracking length must therefore be found. The suitable tracking length for the *in vivo* test case was based on apparent uniform flow in the color flow image, which was found to be approximately 1 cm. A longer tracking length was set for the more uniform *in vitro* flow. The temporal window length was reduced for high velocities because of the tracking distance limitation. Averaging in the flow direction could be done for low velocities, but at the cost of extra computational time. Because of the greater interest in high velocities for this examination, this was not deemed necessary.

Conventional power spectral estimation [(3.5) and (3.13)] was used as a reference in simulations, *in vitro* and *in vivo*. The poor spectral resolution of this approach, found especially in the in vitro comparison, is partly due to the large beam-to-flow angles. The effect is also enhanced by the short temporal excerpt of the flow, containing only small oscillations around the highest velocities of a sinusoidal waveform. These

oscillations were not resolvable by the conventional approach, resulting in a very poor representation of the power spectrum; however, the sinusoidal waveform would be recognizable in a longer temporal segment. The quality of the conventional spectra was also influenced by acquisition parameters, which were more suited for the tracking technique than regular spectral estimation. The short pulse length, which is preferable for tracking, limits the SNR, as will the use of unfocused transmit waves. However, the latter is required for tracking of lateral flow.

2-D tracking Doppler spectra were calculated for different tracking angles by using an extended version of the signal model applied in [5]. The predicted spectra showed good agreement with both the *in vitro* results and the spectra generated from the Field II simulated signal, although the signal model does not contain any restrictions on the size of the transmit aperture. An infinitely large plane wave is assumed and no edge effects are therefore present. Small differences between the spectra generated from the Field II simulated signal and the signal model may be observed in Fig. 3.3 because of estimator variance. It is assumed in the model that the blood flow is in the imaging plane. Presence of out-of-plane flow would shorten the effective tracking length and, hence, broaden the main lobe of the velocity spectrum.

The *in vitro* recordings were done on flow in a straight tube, where a near-parabolic flow profile was expected. The mid-point of the tracking trajectory was placed in the middle of the tube. An erroneous tracking angle was therefore expected to result in broadening toward lower velocities *in vitro*, compared with the spectra predicted using the signal model, for which an infinitely large blood vessel of uniform velocity was assumed. However, no significant difference between the *in vitro* spectra and the signal model spectra was found. This may be due to the short tracking lengths applied for the low velocities. Using the *in vitro* spectra generated with a tracking angle of 63° as an example, the radial distance, R, from the center of the tube can be calculated using the formula $R = 0.5 \cdot N_w/PRF \cdot v \cdot \sin(10°)$. For v = 0.4 m/s, this corresponds to a distance of 0.5 mm, which is much less than the tube radius.

Both the minimum FWHM and the maximum power of the spectra were investigated as candidates for Doppler angle estimation. Repeated measurements of *in vitro* flow were performed and the statistical analysis of the angle estimates (Table 3.2) showed that both methods could provide reliable estimates of the true flow angle, and could therefore be used for automatic angle correction of velocity spectra. However, the standard deviations of the velocity calibration errors were found to be larger for the maximum power method than the minimum FWHM. Also, if the technique is to be used as a guide for the examiner during an investigation, spectral broadening is the most attractive candidate because this may be easier to observe than changes in the SNR. The angles estimated by the minimum FWHM were somewhat biased for two of the investigated beam-to-flow angles. However, angles measured from B-mode images were used as a ground truth in the analysis. A possible inaccuracy in these measurements could explain the calculated bias in the angles estimated by the minimum FWHM.

In Fig. 3.8 the velocity calibration errors for the minimum spectral broadening method were compared with the velocity calibration errors for a conventional method. The results indicated that the 2-D tracking Doppler method gives better velocity

estimates than the conventional approach for large beam-to-flow angles, because all the velocity calibration errors for the 2-D tracking Doppler method were smaller than the velocity calibration errors resulting from a 3° erroneous Doppler angle. The validity of using ±3° as a maximum angle error for the conventional approach can be investigated further in a more comprehensive study. In any case, the maximum velocity calibration errors of the conventional method increase rapidly for large beam-to-flow angles, whereas the estimated velocity calibration errors of the 2-D tracking Doppler method has a standard deviation of less than 6% for all the investigated angles. The increased robustness of the 2-D tracking Doppler method for large beam-to-flow angles may facilitate reliable velocity estimation for angles above 60°. This can improve blood velocity estimation in regions with near-transversal flow, for instance in vascular imaging or when imaging the heart from a parasternal view.

The results in Fig. 3.9 indicate that also *in vivo*, the 2-D tracking Doppler method gives better velocity resolution than the conventional PW Doppler method. The SNR is poor in all spectra, but the velocity-time waveform may be easier to delineate in the 2-D tracking Doppler spectra, because the clutter aliasing is overlapping with the high velocities in the conventional spectrum. This ability of the tracking technique to resolve the ambiguity problem, when the maximum velocity is beyond the Nyquist limit, has earlier been shown for blood flow in the axial direction [4]. The SNR is somewhat better in the conventional PW Doppler spectrum than in the 2-D tracking Doppler spectrum. This may be due to out-of-plane motion, because the sample point for the conventional PW Doppler method was placed near the source of the jet, and not in the middle of the tracking line. The 2-D tracking Doppler spectrum in Fig. 3.9 with $\theta = 50°$ has a better velocity resolution than the other spectra. In the 2-D tracking Doppler spectrum with $\theta = 60°$ the high velocities are blurred, suggesting that the tracking angle is incorrect.

Further studies will include a more comprehensive patient study for evaluation of the 2-D tracking Doppler method, with respect to both spectral estimation and calibration. As a ground truth for the beam-to-flow angle, the results could be compared with vector Doppler or speckle tracking estimates. A challenge *in vivo* is that spatial velocity gradients are expected to broaden the spectra, which may reduce the angle sensitivity of the technique. Also, the flow direction may vary through the heart cycle, and in regions of complex flow the accuracy of the angle estimation may be limited. However, in many applications the primary interest is the quantification of high velocity flow, for instance in cases of valvular insufficiency or in stenotic regions where flow of less complexity can be found, e.g., in the laminar vena contracta of the jet. In these situations, the 2-D tracking Doppler technique should be applicable, and might provide angle-corrected velocity spectra with significantly higher spectral resolution than the conventional approach.

3.6 Conclusion

We have investigated how the 2-D tracking Doppler method depends on the tracking angle. The results showed that the 2-D tracking Doppler method can provide PW

Doppler spectra with improved velocity resolution at large beam-to-flow angles, in addition to information about the Doppler angle. Using a signal model, it was shown that the spectra have lowest bandwidth and maximum power when the tracking angle is equal to the beam-to-flow angle. New techniques for velocity calibration were tested *in vitro*, showing improved performance for large beam-to-flow angles compared with a conventional technique. With an *in vivo* example, it was demonstrated that the method is suitable for vascular Doppler assessment.

References

[1] L. Wilson, "Description of broad-band pulsed Doppler ultrasound processing using the two-dimensional Fourier transform," *Ultrasonic imaging*, vol. 315, pp. 301–315, 1991.

[2] W. Mayo, "Two dimensional processing of pulsed Doppler signals," *US Patent 4,930,513*, 1990.

[3] T. Loupas and R. W. Gill, "Multifrequency Doppler: Improving the Quality of Spectral Estimation by Making Full Use of the Information Present in the Backscattered RF Echoes," *IEEE transactions on ultrasonics, ferroelectrics, and frequency control*, vol. 41, no. 4, pp. 522–531, 1994.

[4] H. Torp and K. Kristoffersen, "Velocity matched spectrum analysis: A new method for suppressing velocity ambiguity in pulsed-wave Doppler," *Ultrasound in medicine & biology*, vol. 21, no. 7, pp. 937–944, 1995.

[5] T. Fredriksen, I. K. Ekroll, L. Lovstakken, and H. Torp, "2-D Tracking Doppler: A New Method to Limit Spectral Broadening in Pulsed Wave Doppler," *IEEE transactions on ultrasonics, ferroelectrics, and frequency control*, vol. 60, no. 9, pp. 1896–1905, 2013.

[6] C. P. Oates, a. R. Naylor, T. Hartshorne, S. M. Charles, T. Fail, K. Humphries, M. Aslam, and P. Khodabakhsh, "Joint recommendations for reporting carotid ultrasound investigations in the United Kingdom.," *European journal of vascular and endovascular surgery : the official journal of the European Society for Vascular Surgery*, vol. 37, pp. 251–61, Mar. 2009.

[7] B. Dunmire, K. W. Beach, K. Labs, M. Plett, and D. E. Strandness, "Cross-beam vector Doppler ultrasound for angle-independent velocity measurements.," *Ultrasound in medicine & biology*, vol. 26, pp. 1213–35, Oct. 2000.

[8] P. Tortoli, G. Bambi, and S. Ricci, "Accurate Doppler angle estimation for vector flow measurements.," *IEEE transactions on ultrasonics, ferroelectrics, and frequency control*, vol. 53, pp. 1425–31, Aug. 2006.

[9] S. Ricci, S. Diciotti, L. Francalanci, and P. Tortoli, "Accuracy and reproducibility of a novel dual-beam vector Doppler method.," *Ultrasound in medicine & biology*, vol. 35, pp. 829–38, May 2009.

[10] J. M. Mari, M. Khoo, C. Riga, G. Coppola, C. Bicknell, and C. G. Caro, "Index proposal and basic estimator study for quantification of oscillation of the secondary flow pattern in tortuous vessels.," *Ultrasonics*, vol. 52, pp. 294–305, Feb. 2012.

[11] J. Kortbek and J. A. Jensen, "Estimation of velocity vector angles using the directional cross-correlation method.," *IEEE transactions on ultrasonics, ferroelectrics, and frequency control*, vol. 53, pp. 2036–49, Nov. 2006.

[12] J. Jensen and N. Oddershede, "Estimation of velocity vectors in synthetic aperture ultrasound imaging," *IEEE Transactions on Medical Imaging*, vol. 25, no. 12, pp. 1637–1644, 2006.

[13] V. Newhouse, E. Furgason, G. Johnson, and D. Wolf, "The Dependence of Ultrasound Doppler Bandwidth on Beam Geometry," *IEEE Transactions on Sonics and Ultrasonics*, vol. 27, pp. 50–59, Mar. 1980.

[14] V. L. Newhouse, D. Censor, T. Vontz, J. a. Cisneros, and B. B. Goldberg, "Ultrasound Doppler probing of flows transverse with respect to beam axis.," *IEEE transactions on bio-medical engineering*, vol. 34, pp. 779–89, Oct. 1987.

[15] V. Newhouse, K. Dickerson, D. Cathignol, and C. J.-Y., "Three-dimensional vector flow estimation using two transducers and spectral width," *IEEE transactions on ultrasonics, ferroelectrics, and frequency control*, vol. 41, no. 1, pp. 90–95, 1994.

[16] P. Tortoli, G. Guidi, and C. Atzeni, "A review of experimental transverse Doppler studies," *IEEE transactions on ultrasonics, ferroelectrics, and frequency control*, vol. 41, no. I, pp. 84–89, 1994.

[17] C.-K. Yeh and P.-C. Li, "Doppler angle estimation using AR modeling.," *IEEE transactions on ultrasonics, ferroelectrics, and frequency control*, vol. 49, pp. 683–92, June 2002.

[18] P.-L. Lee, Y.-H. Chou, J.-C. Hsieh, and H. K. Chiang, "An improved spectral width Doppler method for estimating Doppler angles in flows with existence of velocity gradients.," *Ultrasound in medicine & biology*, vol. 32, pp. 1229–45, Aug. 2006.

[19] J. Jensen, "Field: A program for simulating ultrasound systems," *Med. Biol. Eng. Comput.*, vol. 34, pp. 351–353, 1996.

[20] K. V. Ramnarine, D. K. Nassiri, P. R. Hoskins, and J. Lubbers, "Validation of a new blood-mimicking fluid for use in doppler flow test objects," vol. 24, no. 3, pp. 451–459, 1998.

Chapter 4

Quantification of Mitral Regurgitation Using PW Doppler and Parallel Beamforming

Tonje D. Fredriksen, Hans Torp and Torbjørn Hergum
Medical Imaging Lab and Deptartment of Circulation and Medical Imaging
Norwegian University of Science and Technology (NTNU)
Trondheim Norway

Delayed decision to replace or repair a defective mitral valve may lead to worsening ventricular function. A correct diagnosis of the severity of the regurgitation that results from a defective mitral valve is therefore important. This work takes advantage of the latest developments of ultrasound matrix probes and modern acquisition with many parallel beams to develop a Doppler-based method for a semi-quantitative evaluation of mitral regurgitation.

By using parallel beamforming, several beams from closely-spaced regions can be acquired simultaneously. Velocity spectra from all these regions can then be generated. The idea behind the proposed method is to combine velocity spectra from all the beams into one composite velocity spectrum and add information about the size of a potential regurgitant jet to the spectrum. This is achieved by color coding the composite velocity spectrum with colors representing the number of beams intersecting with the jet.

Ultrasound data produced from simulations of flow in straight tubes were used to evaluate the method. The colored spectra were successful in giving information about the approximate size of the tubes. A colored spectrum generated from an *in vivo* ultrasound recording of a regurgitant jet is also presented, showing that the method is applicable for clinical use.

4.1 Introduction

Mitral regurgitation (MR) is one of the most common valve defects. In fact, it has been observed that a small degree of physiological MR can be detected on Doppler echocardiography in up to 80% of all Americans [1]. MR can add a significant load to the heart and can be a life threatening disease. Correct and timely diagnosis is therefore vital to determine which people are in need of surgery.

Characterization of the severity of regurgitant lesions is among the most difficult problems in valvular heart disease. Two-dimensional color Doppler jet area measurements are widely relied on to estimate mitral regurgitation severity. A number of factors have been reported to influence the accuracy of these measurements. These include instrument settings, geometric orifice characteristics, blood viscosity, and jet properties such as momentum, velocity, pressure gradient, and eccentricity.

Real time 3-D echocardiography is a good tool for evaluating mitral valve diseases such as stenosis and prolapse [2], but the resolution is not yet good enough for direct planimetry of the regurgitant orifice.

Another suggestion for quantification of MR is the proximal isovelocity surface area method (PISA) [3], which seems to work well in some studies [4]. It does, however, underestimate functional MR, and overestimates the regurgitant volume for patients with prolapse because of non-optimal flow convergence regions. The method also assumes circular orifices, while the majority of patients have non-circular orifices as imaged by 3-D color flow [5].

With the recent introduction of commercially available 3D ultrasound scanners, the ability of ultrasound to deliver real time imaging has been challenged due to the large amount of data that needs to be acquired for each volume, and it is common to stitch together data from several heart cycles to obtain good quality images [6]. To speed up the acquisition of ultrasound data it is common to use parallel receive beamforming [7, 8]. This means that the transmitted ultrasound beam is configured to be wide, and that several beamformers processes the received data to obtain several narrow received beams in parallel from within the region of the wide transmitted beam. This means that the acquisition time can be reduced by a factor equaling the number of receive beamformers, enabling real time 3-D images.

For spectral Doppler, parallel beamforming can be used to add spatial information to the spectra. It is possible to insonify the whole region using a single, wide transmitted beam, and just use parallel receive beams to obtain lateral resolution. Such a configuration can be used for instance when imaging regurgitant jets. With a single transmit direction it is possible to use continuous acquisition for the Doppler processing. This will give the same resolution in time as conventional pulsed wave (PW) Doppler, with the added benefit of the lateral resolution provided by the multiple receive beams. With a matrix array transducer these receive beams can cover a three dimensional region in space, enabling the estimation of a Doppler spectrum from each spatial location.

In this study we have explored the possibilities given by the introduction of 3-D ultrasound, using parallel receive processing in combination with HPRF Doppler and continuous acquisition, as described above. We believe that such a combination can

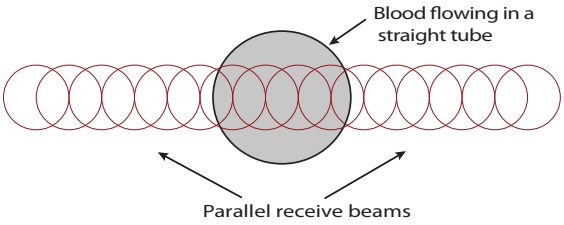

Figure 4.1: 16 parallel beams were aligned across a tube in the simulation setup, spanning a total width of 1.7cm. The tube diameter varied from 2mm to 8mm.

be used to obtain enhanced qualitative and quantitative measures of cardiac function, in particular for evaluation of the severity of regurgitant jets.

4.2 Methods

We have developed a method to semi-quantitatively estimate the size of regurgitant jets using spectral Doppler and parallel beamforming. Using a plane wave on transmit, multiple simultaneous velocity spectra are generated from parallel receive beams, and combined into an enhanced velocity spectrum. This composite velocity spectrum has colors representing the number of beams intersecting the jet.

The algorithm for determining the color of each velocity bin is based on thresholding. After generating Doppler frequency spectra by the Welch's method [9] the data are normalized, using the maximum power of the spectrum. For each beam, the velocity bins in the spectrum are then thresholded and given a value of one or zero. By summing the resulting binary spectra, the velocity bins in the combined spectrum will consist of values from 0 to the total number of beams. These numbers are then represented by different colors.

Both ultrasound simulations and *in vivo* recordings were used for development and testing.

4.2.1 Straight Tube Simulations

To investigate the performance of the method for varying jet sizes, repeated simulations were performed of blood moving in a straight tube with varying diameter (2-8 mm). Backscattered ultrasonic signals were generated using the Field II software [10], which is based on the spatial impulse response estimation as described by Tupholme [11] and Stephanishen [12]. The blood was modeled as a collection of randomly distributed point scatterers with normally distributed scattering amplitude. The density of the scatterers was chosen to assure Gaussian distributed RF-signals. The point scatterers were moved with a uniform and constant velocity of 4 m/s.

A 2-D phased array transducer model was used for all simulations. The parallel beams were aligned across the tube, as sketched in Fig. 4.1. The total receive beam

angle was 10°, giving a measurement width of 1.75 cm at 10 cm depth. Details regarding the ultrasound simulation setup can be found in Table 4.1.

Table 4.1: Simulation Setup

Center frequency	2.5 MHz
Pulse periods	5
PRF	20 kHz
Receive focus Az	0.1 m
Parallel beams	16

The power threshold used for deciding which of the beams that intersect with the flow was chosen to 10 dB below the maximum power. Tube diameters were calculated using the receive beam spacing multiplied with the number of beams above the threshold. Performance was evaluated in terms of the ability to qualitatively distinguish between the different tube sizes, by looking at the colors of the generated spectra.

4.2.2 *In Vivo* Recordings

The method was tested on an *in vivo* recording of mitral regurgitation for feasibility. A Vivid E9 (GE Vingmed Ultrasound, Horten, Norway) equipped with a 4V cardiac probe was modified to acquire 3-D high pulse repetition frequency Doppler data with parallel receive beams.

The recordings were done at the vena contracta, just beneath the orifice. One plane transmit beam and 16 parallel receive beams were used when recording. The region of interests (ROI) was about 9 x 9 mm. The receive beams had a lateral resolution of 3.6 mm and were equally distributed over the ROI, as sketched in Fig. 4.2.

4.3 Results and Discussion

When imaging the heart for diagnostic purposes the sonographer is used to interpret velocity spectra and color flow images. By combining characteristics from both of these image modalities we wanted to develop a method that is easy to employ.

This method adds spatial information to PW Doppler spectra. It gives information about the size of regurgitant jets, but can also be a tool when searching for the jet and positioning the probe. By using many parallel beams it is easier to locate the jet, so the measurement will be easier to perform and less time-consuming.

4.3.1 Straight Tube Simulations

2-D simulations were done of blood moving in a straight tube with a velocity of 4 m/s. Fig. 4.3 shows 16 velocity spectra that are combined into one color coded velocity spectrum. The spectra are generated from a simulation of blood flowing in a tube

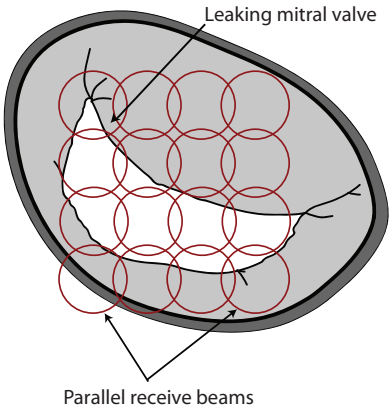

Figure 4.2: 16 parallel beams were equally distributed over the orifice in the *in vivo* setup. Spectra from all of these beams were generated and combined to give information about the number of beams intersecting with the regurgitant jet.

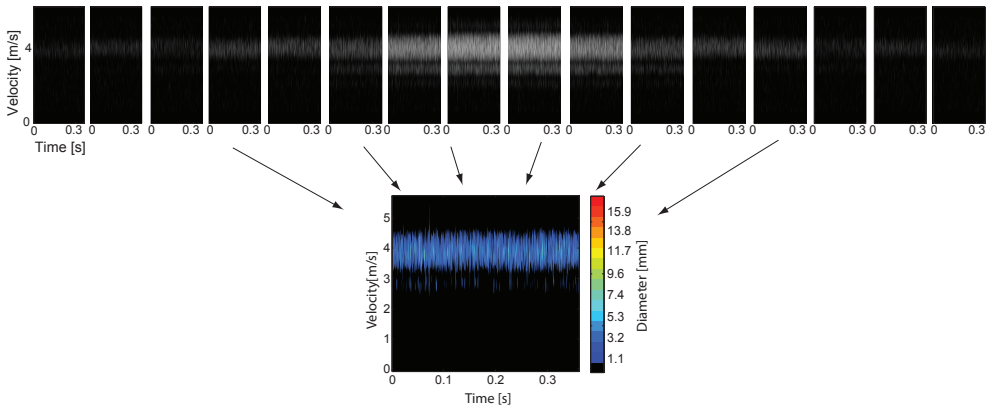

Figure 4.3: Flow in a 2mm in diameter straight tube was simulated and recorded with 16 parallel beams. Velocity spectra from all the beams (top) were combined into a composite velocity spectrum (bottom). The colors and the colorbar gives information about the diameter of the tube.

with a diameter of 2 mm. Only some of the beam's main lobes intersect with the flow. Still signal is found in all of the beams due to sidelobes. Thresholding with a value higher than the noise level is therefore necessary. Fig. 4.4 shows a color spectrum generated from blood flowing in a tube with a diameter of 8 mm. The colors given in the colorbars gives the estimated diameters of the tubes.

The color spectra in Figs. 4.3 and 4.4 are colored with several colors even if the true flow is coherent and fixed in space. This is because of natural variations in the

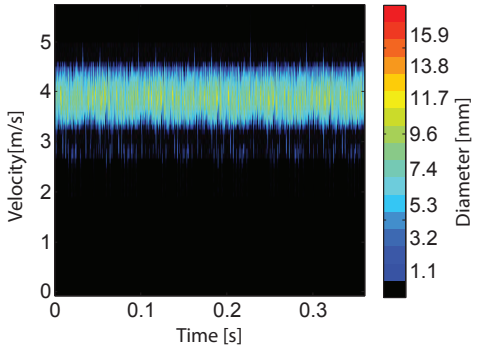

Figure 4.4: Color coded velocity spectra from a Field II simulation of blood flow in a 8 mm in diameter straight tube. The colors and the colorbar gives information about the diameter of the tube. The flow is constant and uniform.

power in the ultrasound data. Still, it is possible to choose the most dominant color in the spectrum, and thereby get a semi-quantitative measure of the tube size. The 2 mm in diameter tube in Fig. 4.3 is mostly colored blue and thus correctly indicates that the tube is about 2 mm in diameter. The 8 mm in diameter tube in Fig. 4.4 is mostly colored green which indicates that the tube is about 7-8 mm in diameter.

4.3.2 *In Vivo* Recordings

Fig. 4.5 shows a color spectrum that was generated from an *in vivo* recording of mitral regurgitation. The velocity spectrum is colored red in the low velocity area and green or yellow in the high velocity area. This indicates that all the beams receive signals from slow moving blood during inflow, while only about half of the beams receive signals from the high velocity jet.

The spatial resolution of the beams limits the differences in jet size that you can measure. A cardiac probe typically has a lateral resolution of $\sim$4 mm, which means that a lot of power is detected in many of the beams adjacent to the jet. Beams that don't intersect with the jet can receive some signal through the sidelobes. Surrounding blood is also pulled along with the jet resulting in a jet that is not well defined. All these factors make it troublesome to decide a robust threshold. The method should therefore only be regarded as an approximate measure of the jet size.

4.4 Conclusion

The method was successful in generating velocity spectra that contains information about the lateral extent of high velocity flow. The spectra give information about the size of regurgitant jets, in addition to all the information the cardiologist is used to from a pulsed wave Doppler recording. The thresholding algorithm and the placement

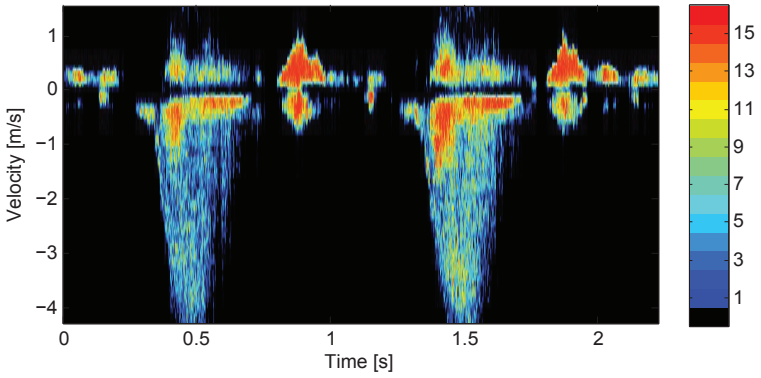

Figure 4.5: Color coded velocity spectrum from a regurgitant jet in a patient. The colors represent the number of beams (0 - 16) that intersects with flow of a certain velocity, and are given in the colorbar. Low velocity flow is colored red which indicates that slow moving blood is found in all of the parallel beams. The high velocities are colored blue/green indicating that a smaller number of beams intersects with the high velocity jet.

of the parallel beams should be optimized in future work. This will be done with the help of computed fluid dynamics simulations together with *in vitro* recordings.

References

[1] C. M. Otto and R. O. Bonow, *Valvular Heart Disease*. Elsevier Inc., 2009.

[2] L. Sugeng, P. Coon, L. Weinert, N. Jolly, G. Lammertin, J. E. Bednarz, K. Thiele, and R. M. Lang, "Use of real-time 3-dimensional transthoracic echocardiography in the evaluation of mitral valve disease," *Journal of the American Society of Echocardiography*, vol. 19, no. 4, pp. 413–421, 2006.

[3] F. Recusani, G. Bargiggia, A. Yoganathan, A. Raisaro, L. Valdes-Cruz, H. Sung, C. Bertucci, M. Gallati, V. Moises, and I. Simpson, "A new method for quantification of regurgitant flow rate using color doppler flow imaging of the flow convergence region proximal to a discrete orifice. an in vitro study," *Circulation*, vol. 83, pp. 594–604, Feb. 1991.

[4] P. Vandervoort, J. Rivera, D. Mele, I. Palacios, R. Dinsmore, A. Weyman, R. Levine, and J. Thomas, "Application of color doppler flow mapping to calculate effective regurgitant orifice area. an in vitro study and initial clinical observations," *Circulation*, vol. 88, pp. 1150–1156, Sept. 1993.

[5] P. Kahlert, B. Plicht, I. M. Schenk, R.-A. Janosi, R. Erbel, and T. Buck, "Direct assessment of size and shape of noncircular vena contracta area in functional versus organic mitral regurgitation using real-time three-dimensional echocardiography," *Journal of the American Society of Echocardiography*, vol. 21, pp. 912–921, Aug 2008.

[6] S. Brekke, S. I. Rabben, A. Støylen, A. Haugen, G. U. Haugen, E. N. Steen, and H. Torp, "Volume stitching in Three-Dimensional echocardiography: Distortion analysis and extension to real time," *Ultrasound in Medicine & Biology*, vol. 33, pp. 782–796, May 2007.

[7] D. P. Shattuck, M. D. Weinshenker, S. W. Smith, and O. T. von Ramm, "Explososcan: A parallel processing technique for high speed ultrasound imaging with linear phased arrays," *Journal of the Acoustical Society of America*, vol. 75, no. 4, pp. 1273–1282, 1984.

[8] T. Hergum, T. Bjastad, L. Løvstakken, K. Kristoffersen, and H. Torp, "Reducing color flow artifacts caused by parallel beamforming," *Ultrasonics, Ferroelectrics and Frequency Control, IEEE Transactions on*, vol. 57, pp. 830 –838, apr. 2010.

[9] P. Welch, "The use of fast fourier transform for the estimation of power spectra: A method based on time averaging over short, modified periodograms," *Audio and Electroacoustics, IEEE Transactions on*, vol. 15, pp. 70 – 73, jun 1967.

[10] J. A. Jensen, "Field: A program for simulating ultrasound systems," in *10th NordicBaltic Conference on Biomedical Imaging, vol. 4, supplement 1, part 1:351–353*, pp. 351–353, 1996.

[11] G. E. Tupholme, "Generation of acoustic pulses by baffled plane pistons," *Mathematika*, vol. 16, no. 02, pp. 209–224, 1969.

[12] P. R. Stepanishen, "Transient radiation from pistons in an infinite planar baffle," *J. Acoust. Soc. Am.*, vol. 49, no. 58, pp. 1629– 1638, 1971.

Chapter 5

Regurgitant Volume Quantification Using 3-D Pulsed Wave Doppler

Tonje D. Fredriksen, Bjørn Olav Haugen and Hans Torp
Medical Imaging Lab and Deptartment of Circulation and Medical Imaging
Norwegian University of Science and Technology (NTNU)
Trondheim Norway

The management of patients with valvular regurgitation is highly dependent on the results from echocardiography examinations. Echo guidelines recommend the use of quantitative methods when assessing the degree of regurgitation, but the existing methods are complex and time-consuming. This work presents and evaluates a new method for estimation of regurgitant flow volume, using only a single PW Doppler recording. By using a broad beam on transmit and many parallel beams on receive, both the vena contracta cross-section and the velocity-time integral may be estimated from the Doppler recording.

In the proposed method the receive beams are evenly distributed in a plane across the vena contracta. The received signals are interpolated in space and velocity spectra from all the interpolated beams are generated. A velocity-time region that only includes the high velocities of the jet is manually chosen from an average of the spectra. The cross-sectional area of the vena contracta is calculated by thresholding the average power in this velocity-time region for all the interpolated beams. The flow volume is then found by multiplying the area with the velocity-time integral.

The method was optimized and tested using simulations. A diverging transmit beam with an opening angle of 6° and Tukey apodization was found to be more suitable than plane wave transmission. Two different scenarios were investigated, where the number of receive beams were restricted to 16 or 64. Regurgitant flow volumes through circular orifices were accurately estimated using 64 parallel beams, whereas 16 parallel beams gave poor results. Power Doppler images were generated to give an indication of area and shape of the vena contracta, showing good correspondence for both circular- and crescent-shaped orifices.

5.1 Introduction

Mitral regurgitation (MR) is one of the most common valvular heart diseases. A severely regurgitant valve cause volume overload of the left ventricle, dyspnea to the patient with the development of heart failure and increased mortality. Surgical treatment may improve symptoms, prevent heart failure, and increase life expectancy. As a surgical procedure is both expensive and may pose a large risk to many patients, it is important to be able to separate between the severities of MR. Echocardiography is the principal imaging method to assess MR severity, but the limited accuracy of the methods is a significant challenge.

It is common to distinct whether MR is caused by abnormalities in the valve itself (organic MR) or if it is caused by left ventricular LV dilation and dysfunction (functional MR). Evaluation of both the anatomy of the mitral valve apparatus and the properties of the regurgitant flow is therefore important when assessing the severity of regurgitation. Today's practice for assessing MR severity is to do a series of measurements using several methods, including gray tone imaging, pulsed wave- (PW), continuous wave- (CW) and color Doppler imaging. The color Doppler images depends on several technical factors, such as display settings and the pulse repetition frequency (PRF), and may cause large interobserver variability.

Several methods have been proposed to improve the robustness of the MR estimates. One method is the proximal isovelocity surface area method (PISA) [1], where MR is evaluated by measuring the flow convergence zone proximal to the regurgitant valve using 2-D color Doppler. A hemispheric shape of the isovelocity surfaces in the inflow region of the regurgitation is assumed, and the size of a hemisphere, together with its velocity value measured by color Doppler, predicts the volume flow rate. By also estimating the maximum velocity in the regurgitant jet from a CW Doppler recording, the effective regurgitant orifice area (EROA) can be calculated. The regurgitant volume can then be found by multiplying the EROA with the velocity-time integral, found from the CW Doppler recording.

Other methods have investigated the narrowest part of the jet, called the vena contracta. The vena contracta represents a direct measure of the EROA and is independent of flow rate and driving pressure for a fixed vena contracta. Generally, the vena contracta width is measured using 2-D color Doppler and a circular geometry is assumed. However, it has been demonstrated that both PISA and vena contracta area underestimates functional MR. Still, current echo guidelines [2] recommend both methods as a quantitative measure of MR severity, when feasible.

With the advent of 3-D color Doppler volumetric data acquisition, it has been possible to provide information about the shape of the regurgitant flow. Asymmetry in the geometry of both PISA and the vena contracta area in functional MR have been shown [3, 4], explaining the underestimation of the EROA by the above described methods. 3-D PISA methods without any geometric assumptions have recently been developed and tested *in vitro* and *in vivo* by several investigators [5–7]. By directly measuring the area of the isovelocity surface, improved volume estimation accuracy has been shown, compared to the 2-D methods. However, the shape of the proximal isovelocity surface may be disturbed by adjacent flow events, such

as the flow through the left ventricular outflow tract. Other recent reports [8–10] have demonstrated improved accuracy in measures of vena contracta area by using multiplanar reformatting of the 3-D color Doppler data. Although there are many promising results, these 3-D color Doppler methods might be limited by variable display settings, low frame rate and time consuming procedures.

The flow volume of a regurgitant jet can be calculated by multiplying the orifice area with the velocity-time integral, found by CW Doppler or PW Doppler. CW Doppler has no depth resolution, but can, for instance, be used to find the maximum velocities along the ultrasound beam. PW Doppler, on the other hand, has depth resolution, but is limited by the Nyquist frequency. A high pulse repetition frequency (HPRF) mode can be applied to obtain a higher Nyquist frequency, meaning that signals from multiple range gates in depth are measured. As the velocity-time integral is calculated by taking the envelope of the velocity spectrum, errors may be introduced due to spectral broadening. Another challenge is that the velocities and the area need to be measured at the exact same location.

Methods for direct quantification of the regurgitant flow volume exist, although none have yet reached clinical practice. In laminar blood flow, such as the vena contracta, the backscattered power is proportional to the amount of blood passing through the sample volume [11]. This principle was used by Buck *et al.* [12], who measured the flow volume from the power-velocity integral by using a single wide transmit beam and a narrow beam for calibration. Hergum *et al.* [13, 14] extended this principle in the method MULDO, by using the sum of several narrow beams as a composite measurement beam and selecting one of these as a reference beam. A more robust estimate was then achieved, but with overestimation of small vena contractas, and some underestimation of large vena contractas as a result of the stochastic nature of the Doppler signals.

The flow volume can also be calculated from a color Doppler image by integrating the velocities over time and area. However, velocity aliasing have previously prevented the quantification of regurgitant jets. A recent study [15] have demonstrated that the velocities can be dealiased when imaging the laminar flow at the vena contracta. However, measurements by both color Doppler and continuous wave Doppler are needed.

We have previously presented a semi-quantitative method for estimation of vena contracta area [16], using a single transmit beam direction. By combining parallel receive beamforming with HPRF Doppler and a continuous acquisition, we showed that information about the size of the regurgitant jet could be added to the PW Doppler spectrum. Using parallel receive beams, multiple scan lines are acquired for each transmit event, hence increasing the information received for each transmission. Spectra from each of the receive beams were generated and combined into one single spectrum. The spectrum was then color coded with information about the number of beams intersecting with the jet. A high end scanner (Vivid E9, GE Vingmed, Horten, Norway) was used to test the method on a patient. The maximum number of receive beams available on the scanner was 16, which restricted the feasible beam density and the field of view. Although information of the vena contracta area was added, the color representation was noisy and no information about the shape was given.

In this work, the method presented in [16] is further developed to produce a more accurate estimate of the vena contracta area, in addition to information about the vena contracta shape and a quantitative measure of the regurgitant volume. Simulation studies are performed to optimize the configurations of the transmit and receive beams. In particular we investigate whether the method may be utilized with 16 parallel receive beams or if more beams are required. In Section 5.2.1 the concept of the new method is presented. In Section 5.2.2 the simulation methods and parameters are described. A suggested beam configuration is presented in Section 5.3, together with results from regurgitant volume estimates of simulated flow.

5.2 Methods

5.2.1 Concept

High pulse repetition frequency PW Doppler signals are acquired from a 2-D plane crossing the vena contracta, using a broad beam on transmit (Tx) and parallel beams on receive (Rx). The receive beams are interpolated in space using 2-D spline interpolation and velocity spectra are generated from each of the interpolated beams. An average of these spectra is calculated, and used to find the velocity-time integral by delineating the spectrum envelope. The same average is then used to identify the velocity-time region that only includes the high velocities of the jet. For each interpolated receive beam, the signal power from the chosen velocity-time region is averaged, and then displayed in a power Doppler image, visualizing the vena contracta cross-section. The area of the vena contracta cross-section is found by thresholding the averaged power in each of the interpolated beams, and by estimating the size of the area above this threshold. The regurgitant volume is then calculated by multiplying the velocity-time integral with the estimated vena contracta area.

5.2.2 Simulations of Regurgitant Flow

The method was tested and optimized using simulations based on the Field II ultrasound simulation software[17] and probe parameters corresponding to the 4V matrix probe (GE Vingmed, Horten, Norway). The acquisition parameters are listed in table 5.1.

Using Field II, the pulse-echo response $h_{pe}(t, \vec{r}_s, \vec{r}_f)$ was calculated for all times t, scatter positions $\vec{r}_s$ and receive focus positions $\vec{r}_f$ at a depth of 10 cm. The receive beams were evenly distributed in the azimuth-elevation plane as illustrated in Fig. 5.1. In-phase and quadrature (IQ) demodulation was performed, resulting in the complex signal $h_{IQ}(t, \vec{r}_s, \vec{r}_f)$. Spline interpolation was done in the $\vec{r}_f$ dimension (for all t and $\vec{r}_s$), resulting in receive beams on a densely sampled grid in the x-y plane.

The expected power $p(\vec{r}_s, \vec{r}_f)$ from a scatterer in position $\vec{r}_s$ was calculated by

$$p(\vec{r}_s, \vec{r}_f) = \sum_t |h_{IQ}(t, \vec{r}_s, \vec{r}_f)|^2 \ . \tag{5.1}$$

Table 5.1: Simulation Parameters

Parameter	Value
Azimuth transducer size	2.05 cm
Elevation transducer size	1.64 cm
Tx center frequency	2 MHz
Pulse periods	5
Tx apodization	Tukey window
Rx apodization	none
Sampling frequency	100 MHz

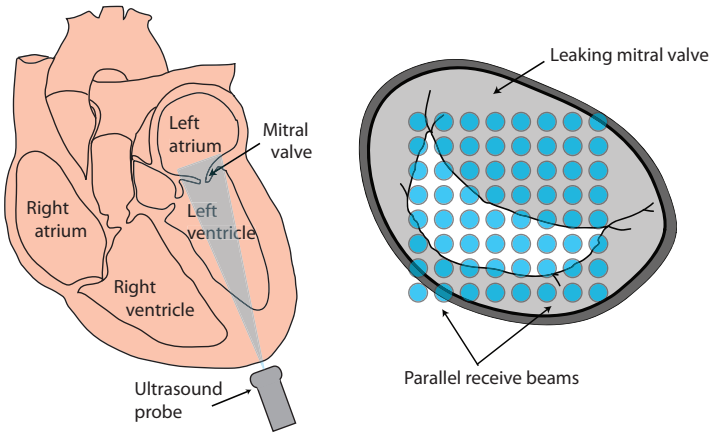

Figure 5.1: Sketch of the heart (left) and the mitral valve (right) with 64 parallel beams indicated across the valve. In the proposed method, PW Doppler signals are acquired from a 2-D plane across the vena contracta, using a broad beam on transmit and parallel beams on receive.

The expected power received in each beam, $\vec{r}_f$, from a jet covering the positions $\vec{r}_j$, was calculated by

$$P_{jet}(\vec{r}_f) = \sum_{\vec{r}_s = \vec{r}_j} p(\vec{r}_s, \vec{r}_f) \ . \tag{5.2}$$

The estimated power could then be displayed in a cross-sectional power Doppler image, as demonstrated for a moderate regurgitation and 8 x 8 receive beams in Fig. 5.2, where the power before and after interpolation is shown.

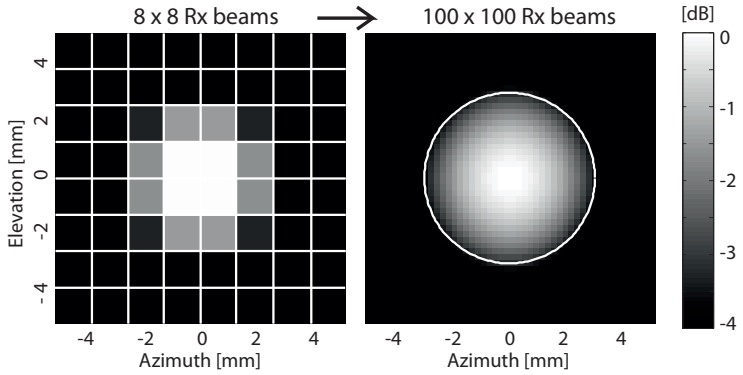

Figure 5.2: Cross-sectional power Doppler images estimated before (left) and after (right) spline interpolation of the receive beams. A circular vena contracta with a diameter of 6 mm centered in the middle of the ROI was simulated.

5.2.3 Flow Volume Estimation

The vena contracta area, A_{VC}, was calculated by thresholding the estimated power in (5.2) at P_{th} decibels below the maximum value, and multiplying the number of receive beams above this threshold with the grid resolution. The regurgitant volume, RgV, was found by

$$RgV = A_{VC} \cdot L_{VTI} \ , \tag{5.3}$$

where L_{VTI} is the velocity time integral. $L_{VTI} = 1.5$ was used in this work, which is the median value of the velocity-time integrals of the mitral regurgitations measured by Skaug *et al.* in [14], using CW Doppler. Different values of P_{th} was tested, and the value that gave the most accurate volume estimates for the configuration with 64 receive beams sampled at 0.5 times the Rayleigh criterion was chosen.

The consistency in the volume estimates for different jet locations was investigated by simulating circular vena contractas in the middle of the ROI (in between the receive beams) or shifted half the beam spacing in azimuth and elevation direction (on a receive beam). The volume estimation results for both scenarios were plotted in the same figure and the intervening area was shaded, indicating the expected variation in the estimation results for different jet locations.

5.2.4 Transmit Beam Optimization

To ensure accurate volume estimates and consistent results for different jet locations and shapes, the transmit beam profile should be approximately uniform in a region large enough to cover large regurgitations. A simulation study was performed to calculate the optimal transmit parameters for a 10 cm depth of interest. Both

unfocused and diverging transmit beams were investigated with varying degree of transmit apodization. Using Field II, diverging transmit beams were simulated with opening angles varying from 4° to 7° with steps of 0.5°, and with Tukey apodization windows with taper ratios varying from 0% to 100% through 21 steps in both azimuth and elevation directions. After averaging the resulting beam profiles with a 4x4 mm filter, the maximum and minimum spatial intensity was found. The transmit beam profile with the minimum difference between the maximum and minimum intensity in a central area of 1x1 cm was chosen as the beam most suited for the proposed method.

A second simulation study was performed to examine the loss in expected SNR for the wide transmit beams used in this method, compared to a focused beam as used in conventional PW Doppler. The spatial peak intensity, I_{max}, at 10 cm depth was chosen as a measure of the signal strength and hence, the SNR. Diverging transmit beams were simulated with opening angles varying from 1° to 15° with steps of 2° and compared with a beam focused at 10 cm. A Tukey window found from the study above (see Table 5.2) was used as transmit apodization for the diverging beams. The beam size at 10 cm depth was estimated as the part of the beam with intensity of at most 4 dB below I_{max}. I_{max} of each beam was normalized with I_{max} of the focused beam and plotted with respect to the estimated beam size.

5.2.5 Receive Beam Optimization

Two different scenarios were investigated where the number of parallel receive beams were set to 16 or 64. When using 64 receive beams, the beam spacing was set to 0.5, 0.75 or 1 times the Rayleigh criterion, which for a rectangular aperture is given by

$$d\theta = \lambda/a \ , \tag{5.4}$$

where $d\theta$ is the beam spacing in radians, λ is the wavelength and a is the aperture size [18]. The same number of receive beams were used in azimuth and elevation direction. Using a non-quadratic aperture and constant beam spacing, this resulted in a two-way beam profile that was wider in the elevation direction.

A minimum width covered by the receive beams was chosen to 1 cm to ensure full inclusion of large circular regurgitations. In order to keep this field of view, the beam spacing was set to 3.4 mm and 4.2 mm in the azimuth and elevation directions, respectively, when using 16 receive beams. This corresponds to a beam spacing of 0.9 times the Rayleigh criterion. When using 16 receive beams, both linear and spline interpolation of the receive beams were tested, as edge effects from the spline interpolation were expected to distort the cross-sectional power Doppler image.

By summing the power for all $\vec{r}_s$ in (5.2), sensitivity maps for the two-way beam profiles were generated.

5.3 Results

Transmit beam profiles for the 4V probe was simulated using Field II. The transmit parameters that were found to give the most uniform beam profile in a 1x1 cm central

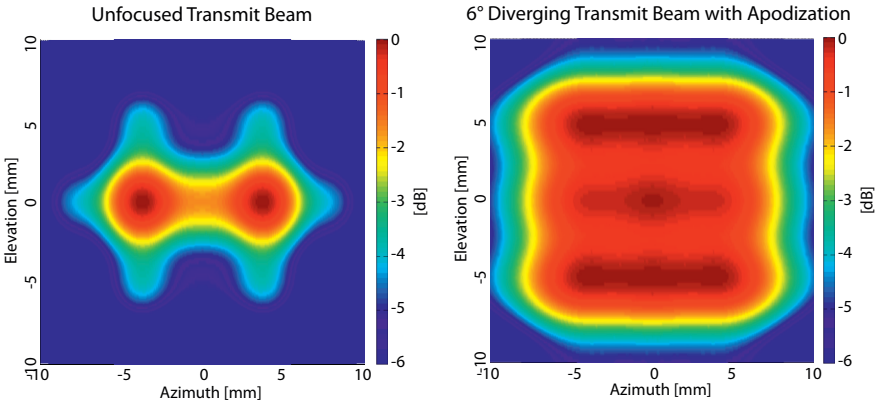

Figure 5.3: Transmit beam profiles at 10 cm depth simulated using Field II with the 4V probe parameters. The left panel shows an unfocused beam profile. The right panel shows a profile of a 6° diverging beam with apodization. The intensity variations in the 1x1 cm central area is less than 1 dB.

area at 10 cm depth is given in Table 5.2, and a cross-sectional image of the beam profile at this depth is shown in the right panel of Fig. 5.3. The intensity variations in the 1x1 cm central area is less than 1 dB. As a comparison, the left panel shows the beam profile of an unfocused beam at 10 cm depth. In this case, the power is separated into two maxima which fall off quickly in both the azimuth and elevation directions.

Table 5.2: Optimized Transmit Beam Parameters

Parameter	Value
Opening angle of diverging beam	6°
Azimuth apodization window	Tukey, 45%
Elevation apodization window	Tukey, 5%

The spatial peak intensity of diverging transmit beams with opening angles of 1° to 15° are marked with crosses from left to right in Fig. 5.4. The beam size increases with increasing opening angle, but the peak spatial intensity decreases, indicating a worsening in SNR for large diverging angles. The peak intensity was found to have an approximate 1/size dependency, given by the function

$$f(A) = 10 \cdot \log_{10}\left(\frac{1/A}{1/A_0}\right) \ , \tag{5.5}$$

where A is the beam size and A_0 is the estimated beam size of the focused beam. $f(A)$ is given by the black line in Fig. 5.4.

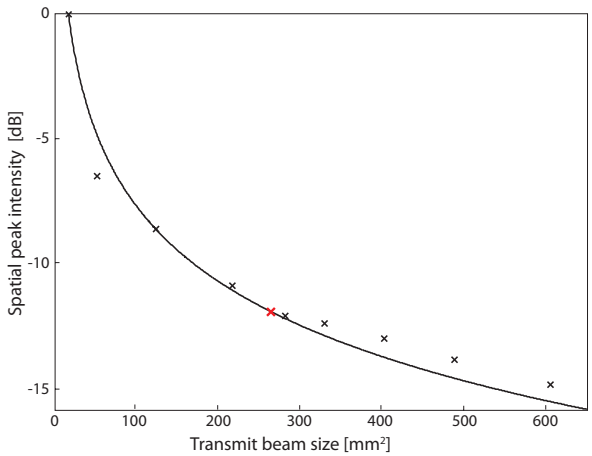

Figure 5.4: Peak spatial intensity (I_{max}) versus beam size for diverging transmit beams with varying opening angles at 10 cm depth. The results are compared with a focused beam; marked in the figure at 0 decibel. The other black crosses are (from left to right) diverging beams with angles from 1° to 15° with steps of 2°. The red cross gives the result for a 6° diverging beam. The black line indicates the 1/size dependency of the spatial peak intensity.

The different receive beam configurations were tested by estimating the regurgitant volumes from circular vena contractas with diameters up to 1 cm. The transmit parameters applied for all the following results are given in Tables 5.1 and 5.2. The threshold that gave the most accurate volume estimates for the configuration with 64 receive beams sampled at 0.5 times the Rayleigh criterion was $P_{th} = 3.3\ dB$. This threshold was used for all the following regurgitant volume estimates. Two simulations were performed for each configuration, where the hole was centered on or in-between the receive beams.

Regurgitant volume estimates using a diverging transmit beam and 16 receive beams are shown in Fig. 5.5. The vena contractas were restricted to circles with diameters of less than 6.7 mm, because of the limited field of view and the non-centered vena contractas. The volume estimation results after linear or spline interpolation of the receive beams are shown in the left panel of Fig. 5.5. In the right panels of Fig. 5.5, sensitivity maps of the corresponding two-way beam profiles are shown. The volume estimates from the simulations using spline interpolation (red) has a gradient that better follows the true volume than the simulations using linear interpolation (green). However, spline interpolation results in a larger estimate distribution.

Regurgitant volume estimation of simulated flow through circular orifices was also done using 64 receive beams with three different receive beam densities. The results are shown in the left panels of Fig. 5.6. In the right panels of Fig. 5.6, sensitivity maps of the corresponding two-way beam profiles are shown. The results show that with a beam spacing of 0.5 times the Rayleigh criterion, the volume estimates correlate well

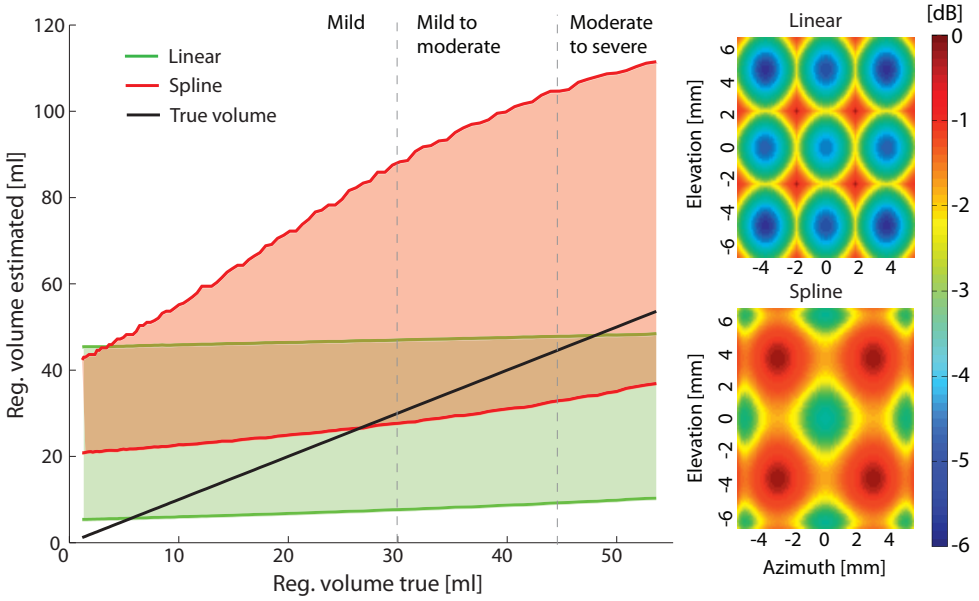

Figure 5.5: Results from simulations using 16 parallel receive beams interpolated using linear or spline interpolation. The receive beam density is 0.9 times the Rayleigh criterion. Estimated regurgitant flow volumes from circular vena contractas are shown in the left panel and sensitivity maps of the two-way beam profiles are shown in the right panels. The volume estimates from the simulations using spline interpolation (red) have a large estimate distribution, however with a mean gradient that better follows the true volume than the simulations using linear interpolation (green).

with the true volume (given by the black line). The volume estimate distribution is larger and the two-way beam profile is less uniform when the beam spacing is larger.

Fig. 5.7 shows power Doppler images from regurgitations of different sizes and shapes, after interpolation of the receive beams. Vena contracta areas of 13, 28 and 50 mm^2 are displayed from left to right, corresponding to mild, moderate and severe regurgitation. When using 16 parallel beams and a beam spacing of 0.9 times the Rayleigh criterion, the vena contracta areas are significantly overestimated. When using 64 parallel beams and a beam spacing of 0.5 times the Rayleigh criterion, the bright area fits well with the true shape (white line), however the images are less accurate for the moon shaped vena contractas than the circular shaped vena contractas. The areas for the moon shaped vena contractas were estimated to 19, 32 and 54 mm^2 for the mild, moderate and severe regurgitations, respectively.

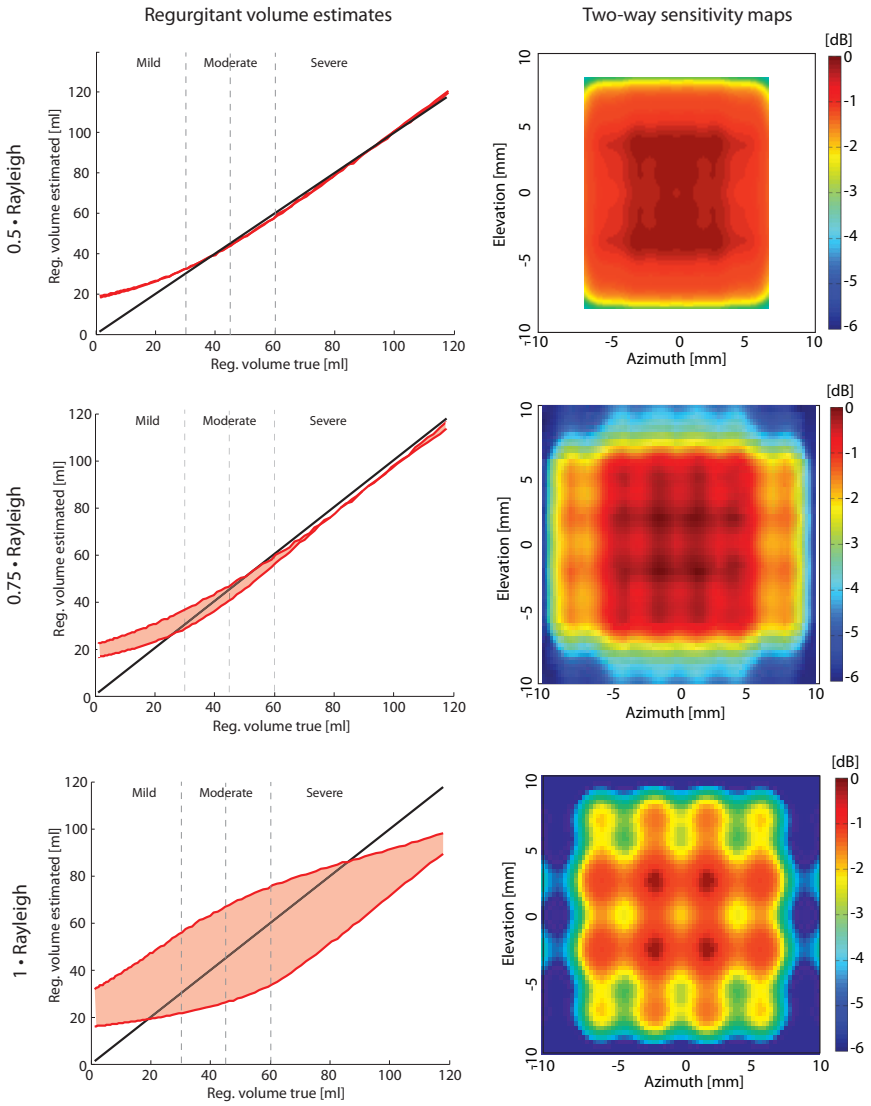

Figure 5.6: Results from simulations using an apodized 6° diverging beam on transmit and 64 parallel beams on receive, sampled with three different sampling densities. Estimated regurgitant volumes from circular regurgitant flow are shown in the left panels and sensitivity maps of the two-way beam profiles are shown in the right panels. Regurgitant volumes up to 118 ml are shown and divided into 4 categories from mild to severe regurgitation. The red lines shows the estimated regurgitant volumes when the hole is placed on or in-between the receive beams. The shaded areas represents possible outcomes for different hole positions. The volume estimates using a sampling density of 0.5 times the Rayleigh criterion, correlates well with the true volume (black line) and have the smallest estimate distribution.

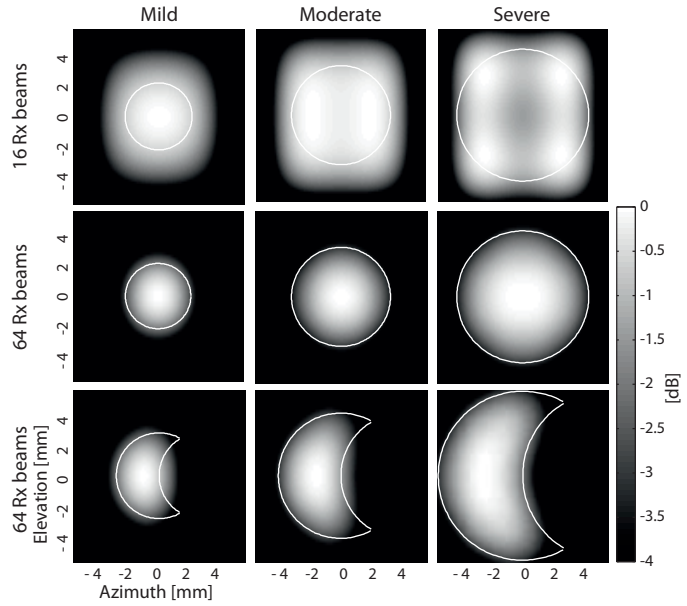

Figure 5.7: Cross-sectional power Doppler images of the simulated regurgitations of different sizes and shapes, after interpolation of the receive beams. Vena contracta areas of 13, 28 and 50 mm^2 are displayed from left to right respectively, corresponding to mild, moderate and severe regurgitation. The white lines indicate the true shape of the regurgitation. 16 receive beams with a beam spacing of 0.9 times the Rayleigh criterion are used in the simulations for the top row panels. 64 receive beams with a beam spacing of 0.5 times the Rayleigh criterion are used in the simulations for the two lower row panels.

5.4 Discussion

In this work, we have developed a 3-D PW Doppler method for quantification of valvular regurgitation. The method was optimized and evaluated using simulations. Flow volumes through circular and crescent-shaped orifices of varying sizes were estimated and cross-sectional power Doppler images were displayed. By applying the optimized acquisition parameters, the regurgitant volumes were accurately estimated for a large range of flow volumes.

A transmit beam with a flat intensity profile at 10 cm depth was searched for, to ensure consistent volume estimates. As seen in the left panel of Fig. 5.3, an unfocused beam has large intensity variations at this depth. The transmit beam found to have the least intensity variations in a 1x1 cm central area was a diverging beam with 6° opening angle and with transmit apodization. Although the intensity variations of this beam was shown to be less than 1 dB in the central area, the intensity drops off quickly outside this area. Larger opening angles of the diverging beam give larger

beam sizes. However, as seen in Fig. 5.4, the spatial peak intensity (I_{max}) is reduced with increasing beam size. The diverging beam with 6° opening angle (red cross in Fig. 5.4) has an I_{max} that is 12 dB lower than the focused beam. A larger opening angle could have been chosen without a substantial loss in SNR. However, because the 6° diverging beam had the least intensity variations in the 1x1 cm central area, it was found best suited for the method.

A beam size of 1x1 cm, as used in this work, will cover large circular orifices. However, large crescent–shaped orifices may extend over a larger distance, and may therefore be underestimated with the proposed beam configuration. Also, a large field of view is desired to ease the clinical procedure when the jet is searched for. Therefore, to ensure robust volume estimates, the acceptable beam size and SNR for the proposed method should be investigated further in an *in vivo* study.

It was shown in Figs. 5.5 and 5.6 that when the two-way beam profile has large intensity variations, different locations of the vena contracta result in large variations in flow volume estimation. Fig. 5.6 also shows that the receive beam density is crucial to ensure a uniform two-way beam profile. When using 16 receive beams, the beam spacing was set to 0.9 times the Rayleigh criterion, in order to keep a field of view of minimum 1x1 cm. However, it was found that a beam spacing of 0.5 times the Rayleigh criterion is advantageous for accurate interpolation of the IQ signal. When using 64 receive beams and a beam spacing of 0.5 times the Rayleigh criterion, the volume estimates were accurate and consistent for different vena contracta sizes and locations.

The choice of 16 and 64 parallel receive beams used in this work was based on the possibilities in the newest high end scanners on the market today. Although the number of parallel receive beams available in most scanners today are limited, an increase in parallel beamformers is expected. If a larger field of view than used in this work is considered, an increased number of receive beams is required to ensure a sufficient sampling density.

The proposed method may have several advantages clinically. First, it measures the regurgitant volume from just one recording, as both the velocity-time integral and the vena contracta area is found from a single PW Doppler measurement. This may improve the workflow for the examiner, but more importantly; it improves the accuracy of the estimate as both measures are done at the exact same location.

In contrast to methods like PISA and the vena contracta width, the proposed method makes no geometric assumptions. Fig. 5.7 shows that the cross-sectional power Doppler images of the vena contractas fits well with the true shape for both circular and crescent-shaped vena contractas. The method may therefore provide more accurate estimates of non-circular orifices and for situations with multiple orifices. However, the regurgitant volumes estimated in this study were more accurate for the circular shaped vena contractas than for the crescent-shaped vena contractas. This may be due to the limited spatial resolution of the ultrasound beam at this depth. This could be overcome by transesophageal echocardiography, where the probe is located in close proximity to the heart.

In the 3-D PISA methods, fewer geometric assumptions are made than in the 2-D methods. However, methods that derive the proximal isovelocity surface area from

volumetric color Doppler data suffer from the fundamental limitation regarding angle dependence of color Doppler imaging. Unlike the single radial measure in 2-D PISA, the 3-D method must identify the entire curvature of the isovelocity surface, which represents a wide range of Doppler angles [19]. The proposed PW Doppler method gives angle-independent flow volume estimates. Even if the ultrasound beam is at an angle with the flow, the property of flow continuity ensures that the volume flow rate can be determined by integrating all the velocity components normal to the imaging plane, as long as the imaging plane completely intercepts the flow path. This principle of flow determination has previously been shown for color Doppler imaging [20, 21].

Another major advantage of the proposed method is that it is not affected by display settings such as gain and tissue priority. The volume estimates are calculated from a fixed threshold and are therefore nearly observer-independent. However, the threshold proposed in this study is given by the maximum intensity of the dataset. This may lead to underestimations of some regurgitations because of statistical fluctuations of the Doppler signals. A threshold that is independent of the maximum value should therefore also be considered.

The suggested algorithm for signal processing and volume estimation, given in 5.2.1, is only preliminary and may need to be adjusted after prospective clinical studies. The suggested method for calculating the velocity-time integral is to trace the envelope of an averaged spectrum. A more advanced procedure could be considered, where more of the velocities in the averaged velocity spectrum is used. By weighting the velocities in the chosen velocity-time region with the corresponding power, and multiplying with the vena contracta area, possible velocity gradients in the jet could be included in the calculations.

The cross-sectional power Doppler image may be used for navigation when searching for the jet. The vena contracta may also be found by examining the PW Doppler spectrum, as the spectrum is at the narrowest when measured inside the laminar area of the jet. Having both image modalities displayed at the same time is therefore advantageous.

When imaging *in vivo*, a lot of averaging of the signal power is required, because of the statistical properties of the Doppler signals. Averaging in time may be challenging, both because the regurgitation may be present only for a limited time, and because the vena contracta can move slightly from frame to frame due to the transient nature of a jet and movement of the operator. These challenges were not considered in this study, but should be investigated further.

In the simulations, the flow was strictly confined inside the vena contracta. In an *in vivo* situation, the flow boundaries are less defined, as surrounding blood are pulled along with the jet. Also, turbulent flow and complex flow patterns may introduce errors in the estimates. The estimated shape and size of the vena contracta cross-section are therefore expected to be less accurate *in vivo*.

5.5 Conclusion

A new method to estimate both the volume and shape of regurgitant flow has been presented. The method was optimized and evaluated using simulations, and a transmit-receive beam configuration was proposed. The regurgitant volume from simulated flow was estimated by thresholding the power in PW Doppler spectra generated from multiple receive beams. The method was successful in estimating the regurgitant volume from both circular and crescent-shaped orifices.

Acknowledgment

The authors would like to thank Jørgen Avdal for many fruitful discussions.

References

[1] F. Recusani, G. S. Bargiggia, A. P. Yoganathan, A. Raisaro, L. M. Valdes-Cruz, H. W. Sung, C. Bertucci, M. Gallati, V. A. Moises, and I. A. Simpson, "A new method for quantification of regurgitant flow rate using color Doppler flow imaging of the flow convergence region proximal to a discrete orifice. An in vitro study," *Circulation*, vol. 83, pp. 594–604, Feb. 1991.

[2] P. Lancellotti, L. Moura, L. Pierard, E. Agricola, B. A. Popescu, C. Tribouilloy, A. Hagendorff, J.-L. Monin, L. Badano, and J. L. Zamorano, "European Association of Echocardiography recommendations for the assessment of valvular regurgitation. Part 2: mitral and tricuspid regurgitation (native valve disease).," *European journal of echocardiography : the journal of the Working Group on Echocardiography of the European Society of Cardiology*, vol. 11, pp. 307–32, May 2010.

[3] Y. Matsumura, S. Fukuda, H. Tran, N. L. Greenberg, D. A. Agler, N. Wada, M. Toyono, J. D. Thomas, and T. Shiota, "Geometry of the proximal isovelocity surface area in mitral regurgitation by 3-dimensional color Doppler echocardiography: difference between functional mitral regurgitation and prolapse regurgitation.," *American heart journal*, vol. 155, pp. 231–8, Feb. 2008.

[4] P. Kahlert, B. Plicht, I. M. Schenk, R.-A. Janosi, R. Erbel, and T. Buck, "Direct assessment of size and shape of noncircular vena contracta area in functional versus organic mitral regurgitation using real-time three-dimensional echocardiography.," *Journal of the American Society of Echocardiography : official publication of the American Society of Echocardiography*, vol. 21, pp. 912–21, Aug. 2008.

[5] S. H. Little, "Quantifying mitral valve regurgitation: new solutions from the 3rd dimension.," *Journal of the American Society of Echocardiography : official publication of the American Society of Echocardiography*, vol. 23, pp. 9–12, Jan. 2010.

[6] J. A. de Agustín, P. Marcos-Alberca, C. Fernandez-Golfin, A. Gonçalves, G. Feltes, I. J. Nuñez Gil, C. Almeria, J. L. Rodrigo, L. Perez de Isla, C. Macaya, and J. Zamorano, "Direct Measurement of Proximal Isovelocity Surface Area by Single-Beat Three-Dimensional Color Doppler Echocardiography

in Mitral Regurgitation: A Validation Study.," *Journal of the American Society of Echocardiography : official publication of the American Society of Echocardiography*, pp. 815–823, June 2012.

[7] P. Thavendiranathan, S. Liu, S. Datta, S. Rajagopalan, T. Ryan, S. R. Igo, M. S. Jackson, S. H. Little, N. De Michelis, and M. A. Vannan, "Quantification of chronic functional mitral regurgitation by automated 3-dimensional peak and integrated proximal isovelocity surface area and stroke volume techniques using real-time 3-dimensional volume color Doppler echocardiography: in vitro and clini," *Circulation. Cardiovascular imaging*, vol. 6, pp. 125–33, Jan. 2013.

[8] M. Shanks, H.-M. J. Siebelink, V. Delgado, N. R. L. van de Veire, A. C. T. Ng, A. Sieders, J. D. Schuijf, H. J. Lamb, N. Ajmone Marsan, J. J. M. Westenberg, L. J. Kroft, A. de Roos, and J. J. Bax, "Quantitative assessment of mitral regurgitation: comparison between three-dimensional transesophageal echocardiography and magnetic resonance imaging.," *Circulation. Cardiovascular imaging*, vol. 3, pp. 694–700, Nov. 2010.

[9] N. A. Marsan, J. J. M. Westenberg, C. Ypenburg, V. Delgado, R. J. van Bommel, S. D. Roes, G. Nucifora, R. J. van der Geest, A. de Roos, J. C. Reiber, M. J. Schalij, and J. J. Bax, "Quantification of functional mitral regurgitation by real-time 3D echocardiography: comparison with 3D velocity-encoded cardiac magnetic resonance.," *JACC. Cardiovascular imaging*, vol. 2, pp. 1245–52, Nov. 2009.

[10] X. Zeng, R. A. Levine, L. Hua, E. L. Morris, Y. Kang, M. Flaherty, N. V. Morgan, and J. Hung, "Diagnostic value of vena contracta area in the quantification of mitral regurgitation severity by color Doppler 3D echocardiography.," *Circulation. Cardiovascular imaging*, vol. 4, pp. 506–13, Sept. 2011.

[11] B. A. J. Angelsen, "A theoretical study of the scattering of ultrasound from blood.," *IEEE transactions on bio-medical engineering*, vol. 27, pp. 61–7, Feb. 1980.

[12] T. Buck, R. A. Mucci, J. L. Guerrero, G. Holmvang, M. D. Handschumacher, and R. A. Levine, "The Power-Velocity Integral at the Vena Contracta : A New Method for Direct Quantification of Regurgitant Volume Flow," *Circulation*, vol. 102, pp. 1053–1061, Aug. 2000.

[13] T. Hergum, T. R. Skaug, K. Matre, and H. Torp, "Quantification of valvular regurgitation area and geometry using HPRF 3-D Doppler.," *IEEE transactions on ultrasonics, ferroelectrics, and frequency control*, vol. 56, pp. 975–82, May 2009.

[14] T. R. Skaug, T. Hergum, B. H. Amundsen, T. Skjaerpe, H. Torp, and B. O. Haugen, "Quantification of mitral regurgitation using high pulse repetition frequency three-dimensional color Doppler.," *Journal of the American*

Society of Echocardiography : official publication of the American Society of Echocardiography, vol. 23, pp. 1–8, Jan. 2010.

[15] B. Plicht, P. Kahlert, R. Goldwasser, R.-A. Janosi, P. Hunold, R. Erbel, and T. Buck, "Direct quantification of mitral regurgitant flow volume by real-time three-dimensional echocardiography using dealiasing of color Doppler flow at the vena contracta.," *Journal of the American Society of Echocardiography : official publication of the American Society of Echocardiography*, vol. 21, pp. 1337–46, Dec. 2008.

[16] T. D. Fredriksen, H. Torp, and T. Hergum, "Quantification of mitral regurgitation using PW Doppler and parallel beamforming," *2011 IEEE International Ultrasonics Symposium*, pp. 434–437, Oct. 2011.

[17] J. Jensen, "Field: A program for simulating ultrasound systems," *Med. Biol. Eng. Comput.*, vol. 34, pp. 351–353, 1996.

[18] J. N. Wright, "Image Formation in Diagnostic Ultrasound," *IEEE international ultrasonics symposium short course*, 1997.

[19] S. H. Little, "Is it Really Getting Easier to Assess Mitral Regurgitation Using the Proximal Isovelocity Surface Area?," *Journal of the American Society of Echocardiography : official publication of the American Society of Echocardiography*, vol. 25, pp. 824–6, Aug. 2012.

[20] Y. Sun, P. Ask, B. Janerot-Sjöberg, L. Eidenvall, D. Loyd, and B. Wranne, "Estimation of volume flow rate by surface integration of velocity vectors from color Doppler images.," *Journal of the American Society of Echocardiography : official publication of the American Society of Echocardiography*, vol. 8, no. 6, pp. 904–14, 1995.

[21] S. Berg, H. Torp, B. O. Haugen, and S. Stein, "Volumetric Blood Flow Measurement with the Use of Dynamic 3-Dimensional Ultrasound Color Flow Imaging," *Journal of the American Society of Echocardiography*, vol. 13, pp. 0393–0402, May 2000.